**M-PM-Sym-1** THE NICOTINIC ACETYLOCHOLINE RECEPTOR: A MODEL FOR CENTRAL AND PERIPHERAL CHEMICALLY GATED ION CHANNELS, Michael A. Raftery, Dept. of Chem., Univ. of MN, Minneapolis, MN 55455

**M-PM-Sym-2** CORRELATIONS BETWEEN THE STRUCTURE, SEQUENCE AND FUNCTION OF ION-CONDUCTING CHANNELS. Robert M. Stroud, Department of Biochemistry & Biophysics, University of California, San Francisco, CA 94143-0448.

The current state of structure analysis of several membrane channel-forming proteins will be discussed in reference to knowledge of conductivity and determinants of conductivity. These include acetylcholine receptors, a colicin channel, bacteriorhodopsin, and an insecticidal toxin that forms pores across membranes. In addition, peptides generated from regions within these sequences have been tested for individual function and in some cases these delineate specific determinants found within these molecules.

**M-PM-Sym-3** THE CONNEXINS: A FAMILY OF GAP JUNCTION PROTEINS. D.A. Goodenough, D.L. Paul, and E.C. Beyer. Dept. of Anatomy and Cellular Biology, Harvard Medical School, Boston, MA 02115.

A cDNA selected from a rat liver cDNA library with an anti-gap junction antiserum codes for a protein with a predicted molecular mass of 32kD (connexin32). This protein is a structural component of the gap junction channel in liver and in other rat organs such as exocrine pancreas, stomach, and kidney. Northern blots fail to demonstrate the presence of the 1.6kb connexin32 mRNA in myocardium and lens. Under conditions of low stringency, however, Northern blots have revealed unique mRNAs in these organs with partial sequence homologies: a ~3.0kb band in myocardium, and a ~2.8 kb band in lens. These bands were observed only following hybridization and washing using low stringency conditions; high stringency conditions abolished the hybridization. Rat heart and lens cDNA libraries were screened with the connexin32 cDNA probe under the permissive hybridization conditions, and positive clones identified and purified. The purified heart cDNAs span 2768 bp containing a single 1146 bp open reading frame coding for a predicted polypeptide with a molecular mass of 43kD (connexin43). The predicted N-terminal amino acid sequence agrees with 20 amino acids determined by Edman degradation for the myocardial gap junction protein. The purified lens cDNA predicts a polypeptide with a molecular mass of 46kD (connexin46). The predicted amino acid sequences for all three connexin molecules have hydrophobic regions with conserved structure, while they differ from each other in area thought to correspond to hydrophilic cytoplasmic domains. Northern analysis under high stringency conditions indicates that the mRNAs for these connexins are not always organ specific, but are found in several instances to coexist. For example, all three connexin mRNAs may be detected by Northern analysis of rat kidney. Supported by GM37751, GM18974, and EY02430.

**M-PM-Sym-4** REGULATION OF FREE INTRACELLULAR CALCIUM IN NON-EXCITABLE CELLS.
E. Neher, R. Penner, G. Matthews, Max-Planck-Inst. f. biophys. Chemie, D3400 Göttingen

Mast cells participate in inflammatory and immunologic processes by liberating histamine and other chemical mediators upon antigenic stimulation. The concentration of free intracellular calcium $[Ca]_i$, plays a major role in the control of secretion in these non-excitable cells (1). Although recent patch-clamp studies have shown that secretion can occur at basal or even reduced $[Ca]_i$ (2,3), it is nevertheless clear that increased $[Ca]_i$ in the range of 0.3 - 1 μM can greatly enhance rates of secretion in response to other stimuli (2). Also, under certain conditions, an increase in $[Ca]_i$ can, by itself, force secretion in the absence of other secretory stimuli, provided $[Ca]_i$ exceeds 1 μM.

The most prominent regulatory mechanism for $[Ca]_i$ in mast cells is the release of calcium from intracellular stores, elicited by PI-breakdown. One or several transient increases in $[Ca]_i$, lasting for 2-10 s and reaching up to several μM, can be elicited by various secretagogues and by intracellularly administered $IP_3$. Voltage-dependent calcium currents have not been found in these cells (4). However, in patch-clamp experiments employing simultaneous measurement of membrane capacitance to monitor secretion, fura-2 fluorescence to monitor $[Ca]_i$, and membrane current, at least three other membrane conductance mechanisms can be distinguished. One of these is activated by secretagogues and is able to induce a slow increase in $[Ca]_i$ at negative membrane potentials.

(1) B.D. Gomperts, TIBS 11, 290 (1986). (2) E. Neher, J. Physiol. 395 (1988, in press). (3) E. Neher & R. Penner, Proc. A. Benzon Symp. 25, Munskgaard, Copenhagen (1988, in press).(4) M. Lindau & J.M. Fernandez, Nature 319, 150 (1986).

**M-PM-Sym-5** CHANNEL-PROTEIN ENGINEERING: A NOVEL APPROACH TO ESTABLISH STRUCTURE-FUNCTION CORRELATIONS IN THE VOLTAGE-DEPENDENT SODIUM CHANNEL.
M. Montal*, S. Oiki† and W. Danho#.
*University of California, San Diego, La Jolla, CA 92093, †Roche Institute of Molecular Biology and #Hoffmann-LaRoche, Inc., Roche Research Center, Nutley, NJ 07110.

The first steps in the application of protein engineering to study channel protein structure-function relationships will be presented. The strategy is shown in the flow chart. The results obtained with synthetic peptides that mimic the sequence of putative pore segments of the voltage dependent sodium channel[1] (this Symposium) and of the Torpedo acetylcholine receptor (Abstract of Oiki, Danho and Montal, this meeting) will be presented. The general validity of this synthetic approach is currently explored with available sequences for the voltage-dependent calcium channel and other ligand-regulated channels.

**CHANNEL PROTEIN ENGINEERING: STRATEGY**

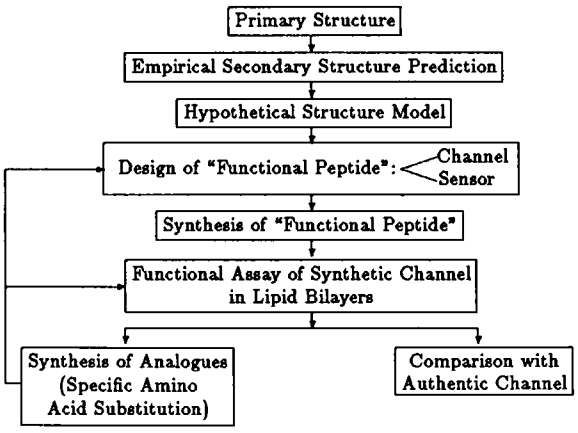


[1] Oiki, S., Danho, W. and Montal, M. (1987) Soc. Neurosci. 13:576 Abstr. 163.2

**M-PM-MinI-1** MEASUREMENTS OF TRANSLOCATION EVENTS IN THE Na/K PUMP CYCLE

B. Forbush, III, Dept. of Cellular & Molecular Physiology, Yale University, New Haven, CT 06510

**M-PM-MinI-2** NEW APPROACHES TO CHEMICAL KINETIC MEASUREMENTS OF RECEPTOR FUNCTION ON CELL SURFACES IN THE μS TO MS TIME REGION. G.P. Hess, Biochemistry, Molecular and Cell Biology, 270 Clark Hall, Cornell University, Ithaca, NY 14853, U.S.A.

Receptor proteins in nerve and muscle cells play a central role in the transmission of signals between cells. However, kinetic investigations of their function have been hampered; endogenous compounds on binding to the protein cause it to form an inorganic ion-conducting transmembrane channel but also induce first-order state transitions in the active protein form to an inactive form with altered abilities to bind ligands. Two new approaches allow kinetic measurements of receptor function to be made on cell surfaces with a time resolution of μs to ms. (1) A method for flowing neurotransmitter-containing solution over cell surfaces is used in combination with measurements of integrated currents, which result when the neurotransmiter binds to the receptor and causes the receptor to form transient transmembrane channels. The time resolution is sufficient to measure the constants that determine the channel-opening process before the receptor is converted to inactive forms. (2) Inactive neurotransmitter precursors have been synthesized that can be photolyzed to the neurotransmitter in the μs time region. The integrated currents that result when the released neurotransmitter binds to the receptor are measured. The technique has a time resolution that allows kinetic measurements to be made of elementary steps in the channel-opening process.

(Supported by grants from NIH and NSF and from the Cornell Biotechnology Program, which is supported by the New York State Science and Technology Foundation, a consortium of industries, and the U.S. Army Research Office.)

**M-PM-MinI-3** Properties and Applications of DM-nitrophen, a New Caged-$Ca^{2+}$. J.H. Kaplan and G. Ellis-Davies. Dept. of Physiology, University of Pennsylvania. Philadelphia, PA 19104-6085.

We have recently synthesized a photolabile chelator for divalent cations, the affinity of which for $Ca^{2+}$ changes by about 5 orders of magnitude on u-v irradiation. The compound, 1-(2'-nitro-4',5'-dimethoxyphenyl)-N,N'-1,2-ethane [N-(carboxymethyl)glycine] or DM-nitrophen, binds $Ca^{2+}$ (Kd 2.7 x $10^{-8}$ M) and $Mg^{2+}$ (Kd 3.0 x $10^{-6}$ M) with relatively high affinity. On irradiation of the DM-nitrophen-$Ca^{2+}$ complex with u-v light in the 350 nm range the chelator is cleaved yielding iminodiacetic acid products with a much lower affinity for Ca(Kd 3 x $10^{-3}$ M) and the free [$Ca^{2+}$] increases. The quantum yield for this process is 0.18. Experimental studies on skinned skeletal muscle fibers where photoreleased Ca rapidly activates contraction and in resealed red cell ghosts where photoreleased Ca activates a K transport pathway will be described. The advantages and disadvantages of this approach compared to other photorelease techniques for increasing [$Ca^{2+}$] will be discussed. Supported by NIH HL15835 to the Pennsylvania Muscle Institute and NIH HL30315.

**M-PM-MinI-4** GATING KINETICS OF THE cGMP-ACTIVATED CHANNEL OF RETINAL RODS. J.W. Karpen, A.L. Zimmerman, L. Stryer and D.A. Baylor, Depts. of Neurobiology and Cell Biology, Stanford Medical School, Stanford, CA 94305.

We have studied the gating kinetics of the cGMP-activated cation channel in excised membrane patches from salamander retinal rods with two methods. In the first, laser flash photolysis of "caged" cGMP (Nerbonne et al. (1984) Nature 310, 74) was used to create fast (<0.2 ms) cGMP concentration jumps in the solution bathing the cytoplasmic face of the patch. After the laser flash, the patch current rose within milliseconds; control experiments showed the rise to result from generation of cGMP. The rate of rise of the current increased with the final cGMP concentration.

In the second method, relaxations of cGMP-induced membrane current were measured after membrane voltage jumps, which perturb activation by cGMP. This method gave results in agreement with those from flash photolysis, but voltage jumps allowed the kinetics to be resolved at high cGMP concentrations, where photolysis did not elicit measurable responses.

The results from both kinds of experiment can be explained by a simple model in which activation involves three sequential cGMP binding steps with bimolecular rate constants close to the diffusion-controlled limit; fully-liganded channels undergo rapid open-closed transitions. Voltage perturbs activation by changing the rate constant for channel closing, which increases with hyperpolarization. The kinetics of activation are limited by the third cGMP binding step at physiological cGMP concentrations. The channel appears to be optimized for rapid response to changes in cytoplasmic cGMP concentration. (Supported by NIH grants EY01543 and EY02005.)

**M-PM-MinI-5** LASER PULSE PHOTOLYSIS STUDIES OF SKELETAL MUSCLE CONTRACTION Y.E. Goldman*, J.A. Dantzig*, J.W. Walker+,*, M. Yamakawa*, E. Homsher# and D.R. Trentham+ Depts. of Physiol., Schs. of Med., Univ. of Penna.*, Phila., PA 19104 and UCLA#, Los Angeles, CA 90024 and Nat. Inst. Med. Res.+, Mill Hill, London NW7 1AA.

Studying the relationship between biochemical, mechanical and structural changes of actomyosin in muscle fibers is a natural application of caged molecules. Rates of elementary reaction steps indicate effects of filament lattice organization and identify candidates for rate limiting control points. Photolysis of caged ATP within glycerol-extracted fibers of rabbit psoas (Biophys. J. 1981 **33**:32a) and soleus muscle (ibid. 1986 **49**:10a) and insect fibrillar flight muscle (ibid. 1985 **47**:288a) showed that the detachment rate of rigor cross-bridges is too high to be rate limiting in the isometric cross-bridge cycle and is insensitive to $[Ca^{2+}]$. In the presence of $Ca^{2+}$, reattachment into the force-generating states is also too high to be rate limiting (ibid. 1986 **49**:268a). Several photolysis experiments link release of product phosphate ($P_i$) with a reversible power stroke. The level of isometric force and the kinetics of tension development following caged ATP photolysis depend on the steady $[P_i]$ (ibid. 1987 **51**:543a). Photolysis of caged $P_i$ in psoas (ibid. 1987 **51**:3a) or insect fibers confirmed the rapid binding of $P_i$ to force-generating cross-bridges. Photolysis of caged G-ATP (ibid. 1985 **47**:25a) and caged ATP($\gamma$S) (ibid. 1987 **51**:475a) rapidly detached rigor cross-bridges, but supported either less tension than ATP (G-ATP), or zero tension (ATP($\gamma$S)). $P_i$ had no appreciable effect on the transients following photolysis, further supporting the linkage between $P_i$ release and the power stroke. Photolysis studies have thus provided quantitative data on actomyosin kinetics in muscle fibers. Support: MDA, MRC and NIH grants HL13835 to the P.M.I. and AM30988 to E.H.

**M-PM-MinI-6** PHOTOCHEMICAL ANALYSIS OF THE LATENCY STEPS BETWEEN ACTIVATION AND CONTRACTION IN SMOOTH MUSCLE. A.P. Somlyo, G. Ellis-Davies, *J.W. Walker, ¶T. Kitazawa, Y.E. Goldman, J.H. Kaplan, *D.R. Trentham, A.V. Somlyo, Univ. of Penna Sch. of Med., Phila., PA, *MRC London, U.K. and ¶Juntendo University, Tokyo, Japan

The elementary steps between surface membrane activation and crossbridge cycling, in smooth muscle, are explored with laser photolysis of photolabile precursors (caged compounds) to circumvent limitations due to diffusion time. We shall present a progress report of studies employing caged precursors of phenylephrine (PE), inositol 1,4,5 trisphosphate ($InsP_3$), $Ca^{2+}$ and adenine nucleotides. Experiments with caged PE were conducted on intact strips, other studies on permeabilized strips of guinea pig portal vein. The latency of contraction following photolysis of PE was ~1.5 sec at 20°C and ~0.6 sec at 30°C; this is longer than the latency that followed photolysis of caged $InsP_3$ or caged $Ca^{2+}$. Increasing [calmodulin] shortened the latency after photolysis of caged $Ca^{2+}$. Photolytic release of ATP (in the presence of 30$\mu$M $Ca^{2+}$+5$\mu$M calmodulin) was followed by a latency of 50ms or less. We conclude that the latency preceeding agonist-activated contraction in smooth muscle is due to at least two significant rate-limiting processes: the first between the binding of the drug to its receptor and $InsP_3$ production, probably due to phospholipase C kinetics and, perhaps, G-protein coupling; the second delay, following the rise in $Ca^{2+}$, is due to the reactions between $Ca^{2+}$, calmodulin and myosin light chain kinase. (Supported by HL15835 to Penn. Muscle Institute)

**M-PM-MinII-1** EPITOPE MAPPING ON ANDROCTONUS AUSTRALIS HEMOCYANIN BY MOLECULAR IMMUNOELECTRON MICROSCOPY AND IMAGE PROCESSING

J.N. LAMY (intr. by S. VINOGRADOV) Université François Rabelais, TOURS (France)

Hemocyanin of the scorpion Androctonus australis is the first protein of which the quaternary structure has been entirely resolved by molecular immunoelectron microscopy (MIEM) (Lamy et al., Biochemistry, 1981, 20, 1849-1856). The original method was based on the observation of native hemocyanin (24 subunits belonging to 8 different polypeptide chains) labelled with subunit-specific polyclonal Fab fragments.

Recently, the precision of the labelling has been considerably improved: (i) Monoclonal antibodies (mAb) are used to produce immunocomplex E.M. views with clearly defined points of contact between the Fab arms and the antigen. (ii) Correspondence analysis, a method of image processing (van Heel and Frank, 1981, Ultramicroscopy, 6, 187-194), allows the separation of E.M. views presenting subtile differences. (iii) The epitope localization, is refined by a systematic investigation of overlaps between pairs of neighboring epitopes. The observation of ring- and/or string-like structure containing one subunit and two different mAb molecules is by far more powerful than the classical immunological (ELISA) test to demonstrate an absence of overlap.

In conclusion, in its present form, this general and direct method, initially developped for hemocyanin, allows an intramolecular localization of epitopes on any antigen visible in the electron microscope.

**M-PM-MinII-2** SEQUENCE AND BIOSYNTHESIS OF MOLLUSCAN HEMOCYANINS. G. Préaux "(Intr. by S. Vinogradov)" KU Leuven, Laboratorium voor Biochemie, Dekenstraat 6, B-3000 Leuven, Belgium

The presence of 8 functional units in the polypeptide chains of gastropodan and cephalopodan hemocyanins (Hcs), as estimated from limited proteolysis followed by $M_r$ and copper analysis of the fragments, was confirmed for some more Hcs, like also the exception of only 7 units in the cephalopodan *Octopi*. The functional units of a given chain differed in carbohydrate composition and in antigenicity and some of them also at the spectroscopical level. Their isolation was greatly improved by the use of a chromatographic step on ConA-Sepharose. The amino-acid sequence of functional units *g* and *h* of the β-Hc of the gastropod *Helix pomatia* and of functional unit *f* of the cephalopod *Sepia officinalis* is being determined. The partial results already revealed a definite degree of homology with functional unit *d* of the β-Hc of *H. pomatia* (Drexel *et al.*, Biol. Chem. Hoppe Seyler 360, 617-635, 1987) but larger for *g* and *f* than for *h*. In functional units *d*, *g* and *h* more than one glycopeptide was found with for *d* even heterogeneity at a given site.

In order to reach the sequence of the Hcs also via that of the cDNAs, a cDNA library was constructed in λgt11 with the Hc-mRNA-rich fraction easily obtained from the branchial glands of *S. officinalis*. It was amplified in *Escherichia coli* Y1090. The immunologically Hc-positive clones were purified and are subcloned in pUC9 before being submitted to cDNA-sequence determination.

A cadmium and copper containing metallothionein was induced in the hepatopancreas of *H. pomatia* by injection of the animals with $Cd(OAc)_2$ or $Cu(OAc)_2$. This protein was apparently able to transfer metal to ApoHc. Its role on the biosynthesis of the Hc in *in vitro* systems is being investigated.

**M-PM-MinII-3** THE STRUCTURE OF OCTOPUS HEMOCYANIN. K. E. van Holde, Department of Biochemistry and Biophysics, Oregon State University, Corvallis, OR 97331.

The research to be described is a collaborative effort between our laboratory and that of Dr. J. Lamy, Université Francois Rabelais, Tours, France.

The hemocyanin of Octopus dofleini exists in vivo as a decamer of $3.6 \times 10^5$ dalton subunits. We have shown that there is only one type of subunit, and that this is a 7-domain structure, each domain corresponding to one oxygen-binding site. The domains can be separated, in various combinations, by limited proteolysis, and are immunologically distinct. The order of domains has been nearly completely established, and the C-terminal domain (Od-1) has been purified and characterized. The dissociation of the decamer to monomer upon removal of divalent cations is completely reversible, and the monomer-decamer equilibrium has been studied as a function of pH and ionic environment. Studies of the kinetics of reassociation indicate that the rate-limiting step is a second-order dimerization, following a first-order process of unknown nature.

Oxygen binding studies show that the whole hemocyanin is highly cooperative, with a strong Bohr effect. The subunits and Od-1 exhibit non-cooperative $O_2$ binding, and a much weaker Bohr effect.

C-DNA clones of the hemocyanin gene have been obtained, and sequencing is in progress, with most of Od-1 completed. The sequences show considerable homology to Helix pomatia hemocyanin and tyrosinase, but little homology to arthropod hemocyanins. Supported by NSF-DMB 85-17310 and CNRS-RCP 080816.

**M-PM-MinII-4** **DESCRIPTION OF HEMOCYANIN FUNCTIONAL PROPERTIES BY ALLOSTERIC NESTING MODELS**

**Stanley J. Gill, Charles H. Robert, Patrick Connelly, and Heinz Decker†**
**Department of Chemistry and Biochemistry, University of Colorado, Boulder, CO 80309; †Zoologisches Institut der Universität, D8000 Munchen 2, Luisenstr. 14, FRG**

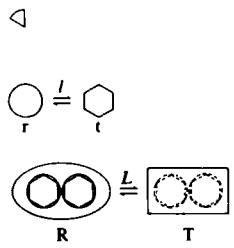


The high cooperativity of large respiratory proteins such as the hemocyanins suggest the presence of large-scale allosteric control. However, the complexity of the binding curves leads one to consider that allosteric interaction occurs within the large scale allosteric structures, as might be envisioned in the figure at left for a 12 subunit protein. This approach to modelling the functional chemistry of multisubunit macromolecules is termed "nesting" [Wyman (1984) Quart. Rev. Biophys. **17**, 453-488]. The basic idea finds expression in the relation of the overall binding potential $\prod$ for a structure in terms of that for each of its substructures: $\prod = \ell n \sum v_i^o \exp(\prod_i)$ where the potentials are defined in RT units and $v_i^o$ indicates the mole fraction of the unligated structure in the ith allosteric state. (The extent of binding $\bar{X}$ is given by the derivative $\partial\prod/\partial\ell nx$ where x is the ligand X activity.) The "flyaway" nature of $\prod$ allows one to formulate $\prod_i$ itself in the same way, and in this manner a nested model is constructed to any desired degree of hierarchy. The particular form of the equations will properly reflect the structural features of the system. In this talk we will discuss the development and application of these ideas to the binding of a single ligand (oxygen) and to the identical linkage of two competing ligands (oxygen and carbon monoxide) for two arthropod hemocyanin systems [Robert et al (1987) Proc. Natl. Acad. Sci. USA **84**, 1891-1895]. Supported by NIH grant HL 22325.

**M-PM-MinII-5** LIGAND BINDING BY HEMOCYANINS. Joseph Bonaventura and Celia Bonaventura. Duke University Marine Laboratory, Beaufort, NC 28516.

The ability of hemocyanins to bind oxygen reversibly at a binuclear copper center is exemplary of the novel metal-ligand interactions that a protein matrix can make possible. The hemocyanins differ among themselves both structurally and functionally. Studies of arthropod and molluscan hemocyanins clearly illustrate that significantly different active-site geometries can occur within a single type of metalloprotein. Active-site heterogeneity can be better understood in light of recent structural studies. Notable among these are x-ray crystallographic studies on lobster hemocyanin and the amino acid sequences determined by a number of laboratories on hemocyanins of varied species. These results reveal differences in the ligand fields of the two copper atoms that make up the oxygen binding site. For only one of the copper atoms does the ligand field seem to be similar in both arthropods and molluscs. Thus, a long-standing argument about similarities vs. differences in arthropod and molluscan hemocyanins reaches the happy conclusion that defenders of both views were justified.

Another aspect of hemocyanin study that has far-reaching consequences is that of allosteric modulation of function in high molecular weight aggregates. Both the kinetics and equilibria of ligand binding to the hemocyanins are of interest in evaluating the extent to which cooperative interactions in large aggregates occur within "allosteric units" or are propagated throughout an extended protein assemblage. The ability to create molecules with modified active sites in defined subunits will allow our increased structural knowledge to be used in a predictive and insightful way in evaluation of allosteric mechanisms.

**M-PM-MinIII-1 CHARACTERIZATION OF AN AMINOPHOSPHOLIPID TRANSLOCASE IN HUMAN ERYTHROCYTES**

P.F. Devaux, A. Zachowski, M. Bitbol and P. Fellmann
Institut de Biologie Physico-Chimique, 13, rue Pierre et Marie Curie, 75005 Paris, France

Using spin-labeled phospholipids, we have demonstrated the selective inward translocation of aminophospholipids in red blood cells. This transport requires intracellular $Mg^{2+}$-ATP (1 mM) and can be inhibited by NEM (1 mM), intracellular $Ca^{2+}$ (0.2 μM), vanadate (50μM) and vanadyl ions (30μM). The active translocation requires not only specific head groups but also an ester bond at the β position. These observations led us to postulate the existence of a specific carrier protein ("Amino Phospholipid Translocase") in the red cell membrane. Competition experiments between spin labeled analogues of phosphatidylserine and phosphatidylethanolamine have indicated that the same pathway is used by both lipids, the former having a higher affinity for the protein than the latter. Experiments have been carried out also to measure the inside-outside diffusion of aminophospholipids in red cells. This phenomenon is also protein mediated and can be blocked by the same concentration of NEM as the inward diffusion. Half-time for inside-outside passage is similar for both aminophospholipids but longer than the half-times of outside-inside translocation. Iodinated photoactivable phosphatidylserine has been used in an attempt to determine which protein(s) is (are) involved. Comparison between red cells of various mammals have been carried out.

M-PM-MinIII-2 AMINOPHOSPHOLIPID FLIPPASE ACTIVITY IN HUMAN ERYTHROCYTES. David L. Daleke[a] and Wray H. Huestis[b], [a]Cancer Research Institute, University of California, San Francisco, California 94143 and [b]Department of Chemistry, Stanford University, Stanford, California 94305.

The activity of an aminophospholipid transporter in the plasma membrane of erythrocytes, platelets, and lymphocytes is studied by observing changes in cell morphology resulting from the incorporation of exogenous phospholipids (*Biochemistry* 24 (1985) 5406) and by measuring the transmembrane distribution of incorporated radiolabeled lipids. Erythrocyte morphology accurately reflects the incorporation and subsequent transmembrane distribution of short chain saturated phosphatidylserines and phosphatidylcholines. Using cell morphology as an assay for phospholipid distribution, studies in human erythrocytes reveal that the aminophospholipid transport mechanism is inhibited by specifically modifying cellular sulfhydryl or arginine residues or by depleting intracellular ATP or magnesium. Phosphatidylserine transport requires ATP hydrolysis and is inhibited by vanadate. These data suggest that the process is protein mediated, energy dependent, and likely involves an ATPase. In addition, the transport of phosphatidylserine is strongly dependent on temperature; low temperature incubation reversibly inhibits phosphatidylserine transport. The energy of activation for phosphatidylserine transport derived from these temperature studies is similar to values reported for other transmembrane transport processes and to those values obtained using spin labelled lipids (Zachowski et al., *Biochemistry* 25 (1986) 2585). Further studies reveal that transbilayer phosphatidylserine transport is independent of acyl chain length. In contrast, phosphatidylcholine movement across the blayer is passive, exhibits an activation energy similar to that found for flip-flop in model membranes and is strongly dependent on acyl chain length. This energy dependent aminophospholipid transporter may participate in the maintenance of transmembrane phospholipid asymmetry in erythrocytes and other cells.

M-PM-MinIII-3 TRANSPORTERS OF PHOSPHATIDYLCHOLINE AND ITS METABOLITES IN RAT LIVER ENDOPLASMIC RETICULUM W. Robert Bishop, Yoichi Kawashima, and Robert M. Bell. Department of Biochemistry. Duke University Medical Center. Durham, North Carolina. 27710

Rapid transmembrane movement of phosphatidylcholine (PC) occurs in rat liver endoplasmic reticulum (ER). Transmembrane movement of PC is considerably slower in other biological membranes (eg. plasma membrane) and in liposomes. In contrast, diacylglycerol undergoes rapid and spontaneous transmembrane movement in liposomes, indicating that it is the polar headgroup which prevents spontaneous PC movement. Therefore, the ER must possess a mechanism to facilitate the rapid transmembrane movement of the phosphocholine headgroup of PC. We have investigated PC transmembrane movement using a short-chain, water-soluble PC, dibutyroyl PC ($diC_4PC$). This molecule remains in aqueous compartments allowing the use of standard methodologies for examining the transport of water-soluble metabolites. $DiC_4PC$ is transported into the lumen of rat liver microsomal vesicles. Transport is dependent on time, microsome concentration and an intact permeability barrier. $DiC_4PC$ transport is saturable and inhibited by proteases, protein modification reagents and structural analogs. Transport of $monoC_4PC$, a homolog of lysoPC, also occurs and exhibits similar kinetic and inhibitory characteristics. This suggests that microsomal transport of PC and lysoPC is mediated by protein "flippases". Glycerophosphorylcholine (GPC) is also transported by rat liver ER vesicles. GPC uptake is insensitive to proteases or modification reagents; therefore, a transporter distinct from that for $diC_4PC$ is inferred. Recently we have successfully reconstituted the $diC_4PC$ and GPC transporters into proteoliposomes using detergent-solubilized protein from rat liver microsomes.

**M-PM-MinIII-4** IS SPECTRIN INVOLVED IN THE ERYTHROCYTE PHOSPHOLIPID ASYMMETRY ?
A. Zachowski, J.Y. Calvez and P.F. Devaux. Institut de Biologie Physico-Chimique 13, rue Pierre et Marie Curie, F-75005 Paris, France.

In the human red cell membrane, phosphatidylcholine (PC) and sphingomyelin (SM) are the predominant phospholipids of the bilayer outer half, while phosphatidyl-serine (PS) and -ethanolamine (PE) occupy mostly the inner layer. We have demonstrated that an enzyme (Amino-Phospholipid Translocase or APT) translocate both PS and PE from the outer to the inner leaflet to the expense of ATP hydrolysis. However one cannot exclude a role of spectrin through interactions with PS and PE. Using spin-labeled phospholipid analogues suitable for these studies, we looked at the APT carrier activity in membrane vesicles obtained by heat-treatment of erythrocytes (15 min, 50°C). These vesicles are practically devoided of spectrin on their membrane. ATP-repletion by incubation in a metabolite-rich medium restored some APT activity : equilibriums obtained were lower than in fresh cells, however there was a clear discrimination between PS, PE and PC, SM. For instance, at equilibrium we recovered 62% of PS, 50% of PE and 29% of PC on the cytoplasmic leaflet. A similar behavior was obtained with the remaining, heat-treated erythrocytes. Thus the carrier activity by itself is capable of generating and maintaining a phospholipid asymmetry. The decrease of the plateau levels of PS and PE can be explained by a partial thermo-denaturation of the AminoPhospholipid Translocase. Alternatively, the small difference between fresh erythrocytes and the heat-treated vesicles can reflect the contribution of spectrin to the phospholipid asymmetry.

**M-PM-MinIII-5** ATP-DEPENDENT TRANSLOCATION OF PHOSPHATIDYLSERINE TO MAINTAIN ITS ASYMMETRIC DISTRIBUTION IN SICKLED ERYTHROCYTES.
B. Roelofsen[1], E. Middelkoop[1], J.A.F. Op den Kamp[1], L.L.M. van Deenen[1], R.F.A. Zwaal[2], D.T.-Y. Chiu[3] and B.H. Lubin[3]; [1] Dept. of Biochemistry, University of Utrecht, the Netherlands; [2] Dept. of Biochemistry, University of Limburg, Maastricht, the Netherlands; [3] Children's Hospital Oakland Research Institute, Oakland, CA 94609.

Two mechanisms are considered to be responsible for maintaining the marked asymmetric distribution of phospholipids in the erythrocyte membrane, i.e. (i) an ATP-dependent translocation of both amino-phospholipids (PE andPS) towards the inner membrane leaflet and (ii) an interaction of those lipids with the membrane skeleton. Prolonged incubation of ATP-depleted reversibly sicklable cells (RSCs) under nitrogen causes a time-dependent appearance of appreciable amounts of PS in the outer membrane layer, when probed with the so-called prothrombinase assay. This phenomenon is not observed when fresh (ATP containing)RSCs are subjected to prolonged deoxygenation. Since sickling of RSCs, as induced by deoxygenation, involves a (local) uncoupling of the lipid bilayer from the membrane skeleton, these observations support the view that the absolute asymmetric distribution of PS in the red cell membrane is maintained by both an interaction with the membrane skeleton and an ATP-dependent translocation towards the inner monolayer. This also implies that, in contrast to what nowadays seems to be a generally accepted phenomenon, sickling of RSCs does not give rise to an appreciable loss of phospholipid asymmetry in their membranes. Despite the local uncoupling of the lipid bilayer from the membrane skeleton, phospholipid asymmetry in the membrane of the sickled cell will be largely maintained because of the action of the ATP-dependent, amino-phospholipid specific, translocase.

**M-PM-MinIII-6** ROLE OF PHOSPHATIDYLSERINE SPECIFIC FLIPASES IN THE MAINTENANCE OF HOMEOSTASIS.
Jerome Connor, John Madsen and Alan J. Schroit, Department of Cell Biology, The University of Texas M. D. Anderson Hospital and Tumor Institute at Houston, Houston, Texas 77030.

The expression of phosphatidylserine (PS) in the outer leaflet of red blood cells results in the recognition of these cells by the reticuloendothelial system. Red cells which contain exogenously supplied fluorescent analogs of PS inserted into their outer leaflet, or cells which express endogenous outer leaflet PS (sickled red cells) avidly bind to macrophages as opposed to cells expressing a fluorescent analog of phosphatidylcholine.

Since the equilibrium distribution of PS appears to be controlled by a specific protein, we have developed techniques, based on resonance energy transfer, to monitor the transbilayer transport of PS in intact cells. In addition, a series of probes have been synthesized in an attempt to identify and isolate this PS specific flipase. Two independent protein labeling procedures have indicated that this flipase, which specifically translocates exogenously supplied PS from the cells' outer to inner leaflet, is a 30,000 dalton protein.

Supported by NIH/NCI grant CA-40149.

**M-PM-A1** MULTIPLE LIQUID CRYSTALLINE PHASES OF DNA. Randolph L. Rill, Teresa Strzelecka and M. W Davidson, Department of Chemistry and Institute of Molecular Biophysics, The Florida State University, Tallahassee, Florida, USA 32306.

Aqueous solutions of near persistence length DNA (ca. 146 base pairs) with simple monovalent counterions spontaneously form ordered, liquid crystalline phases at concentrations in the in vivo range (> 120 mg DNA/ml). At a supporting electrolyte concentration of 0.3 M monovalent cation, a weakly birefringent mesophase with microscopic textures intermediate between those of a nematic and true cholesteric phase forms at the lowest DNA concentrations required for phase separation. Large scale dynamic fluctuations of the nematic director occur in this phase, which we have termed "precholesteric". The concentration and temperature dependencies of isotropic/biphasic and biphasic/precholesteric phase transitions were determined by solid state $^{31}$p NMR methods. These phase boundaries were in good agreement with behavior predicted from Flory's lattice statistics theory assuming a scaled effective DNA radius of 22A. At least two additional phase transitions occur at higher DNA concentrations. The second mesophase is strongly birefringent and has been unambiguously identified by optical and electron microscopic methods as a well-ordered cholesteric phase with a pitch ranging from ca. 2 to 5 um, depending on DNA concentration and temperature. Polarized light microscopy and electron microscopy indicate that the phase or phases formed at the highest DNA concentrations examined (300 - 350 mg/ml) are two dimensionally ordered and appear similar to smectic phases of thermotropic small molecule liquid crystals. Transitions between all phases occur over relatively narrow concentration ranges, indicating that the precise DNA molecular ordering is highly sensitive to environment. Supported in part by NIH grant GM37098.

**M-PM-A2** UV PHOTOELECTRON AND AB INITIO MOLECULAR ORBITAL INVESTIGATIONS OF VALENCE ELECTRONIC STRUCTURES IN PHOSPHATE ESTERS.
Pierre R. LeBreton and Shigeyuki Urano, Department of Chemistry, University of Illinois at Chicago, Chicago, Illinois 60680

The He I UV photoelectron spectrum of trimethyl phosphate (TMP) has been interpreted with the aid of SCF molecular orbital calculations carried out with STO-3G, STO-3G* and 4-31G basis functions. For TMP ($C_3$ symmetry) the vertical ionization potentials of the upper occupied orbitals are 10.81 eV (8e), 11.4 eV (9a), 11.93 eV (7e), 12.6-12.9 eV (8a and 6e), 14.4 eV (7a) and 15.0-16.0 eV (5e and 6a). This assignment agrees with the ordering of SCF orbital energies predicted by all of the calculations. The nine uppermost occupied orbitals from 8e to 7a are made up primarily from oxygen atomic orbitals. In these molecular orbitals the phosphorus contributions are less than 17% and the carbon and hydrogen contributions are less than 30% according to both STO-3G and STO-3G* calculations. In the 5e and 6a orbitals, the STO-3G and STO-3G* calculations predict that the carbon and hydrogen content increases to over 60%.

The results of these studies on phosphate esters, when combined with previously reported results for DNA bases and nucleosides, provide the opportunity to obtain photoelectron scaled descriptions of valence electrons in neutral nucleotides. In preliminary studies these methods have also been applied to nucleotide anions. The results suggest that accurate valence orbital descriptions of nucleotides can provide information which is useful in rationalizing DNA reactions with electrophiles.

Support of this work by the Petroleum Research Fund (Grant #19245-AC) and the National Cancer Institute of the National Institutes of Health (Grant #CA41432) is gratefully acknowledged.

**M-PM-A3** ELECTRONIC IMAGING SYSTEM FOR DIRECT AND RAPID QUANTITATION OF FLUORESCENCE FROM ELECTROPHORETIC GELS: MEASUREMENT OF STRAND BREAKS IN DNA AND OTHER APPLICATIONS.*
John C. Sutherland, Denise C. Monteleone and John Trunk, Biology Department, Brookhaven National Laboratory, Upton, NY 11973

The frequency of single- and double strand breaks induced in DNA by various treatments is given by the difference between the number average molecular lengths of treated and untreated samples. Calculation of number average lengths requires 1) measurement of the mass of DNA as a function of its mobility on an agarose gel and 2) determination of the dispersion function of the gel [1,2]. We have developed an electronic imaging system to replace photography in determining the distribution of fluorophore stained DNA in gels [3]. Unlike photographic film, our solid state detector responds linearly to the intensity of fluorescence. Exposure times can exceed a minute and the entire 200,000 pixel image is digitized and stored in random access computer memory within 33 msec after completion of an exposure. Electronic imaging increases the accuracy, sensitivity and speed of analysis of strand breaks, and can be applied to other tasks that require the quantitation of biomolecules on electrophoretic gels and blots.

1. S. E. Freeman et al., Analytical Biochemistry 158, 119-129 (1986).
2. J. C. Sutherland et al., Analytical Biochemistry 162, 511-520 (1987).
3. J. C. Sutherland et al., Analytical Biochemistry 163, 446-457 (1987).

*Research supported by the Office of Health and Environmental Research, U.S. Department of Energy.

**M-PM-A4** DISTRIBUTION OF IONS AROUND DNA: POISSON-BOLTZMANN THEORY AND EXPERIMENT.

Gene Lamm* and Attila Szabo, Dept. of Biomedical Sciences, Universiy of Illinois College of Medicine, Rockford, IL 61107 and Laboratory of Chemical Physics, NIDDK, National Institutes of Health, Bethesda, MD 20892.

Two recent experiments which reflect the distribution of ions around DNA are reconsidered in light of the Poisson-Boltzmann theory. Bleam et al. (Biochemistry 22, 5418 (1983)) have reported measurements of $Na^{23}$ NMR relaxation line widths in the presence of DNA and varying amounts of added Na and Mg salt. They find that the Na relaxation rate is inversely proportional to the total Na concentration and varies linearly with small amounts of added Mg. Within the framework of a two-state model, Poisson-Boltzmann theory as applied to a uniformly charged cylinder correctly predicts the added-salt concentration dependence of the Na relaxation rates.

The paper by Wensel et al. (Proc. Natl. Acad. Sci. USA 83, 3267 (1986)) reports measurements of charged donor-acceptor energy transfer rates in the presence of DNA. These rates reflect the pair correlation function of the ions. Since Poisson-Boltzmann theory only describes the distribution of ions with respect to DNA and not their relative distribution with respect to each other, the experimental observables can only be related to Poisson-Boltzmann distributions if the Kirkwood superposition approximation is employed and the donor-acceptor pair correlation function is assumed to be unaffected by the DNA. Using this approach ot include the effect of finite ion size we have reinvestigated the applicability of Poisson-Boltzmann theory to the description of these experiments.

**M-PM-A5** MONTE CARLO CALCULATIONS OF THE COUNTERION DISTRIBUTION AROUND DNA USING A PSEUDO-HYDRATION INTERACTION POTENTIAL.

George R. Pack, Gene Lamm*, Linda Wong*, and C.V. Prasad*, Dept. of Biomedical Sciences, University of Illinois College of Medicine, Rockford, IL 61107.

Monte Carlo simulations of the counterion atmosphere of DNA using a newly devised potential function have been performed to investigate the effect of the structuring of individual water molecules on the three-dimensional distribution of these counterions. The calculations consider $Na^+$ ions carrying a 'soft' hydration shell that interact with each other and with a realistic model for DNA in a dielectric continuum. The potential function is an electrostatic plus Lennard-Jones potential fit to the results of ab initio quantum chemical calculations of the interaction of $Na^+$ with $H_2PO_4^-$ in the presence of four water molecules. This yields an interaction potential that has a minimum at a distance greater than that of a bare $Na^+$ ion but less than a fully hydrated $Na^+$. For the $Na^+$ - $Na^+$ interactions, fully hydrated ions are assumed.

The results of these calculations are compared with the results of previous three-dimensional Poisson-Boltzmann calculations on this system. Average local concentrations in the major and minor grooves and the forces generated by the ion atmosphere on the DNA atoms are presented.

**M-PM-A6**

## THEEORY OF MONOVALENT SALT EFFECTS ON THE HELIX-COIL TRANSITION OF DNA

**Angel E. Garcia and Dikeos Mario Soumpasis.**

T10 MS K710, Theoretical Biology and Biophysics, LANL, Los Alamos, New Mexico 87545 (USA).

We use the *Potential of Mean Force* framework [1] that has succesfully been applied to describe the stability and structural transitions of A, B and Z DNA in 1:1 electrolytes to calculate salt effects on the *helix-coil* transition of DNA.

It is found that this theory can account, for both , the *stabilization* of the helix state at lower salt concentrations, and its experimentally observed *destabilization* [2,3]at higher salt concentrations. Widely used idealized theories of polyelectrolytes such as the Counterion Condensation Theory and the Poisson Boltzmann approach do not describe the observed desstabilization at higher salt concentrations. The observed destabilization is due to both , many body hard core effects and screened Coulomb interactions.

1. D. M. Soumpasis, *Proc. Natl. Acad. Sci.(USA)*,**81**,5116(1984)
2. D. W. Gruenwedel, C-H Hsu, and D. S. Lu, *Biopolymers*,**10**,47(1971)
3. S. A. Kozyavkin, S. M. Mirkin, and B. R. Amirikyan, *J. Biomol. Struc. & Dyn.*,**5**,119(1987).

**M-PM-A7** ANOMALOUS CORRELATION BETWEEN ETHIDIUM BROMIDE LIGAND -- SUPERCOILED DNA LINEAR DICHROISM PROPERTIES. C. E. Swenberg, RSD, Armed Forces Radiobiology Research Institute, Bethesda, MD., S. E. Carberry*, and N. E. Geacintov+, Department of Chemistry, New York University, New York, N.Y.

We have used the flow linear dichroism method to study the influence of drug molecules and polycyclic aromatic mutagens and carcinogens on the degree of superhelicity of DNA. Here we report measurements of the linear dichroism spectra of ethidium bromide interacting with supercoiled ØX-174, SV40 and pBR322. DNA was dissolved in 5 mM Tris, 1 mM EDTA at pH 7.9 at a concentration of 75 μM (0.5 absorption units at 260 nm). In order to follow the conformational changes as a function of ethidium bromide (EtBr) concentration, DNA samples were repeatedly injected with aliquots of EtBr and the spectra were scanned from 240 nm to 595 nm at a speed of 120 nm/min after each injection. Spectra were recorded for $r_b$ (moles of EtBr bound / moles of DNA) between 0 and 0.16. It was shown earlier (Yoshida et al., 1987) that the magnitude of the linear dichroism signal at 260 nm reflects the hydrodynamic shapes of the DNA molecules as observed in sedimentation coefficient measurements. The linear dichroism signal at 520 nm due to bound ethidium was negative in sign, as expected for intercalative binding, and increased approximately linearly with increasing ethidium concentration in contrast to the biphasic response at 260 nm. The apparent contradiction in the linear dichroism signal at 260 nm and 520 nm are interpreted in terms of a two domain model of DNA conformation.

H. Yoshida, C. E. Swenberg, and N. E. Geacintov, Biochemistry 26: 1351, 1987.

+This work was supported in part by grants from NIH (CA20851) and DOE.

**M-PM-A8** MELTING TRANSITIONS OF DNA: AMINOTHIOL RADIOPROTECTANT COMPLEXES. S. A. Knizner*, E. A. Holwitt*, and C. E. Swenberg. Armed Forces Radiobiology Research Institute, Bethesda, MD.

Polyamines are aliphatic polycationic compounds endogenous to most cells. Polyamines are thought to play a significant role in the regulation of normal and malignant cell proliferation, and their concentrations vary during the cell cycle. Extensive experimental studies have shown that polyamines interact strongly with nucleic acids and have a variety of effects on both DNA synthesis and metabolism. The radioprotective drugs WR-2721 (S-2-(3-aminopropylamino) ethyl phosphorothioic acid) and its derivatives WR-1065 (2-(3-aminopropylamino) ethyl mercaptan) and WR-33278 (symmetrical dissulfide of WR-1065) have structures analagous to naturally occurring polyamines. These chemicals are non-intercalating and are presumed to bind to DNA by electrostatic interactions between the positively charged amino groups and negatively charged phosphate backbone of DNA. We report the melting transitions of calf thymus DNA, poly (dA-dT)•poly(dA-dT), and poly(dG-dC)•poly(dG-dC) in the presence of WR-2721, WR-1065 and WR-33278. All solutions (buffer 5mM $Na_2HPO_4$, pH7.2) were thoroughly saturated with $N_2$ and handled in a nitrogen atmosphere, to prevent the oxidation of the drugs. For these conditions, ratios of concentrations of WR-1065 to DNA-phosphate as high as 5:1 were obtainable, without precipitation of the complex. In the presence of $O_2$ precipitation, these complexes occurred at ratios of 1:1. The melting point (Tm) of these DNA-drug complexes increased linearly with increasing concentration of added drugs for ratios less than 2:1. At higher concentrations, no further increase was observed. The possible significance of these DNA-complex interactions for radioprotection will be discussed.

**M-PM-A9** STRUCTURE OF DNA HYDRATION SHELLS STUDIED BY RAMAN SPECTROSCOPY. N.J. Tao, S.M. Lindsay. Department of Physics, Arizona State University, Tempe, AZ 85287 and A. Rupprecht, Arrhenius Laboratory, University of Stockholm, S-106 Stockholm, Sweden.

We have used Raman scattering to study the water O-H stretching mode (~3450$cm^{-1}$) and the collective O-H stretch mode (~3220$cm^{-1}$) in DNA films as a function of relative humidity (r.h.). The intensity of the collective mode vanishes as the r.h. decreases from 98% to around 80%, which indicates that the hydrogen bond network of water is disrupted in the primary hydration shell which therefore cannot have an 'ice-like' structure. The number of water molecules in the primary hydration shell was determined from the intensity of the collective mode as about 30 water molecules per base pair. The O-H stretch mode persists at 0% r.h., implying that 5 to 6 tightly bound water molecules remain at 0% r.h. The frequency of the O-H stretch mode is lower by 30 to 45$cm^{-1}$ in the primary hydration shell. The water content v.s. r.h. obtained from these experiments agrees with gravimetric measurements. The disappearance of the collective mode, and the shift of the O-H stretch band, provide a more reliable definition of the primary shell than swelling experiments.

**M-PM-A10** DYNAMIC COUPLING BETWEEN DNA AND ITS PRIMARY HYDRATION SHELL STUDIED BY BRILLIOUN SCATTERING. S.M. Lindsay, N.J. Tao. Department of Physics, Arizona State University, Tempe, AZ 85287 and A. Rupprecht, Arrhenius Laboratory, University of Stockholm, S-106 Stockholm, Sweden.

We have studied the dispersion of Brillioun linewidths and shifts in DNA films as a function of their water content. The strength of the primary shell relaxation increases with water content until the primary shell is completed, thereafter remaining constant. The relaxation time remains essentially constant at about 40 pS for all water contents at room temperature. Thus viscous damping of vibrational modes is at a maximum at frequencies around 4 GHz at room temperature for a wide range of water contents. This relaxation may be due to Debye-like reorientation of the molecules in the primary shell, and there is some evidence of another loss maximum at very much higher frequencies ($10^{12}$ Hz) possibly associated with hydrogen-bond relaxation.

**M-PM-A11** LOW FREQUENCY RAMAN SPECTRA OF OLIGONUCLEOTIDE CRYSTALS, HOMOPOLYMER FIBERS AND HIGHLY CRYSTALLINE DNA FILMS. Qi Rui, T. Weidlich, G.D. Lewen, S.M. Lindsay, W.L. Peticolas*, G.A. Thomas*, and A. Rupprecht+. Dept. of Physics, Arizona State University, Tempe, AZ 85287, *Chem. Dept., University of Oregon, Eugene, OR 97403 and +Arrhenius Laboratory, University of Stockholm, S-106 Stockholm, Sweden.

Raman spectra of inhomogeneous DNA fibers and highly crystalline DNA films shown a rather small number of modes below 150 cm-1 (there are 3 Raman active modes in B-form DNA and 4 or 5 Raman active modes in A-form DNA). We have taken Raman spectra of two oligonucleotide crystals, the B-form dodecamer $d(CGCGAATTCGCG)_2$ and the A-form octamer $d(GGTATACC)_2$. Although the packing of DNA in these crystals is very different from the packing in films, the low frequency Raman spectra are very similar: the B-form spectra of films and crystals are nearly identical and in the A-form crystals, the 34 cm-1 mode of the fibers is replaced by a very low frequency mode at about 12 cm-1. From these results and additional spectra of homopolymers we are able to distinguish between intrahelical vibrations (i.e. they can occur on a single DNA molecule) and lattice vibrations, which depend strongly on the 3-dimensional arrangement of neighboring DNA molecules.

**M-PM-A12** HOMOGENEOUS AND INHOMOGENEOUS BROADENING IN LOW FREQUENCY RAMAN MODES OF DNA. T. Weidlich, S.M. Lindsay, A. Rupprecht*, W.L. Peticolas+ and G.A. Thomas+. Dept. of Physics, Arizona State University, Tempe, AZ 85287, *Arrhenius Laboratory, University of Stockholm, S-106 Stockholm, Sweden and +Chem. Dept., University of Oregon, Eugene, OR 97403.

The widths of Raman modes depend on two effects: homogeneous broadening (due to population lifetimes and dephasing processes) and inhomogeneous broadening (e.g. due to site specific interactions, anharmonicities, etc.). The widths of low frequency modes in DNA films and two oligonucleotide crystals ($d(CGCGAATTCGCG)_2$ and $d(GGTATACC)_2$) behave very similarly: they are rather broad (between 5 and 30cm-1 HWHM) and the width is approximately proportional to the phonon frequency. We have also studied the temperature dependence of the widths of these modes between 77K and 300K. Using all these results we were able to estimate the contributions of homogeneous and inhomogeneous broadening effects for the different modes.

**M-PM-B1** STRUCTURE AND FREE ENERGY OF COMPLEX THERMODYNAMIC SYSTEMS. Zhenqin Li and Harold A. Scheraga, Baker Laboratory of Chemistry, Cornell University, Ithaca, NY 14853-1301.

Biological systems are intrinsically complex, involving large degrees of freedom, heterogeneity, and strong interactions among components. For the simplest of biological systems, e.g., biomolecules, which obey the laws of thermodynamics, we may try to investigate them by means of a statistical mechanical approach. Even for these simplest many-body systems, assuming all microscopic interactions are completely known, current physical and chemical methods of characterizing the overall structure and free energy face the fundamental challenge of an exponential amount of computations as the number of degrees of freedom of these systems increases. As a response to this problem, two general procedures are developed to compute the structure (Monte Carlo-minimization method) and free energy (Monte Carlo recursion method) of a complex thermodynamic system. The Monte Carlo-minimization procedure has been applied to determine the structure of a pentapeptide Met-enkephalin, leading to a stable β-bend structure consistently, starting from random initial conformations. The Monte Carlo recursion method has been applied to a Lennard-Jones fluid, with results in agreement with previously published free energy values obtained from other procedures.

**M-PM-B2** **The Use of Coupled Molecular-Dynamics X-ray Structure Factor Refinement to Analyze the Charge State of Catalytically Important Residues**

Robert C. Davenport, Department of Biology, M.I.T. and Paul A. Bash, Harvard University

Triose phosphate isomerase is one of the most efficient and extensively studied enzymes known, yet its exact mechanism of catalysis is unknown. The reaction proceeds from DHAP to GAP through a kinetically significant intermediate of uncertain structure. The enzyme may stabilize this intermediate through protonation of the DHAP carbonyl and the intermediate is a cis-enediol, or the enzyme may stabilize the intermediate electrostatically, then the intermediate would be an enediolate. Central to this question is the protonation state of His-95, shown by X-ray crystallography positioned to interact with the catalytically important oxygens of the substrate. The side chain of this residue could act as an acid-base catalyst in the formation and decomposition of the enediol. However, these studies also suggest that the imidazole N-delta of His-95 is within hydrogen bonding distance of the amide N-H at the N-terminus of an alpha helix comprising residues 96 to 103. The unprotonated side chain of His-95 could act as a conduit of the helix dipole moment to stabilize an enediolate intermediate. Various methods have been utilized to determine the charge state of His-95 with ambiguous results. New protocols utilizing a combination of molecular dynamics calculations and X-ray structure-factor refinement (Brunger et al., Science, (1987), 235: 458-460) permit an experimental test of the protonation state of His-95; i.e. which protonation state(s) are compatible with both the X-ray data and the molecular-mechanics force fields. Results of this analysis applied to two different crystal forms of triose phosphate isomerase will be presented, with conclusions pertinent to the enzymatic mechanism. R.C.D is supported by the Jane Coffin Childs Memorial Fund.

**M-PM-B3** **A Combined Quantum Mechanical and Molecular Mechanical Technique for Studying Chemical Systems in the Condensed Phase**

M.J.Field, P.A.Bash and M.Karplus
Department of Chemistry,Harvard University, Cambridge, MA 02138.

We have developed a combined quantum mechanical (QM)/ molecular mechanical (MM) technique which we are using to investigate chemical reactions in the condensed phase. Traditional molecular mechanics methods are unsuitable for studying reactions as they do not have the appropriate form to describe the breaking and forming of bonds, whereas wholly quantum mechanical methods are too time consuming to use on systems that are more than, at most, a few tens of atoms in size. In our method we treat a small group of atoms with a semi-empirical (SE) or an *ab initio* (AB) Hartree-Fock molecular orbital approximation and represent the atoms making up their environment molecular mechanically. The MM atoms are modelled by a point charge inside a van der Waal's sphere. The QM/MM electrostatic interactions are accounted for by calculating QM nuclear / MM charge terms and by incorporating one-electron / MM charge integrals into the normal SCF procedure. Van der Waal's spheres can be put onto the QM atoms in which case QM/MM van der Waal's interactions are determined too. Regions in which there is bonding between QM and MM atoms are dealt with specially. The method is being carefully calibrated so that its reliability can be ascertained. Tests are being performed on a variety of systems using both the SE and AB QM Hamiltonians. In practice the SE approach is fast enough so that minimisations, molecular dynamics simulations and free energy perturbation calculations can be performed on a maximum of about 20 non-hydrogen atoms. The QM energy and forces are calculated at each step. AB point energy calculations or limited minimisations are used to check the accuracy of the SE results. We are using the QM/MM program particularly to investigate the mechanisms of certain enzyme reactions but it is also being applied to study simple organic reactions in solution and to determine pKas. Extensions to electron and proton transfer and light-activated processes in proteins and elsewhere are planned.

M-PM-B4

## A Quantum Molecular Dynamic Free Energy Perturbation Method Applied to Chemical Reactions in the Condensed Phase

Paul A. Bash, Martin J. Field, and Martin Karplus
Department of Chemistry, Harvard University, Cambridge, Massachusetts 02138

A semiempirical quantum mechanical method is combined with molecular mechanics to obtain a potential function for studying chemical reactions in condensed phase systems. Molecular dynamics simulations based on this potential function are implemented to perform thermodynamic perturbation calculations. The method is utilized to calculate the free energy activation barrier for an $S_N2$ reaction in solution. The results compare well with experiment and those from other theoretical treatments. This technique is also used to study the isomerization of dihydroxyacetone phosphate (DHAP) to glyceraldehyde phosphate (GAP) catalyzed by the enzyme triose phosphate isomerase (TIM). Plausible pathways for the reaction are determined starting from the 1.9 Å resolution x-ray crystal structure for TIM complexed with the inhibitor phosphoglycolohydroxamic acid (PGH) (Davinport et al.). Free energy profiles are calculated from these pathways and compared with experimental values (Knowles et al.). Calculations using a model with His-95 both singly and doubly protonated are carried out to investigate alternative mechanisms that result from the protonation state of this residue. P.A.B. is supported by the Damon Runyon - Walter Winchell Cancer Fund.

M-PM-B5 MOLECULAR DYNAMICS STUDIES OF T4 LYSOZYME MUTANTS. Dan Harris, Lawrence McIntosh, Larry Weaver, Terry Gray and Bruce Hudson, Institute of Molecular Biology and Department of Chemistry, University of Oregon, Eugene, OR 97403.

A comparison is presented of 300 ps molecular dynamics studies for wild type and mutant T4 lysozymes. Particularly important are the differences in the dynamics of the buried tryptophan W138 as determined by the nature of the amino acid environment proximate to W138. These results are compared with time resolved polarization data for these multitryptophan mutants as well as single trp cases. The data is collected on multiple time ranges and analyzed globally (G.R. Holton Biophys. J. 51, 286a (1987)). Use of global analysis facilitates a quantitatively accurate experimental determination of the average short time dynamics of W138 in these proteins. For the first time a fair comparison of experimental rotational correlation times due to fast internal motions with molecular dynamics studies of T4 lysozyme mutants is possible. Such detailed comparisons are essential to determination of the adequacy of existing potential functions in predicting biomolecular structure and function.

M-PM-B6 STRUCTURE-ACTIVITY OF RENIN INHIBITORS HAVING DIFFERENT $P_1$-$P_1'$ PSEUDODIPEPTIDE MODIFICATIONS: ANALYSIS OF LIGAND-ENZYME INTERACTIONS BY COMPUTER-ASSISTED MOLECULAR MODELING. Tomi K. Sawyer$^{\delta*}$, Boryeu Mao$^{\ddagger}$, Linda L. Maggiora$^{\delta}$, Douglas J. Staples$^{\delta}$, Anne E. deVaux$^{\delta}$, John H. Kinner$^{\delta}$ Clark W. Smith$^{\delta}$ and Donald T. Pals$^{\dagger}$ ($^{\delta}$Biopolymer Chemistry, $^{\dagger}$Cardiovascular Diseases Research and $^{\ddagger}$Computational Chemistry Units, The Upjohn Company, Kalamazoo, MI, USA 49001).

Based on the angiotensinogen$_{6\text{-}11}$ sequence (His-Pro-Phe-His-Leu-Val), chemical modifications of the $P_1$-$P_1'$ Leu$^{10}$-Val$^{11}$ were examined in a series of substrate-based inhibitors of human renin. Noteworthy was the hexapeptide, Ac-Ftr-Pro-Phe-His-Phe$\psi$[$CH_2NH$]Phe-$NH_2$, which was a highly potent ($IC_{50} < 10^{-9}$ M, human plasma renin) inhibitor and provided a useful template to compare the effects of other $P_1$-$P_1'$ substitutions (*e.g.*, Leu$\psi$($CH_2NH$)Val, Leu$\psi$(CH[OH]$CH_2$)Val and Sta) as well as $P_5$-$P_4$ modifications. Molecular modeling of selected $P_1$-$P_1'$ Phe$\psi$[$CH_2NH$]Phe substituted inhibitors was performed to identify and characterize potential inhibitor·enzyme intermolecular interactions. These data are compared to a recently determined 1.8Å resolution x-ray crystallographic structure of H-D-His-Pro-Phe-His-Phe$\psi$[$CH_2NH$]Phe-Val-Tyr-OH bound to the active site of the aspartyl protease, rhizopus chinensis. The scope and limitations of this structure-conformation-activity strategy will be discussed.

**M-PM-B7** MOLECULAR DYNAMICS STUDIES OF METHIONINE CRYSTALS. Dan Harris, E.V. Curto and Bruce Hudson, L. Mayne. Dept. of Chemistry and Inst. of Molecular Biology, Eugene, Oregon, 97403

T4 lysozyme is an excellent subject for the evaluation of molecular dynamics simulations. This 164 residue protein contains 5 methionines. We are conducting fluorescence and computational studies with the purpose of accessing the reliability of existing amino acid potential functions. To augment this we are initiating a program of small molecule spectroscopic/simulation studies.

Crystal structures of l-methionine have been determined as a function of temperature from -20°C to 75°C by Curto et al. The sidechain dynamics of crystalline L-(3,3-$^2H_2$) methionine have been studied by deuterium quadrupolar nmr by Torchia and coworkers. There is a large degree of torsional flexibility for this amino acid even in the crystalline state. Above 0°C as determined by both nmr and crystallographic studies at least two distinct molecular conformations exist in the methionine unit cell. The values of the generalized order parameters of the A and B molecule sidechains decrease from unity at -35°C to 0.69 and 0.25 at 106°C. Using a two-site jump model Torshia and coworkers have found that for the A and B molecules, respectively, the reorientational correlation times decrease from 0.45 to 0.019 ns and from 4.2 to 0.049 ns in the -19°C to 77°C temperature range.

Molecular dynamics studies of crystalline l-methionine have been conducted as a function of temperature. The time average crystal structures, the calculated generalized order parameters and the reorientational correlation times are compared with the above experimental studies. We will discuss the adequacy of the existing methionine potential function in CHARMM.

**M-PM-B8 ROLE OF ELECTROSTATICS IN THE T->R STRUCTURAL TRANSITION OF *E. COLI* ASPARTATE TRANSCARBAMOYLASE.** M. Glackin and N. Allewell, Wesleyan University, Middletown, CT 06457; J. B. Matthew, du Pont Experimental Station, Wilmington, DE 19898.

Aspartate transcarbamoylase undergoes a large change in tertiary and quaternary structure when the bisubstrate analog PALA binds {Krause *et al.*, J. Mol. Biol. 193, 527 (1987)}. This conformational change is thought to play a major role in the allosteric mechanism. We have used modified Tanford-Kirkwood theory {Matthew *et al.*, Biochemistry 18, 1919 (1979)} to compare the electrostatic properties of the unliganded and liganded structures. Although the results are quantitatively sensitive to the charge distribution on PALA, the calculations indicate that, in the pH range 6-8, the difference in the electrostatic component of the free energy of stabilization of the liganded and unliganded structures is approximately -50 kcal, of which ~ -30 kcal is due to interactions involving PALA. The pK values of virtually every ionizable residue differ between the two structures. The largest shifts (more than 2 pH units) are those of Arg 54, Lys 84, and Arg 105 at the active site. The pK values of Asp 19, Lys 56 and Asp 87 in the r chain decrease by 1.7, 1.7 and 2.5 pH units, respectively. The groups whose charges change most at pH 8 are His 147 of the r chain, His 170, His 212, His 265, and the N-terminal amino group, all in the c chain. The changes in charge are -0.3, 0.4, 0.6, 0.3 and -0.2 esu, respectively. Since many of the groups whose charges and pK values change are several angstroms from the active site, these results suggest that electrostatic interactions may transmit information between active sites and to the nucleotide binding sites. Supported by NIH grant AM-17335.

**M-PM-B9** THEORY OF RELAXATION OF MOBILE WATER PROTONS INDUCED BY PROTEIN NH MOIETIES, WITH APPLICATION TO HEART MUSCLE AND LENS HOMOGENATES
Seymour H. Koenig, IBM T. J. Watson Research Center, Yorktown Heights, NY 10598

Beaulieu et al. (Soc. Magn. Reson. Med., Sixth Ann. Mtg., 1987) reported structured peaks in the magnetic field-dependent relaxation rate ($1/T_1$) of the water protons of calf eye lens homogenates, essentially concentrated protein (crystallin) solutions. The peaks, in the range 0.5-5 MHz proton Larmor frequency, could be decomposed into a pair of triplets and the intrinsic linewidths determined. Less resolved peaks were first reported by Kimmich et al. (cf. Winter, F. and Kimmich, R., Biochim. Biophys. Acta 1984, *719*:292-298) in muscle tissue, cells, and dehydrated protein, and more recently by Koenig et al. in rat heart (Invest. Radiol. 1984, *19*:76-81). Kimmich et al. argued that the peaks arise from cross relaxation between proton Zeeman levels and $^{14}N$ quadrupolar splittings of protein NH groups. The results of Beaulieu et al. are the first reported for protein solutions, though the peaks are most apparent when the crystallin concentration is above a critical density associated with ordering that contributes to lens transparency. Here, we analyze the data for lens homogenate and heart, and suggest a pathway for cross relaxation to which we apply the theory of relaxation quantitatively: when the Zeeman energy of the NH protons matches an $^{14}N$ quadrupolar splitting, NH protons cross relax to the $^{14}N$ nuclei, which transfer excess energy to the protein "lattice." The correlation time for the cross relaxation is $T_2$ of the $^{14}N$ nuclei, $\sim 10^{-6}$ s, faster than $T_1$ of the NH protons, $\sim 10^{-3}$ s. At these level crossings, NH protons become relaxation sinks for protons of rapidly exchanging ($\sim 3 \times 10^9\ s^{-1}$) solvent water molecules hydrogen bonded to the same backbone carbonyl oxygens as the NH protons. The hydrogen bond lifetime ($\sim 3 \times 10^{-10}$ s) is the correlation time for the water proton-NH proton interaction and, though short, is much longer than that in pure water ($\sim 5 \times 10^{-12}$ s); the enhanced interaction results in dramatic peaks in $1/T_1$ of solvent protons. The precise data of Beaulieu et al., combined with a quantitative theory and the fact that the magnitude of the $^{14}N$ peaks is very sensitive to protein concentration, allow—at least for lens proteins—a study of protein-protein interactions and ordering, difficult to investigate by other methods.

**M-PM-B10** CONFORMATIONAL STUDIES OF α-MSH AND THE SUPERPOTENT ANALOGUE [Nle$^4$, D-PHe$^7$]α-MSH

Fahad Al-Obeidi, Lung-Fa Kao, and Victor J. Hruby, Department of Chemistry, University of Arizona, Tucson, Arizona 85721 U.S.A.

α-MSH, a tridecapeptide (Ac-Ser-Tyr-Ser-Met-Glu-His-Phe-Arg-Trp-Gly-Lys-Pro-Val-$NH_2$) is one of the major peptides secreted by the pituitary gland of vertebrates, birds and mammals. α-MSH has many important physiological and morphological functions in biological systems including skin and hair coloration, CNS effects on learning and behavior, etc. Based on conformational considerations and structure-biological activity studies we have developed a number of super potent, super prolonged acting α-melanotropin analogues including [Nle$^4$, D-Phe$^7$]α-MSH. Using a number of interrelated biophysical methods including 1D and 2D NMR, CD spectroscopy, molecular mechanics energy minimization calculations, and molecular dynamics simulations in conjunction with classical structure-biological activity studies, the accessible molecular conformations of α-MSH have been explored and evaluated with respect to its dynamic properties. The theoretical and experimental studies have produced several interesting conformers which can be correlated very well with the results from the structure-biological activity studies. Descriptions of the conformations, including the spatial arrangements of different side chain groups in relation to backbone conformations of α-MSH will be described, and their relationships to known biological activities will be presented. The use of these data in designing new agonist or antagonist analogues for this peptide hormone and the biological activities of these new analogues will be discussed. A new class of potent and prolonged acting agonist analogues have been discovered by this itnerdisciplinary approach.

**M-PM-B11** A Study of the Conformation of the Zn(II) Complex of Bleomycin Using Nuclear Overhauser Effects and Distance Geometry Calculations.

Ian J. McLennan*, Michael P.Gamcsik*,Jerry D.Glickson*,and Ad Bax#

* NMR Research, Department of Radiology Johns Hopkins School of Medicine, Baltimore MD 21205 #National Institutes of Health Bldg #2 Bethesda MD

Bleomycin is a glycopeptide (Mol Wt. 1400) that has been found to be an effective antitumor agent for a variety of soft tumors including testicular carcinoma. We have investigated the conformation of the Zn(II) complex of bleomycin in solution using 2D nuclear Overhauser enhancements (NOE) in the rotating frame. The advantage of performing the NOE experiments in the rotating frame is that the intensity of the NOE is not dependent on the nuclear Larmor frequency ($(\omega_L \cdot \tau_C \approx 1)$ for Zn(II) bleomycin at 8.5T to 11T). A series of 2D NOE experiments were performed in which the spin-locking time was varied from 70ms to 110ms. Based on the results of these experiments,quantitative NOE's were obtained which corresponded to 120 distances in the Zn(II) bleomycin complex. In addition to the NOE experiments, the conformation of the Zn(II)-bleomycin complex was further constrained with the identification of five of the six possible coordination sites of the Zn(II) atom (based on natural abundance $^{15}N$ NMR experiments).A series of conformations, consistent with the above information was generated using a distance geometry program that is based on the work of Crippen and Kuntz. The study has implications regarding the nature of the binding of metal comlexes of bleomycin to DNA.

**M-PM-B12** **ELUCIDATION OF INTERMEDIATE AND SLOW PROTEIN ROTATIONAL MOTIONS IN BOVINE LENS HOMOGENATES BY C-13 NMR SPECTROSCOPY.** C.F. Morgan, T. Schleich, R.L. Haner, G.H. Caines, and P.N. Farnsworth* (Intr. by A.L. Fink), Dept. of Chemistry, Univ. of California, Santa Cruz, CA 95064 and *Dept. of Physiology, New Jersey Medical School, Newark, NJ 07103.

Two NMR techniques have been employed for the study of intermediate ($\tau_c$ range of 1000 to 1 nsec) and slow ($\tau_c$ > 0.1 nsec) protein rotational molecular motion time scales in calf lens homogenates: $^{13}C$ off-resonance rotating frame spin-lattice relaxation and the solid state double resonance NMR techniques of dipolar decoupling and cross polarization (CP). The peptide bond carbonyl spectral intensity ratio dispersion of the lens proteins present in a cortical homogenate at 35° and 1° C indicates the presence of a polydisperse "mobile" protein fraction with mean $\tau_c$ values of 28 and 46 nsec, respectively. Comparison of proton dipolar decoupled and un-decoupled $^{13}C$ NMR spectra of the cortical homogenate lens proteins indicate the absence of significant contributions from slowly tumbling protein environments. This interpretation was confirmed by the failure to detect significant lens protein $^{13}C$-$^{1}H$ cross polarization in cortical homogenates. For nuclear homogenates the spectral intensity ratios for the carbonyl resonance of a nuclear homogenate gave mean $\tau_c$ values of 47 and 40 nsec at 35° and 1° C, respectively. In contrast to the behavior observed for the cortical homogenate, lowering the temperature to 1° C, a temperature which supports the cold cataract, results in an overall decrease in $\tau_c$. The presence of a solid-like protein fraction was established by dipolar decoupling and CP. These studies establish the presence of both a mobile and a solid-like protein phase in calf lens nuclear homogenates, whereas for the cortical homogenate the predominant protein phase is mobile. (Supported by NIH)

**M-PM-B13 PROTEIN ROTATIONAL DIFFUSION BY C-13 OFF-RESONANCE ROTATING FRAME SPIN-LATTICE RELAXATION: EFFECT OF POLYDISPERSITY AND ANISOTROPIC TUMBLING.** T. Schleich, C.F. Morgan, G.H. Caines, R.L. Haner, and D. Michael, Dept. of Chemistry, Univ. of California, Santa Cruz, CA 95064.

The original formalism of the $^{13}C$ off-resonance rotating frame spin-lattice relaxation experiment for the evaluation of protein rotational correlation times was limited to the case of random isotropic rotation of a monodisperse protein population. We have extended the formalism to include polydispersity and anisotropic particle tumbling. The dependence of the spectral intensity ratio ($R = T_{1\rho}(off)/T_1$) for a given resonance on the precessional frequency of the nuclear spins about the effective field in an off-resonance dispersion experiment (at fixed $B_1$) was calculated. For isotropic tumbling each peptide bond carbonyl of the ith residue is equivalent to all other residues in terms of its contribution to the resonance intensity, assuming identical local peptide bond geometries and principal values of the peptide bond chemical shift tensor. By contrast, for an anisotropic tumbling particle of a given axial ratio, each carbonyl carbon contributes to the resonance intensity in a way which is explicitly dependent on the orientation of the CSA principal axis system (defined by the Euler angles $\beta$ and $\gamma$) and the C-H internuclear vector angle with the long axis of the anisotropic particle. These angles are calculated for each peptide carbonyl from X-ray crystal data. The effects of polydispersity on the spectral intensity ratio is incorporated by considering the weight fraction of each protein species j. Application is made to lysozyme, BSA, lysozyme-BSA mixtures, the alkaline pH induced association of lysozyme, and to the phase separation of lysozyme salt water mixtures induced by low temperature, which has been used to model the "cold cataract" occurring in juvenile mammalian lenses. (Supported by NIH)

**M-PM-C1** CHANNELS INCORPORATED INTO PLANAR LIPID BILAYER MEMBRANES (BLM) FROM HPLC PURIFIED MIP 26 OR FROM MEMBRANE FRAGMENTS ENRICHED FOR LENS FIBER JUNCTIONS ARE NEARLY IDENTICAL. G.R. Ehring[1], G.A. Zamphigi[2], J. Horwitz[3], D. Bok[3] and J.E. Hall[1]. [1]Dept. of Physiology and Biophysics, UCI, 92717. [2]Dept. of Anatomy and [3]Jules Stein Eye Institute, UCLA 90024.

Urea extracted lens fiber membrane fragments are enriched for lens junctional membrane. SDS-PAGE analysis indicates that the predominant protein in this extract is MIP26. Octyl-beta-D-glucopyranoside (OG) solubilized membrane fragments (OG-MEMB) were reconstituted into phosphatidylcholine (PC) vesicles. Addition of these vesicles to phosphatidylethanolamine-squalane BLMs resulted in the incorporation of voltage-dependent channels. We have previously proposed that these channels were due to MIP 26. To test this hypothesis, we further purified urea-extracted lens-fiber membrane fragments using HPLC with a Toyosoda TSK 3000SW column. This procedure yielded monomeric MIP 26 (HPLC-MIP), which was reconstituted into PC vesicles and added to BLMs as before. In 1.0 M KCl, pH 5.8, the channels induced by the HPLC-MIP had a similar voltage-dependence to those previously reported. These channels were fully open at voltages less than 20 mV and closed to a minimum conductance state with increasing voltages. Boltzman fits to GV curves gave that $G_{min}/G_{max}$ was 0.49 ± .09, that apparent gating charge was 2.61 ± .57 e and that the voltage where half the channels closed was 57 ± 9 mV (mean±s.d., n=14). The step conductance for HPLC-MIP induced channels was nominally 2.0 nS closely agreeing our previous measurements. In contrast to the OG-MEMB-induced channels, the HPLC-MIP channels could be readily incorporated in 1.0 M KCl, pH 7.2. There was no significant effect of pH on the gating properties of these channels. Supported by NIH grants EY05561 and EY04110.

**M-PM-C2** SEROTONIN MODULATES $K^+$ CHANNELS ON LYMPHOCYTES THROUGH TWO DISTINCT RECEPTOR TRANSDUCTION SYTEMS. D.CHOQUET & H.KORN, Lab. de Neurobiologie Cellulaire, INSERM U261, Institut Pasteur, 25 rue du Dr. Roux, 75724 PARIS CEDEX 15, FRANCE.

Despite a large body of data relative to modulation of immune functions by neuro-transmitters and hormones, there is little evidence that these substances act on specific and defined targets. We have used the whole-cell patch-clamp technique to investigate the action of serotonin (5-HT) on the 18-81 pre-B cell line, where the presence of voltage-dependent $K^+$ channels has previously been described (see Choquet et al., Science, 1987, 235: 1211). Perfusion of the bathing medium with 5-HT (1-20 µM) induces in 1-2 minutes two different effects on the same $K^+$ current: a transient (2-5 minutes) increase of the peak current elicited by depolarizing pulses (46%±29, n=32), and a nearly irreversible increase in the rate at which it inactivates (28%±20, n=14), the latter developing more slowly than the former. The relative magnitudes of these two effects varied from cell to cell, and could be pharmacologically dissected. i) The 5-HT induced increase of the peak current was fully blocked by methiotepin (1 µM) and by metergoline (1 µM) ($5HT_{1-2}$ antagonists). But the $5\text{-}HT_2$ receptor antagonist ketanserin (10 µM) had no effect. These data suggest that this first effect is mediated through $5\text{-}HT_1$ receptors. ii) The enhanced inactivation was blocked by the $5\text{-}HT_3$ receptor antagonists ICS205-930 (10-20 µM) and MDL7222 (20-100 µM). Furthermore, we found evidences that elevation of intracellular cGMP could be implicated in the increase of the peak current. Other transmitters, namely histamine and substance P, also affect lymphocytes through modulation of their $K^+$ conductance.

**M-PM-C3** ASYMMETRY OF GAP JUNCTION FORMATION IN *XENOPUS* OOCYTES ALONG THE ANIMAL-VEGETAL AXIS. E. Levine, R. Werner, G. Dahl, Depts. of Physiology and Biophysics and of Biochemistry, University of Miami, FLorida 33101.

Expression of functional cell-cell channels can be obtained in pairs of oocytes by injection of an *in vitro* transcript of rat liver gap junction cDNA (Dahl et al., Science 1987). When gap junction-specific mRNA is injected into paired oocytes, junctional conductance becomes detectable after about 6 hrs and increases with time. However, if pairing of oocytes is delayed by 18-42 hrs after mRNA injection, junctional conductance appears more rapidly and increases with a steeper slope, indicating that single oocytes can accumulate a pool of junctional precursors. Surprisingly, the formation of cell-cell channels from this pool is highly asymmetric. Junctions are preferentially formed in oocyte pairs with the vegetal poles facing each other. In contrast, oocytes paired before mRNA injection show little or no such asymmetry. The animal-vegetal pole asymmetry therefore appears to be restricted to the formation of junctions from an existing pool of precursors. Localization or translocation of the mRNA, and involvement of cytoskeletal elements are unlikely to be solely responsible for the asymmetry. The asymmetry, however, was found to be dependent on the membrane potential of the oocytes during the preincubation (before pairing). Furthermore it is effected by externally applied electric fields. We propose the hypothesis that gap junction precursors are translocated by an electric field. Such a field has been shown to be present along the animal-vegetal axis in *Xenopus* oocytes (Robinson, PNAS 1979). A translocation mechanism of this kind may play a role in placing gap junctions at strategic points in organized tissues and in the developing embryo. Supported by NSF (grant DCB-8605510)

M-PM-C4 FURA-2 FLUORESCENCE REVEALS THAT INTERCELLULAR COMMUNICATION ELEVATES INTRACELLULAR CALCIUM IN TRACHEAL CILIATED CELLS. Michael J. Sanderson and Ellen R. Dirksen, Department of Anatomy, UCLA School of Medicine, University of California, Los Angeles, CA, 90024.

Rabbit tracheal ciliated cells, grown in culture, responded to mechanical deformation of their cell surface by displaying a rapid, transient increase in ciliary beat frequency (PNAS 83; 7302, 1986). This response was not restricted to the stimulated cell but was communicated to adjacent cells in all directions. The display of a frequency response by a neighboring cell occurred after a lag-time that was proportional to the distance of the cell from the stimulated cell (Am. J. Physiol. 1987, in press). We have recently discovered, by examining changes in Fura-2 fluorescence, that the frequency response in both the stimulated cell and the communicating cells was associated with an elevation of intracellular calcium. Non-ciliated cells also showed similar calcium changes. Digital video microscopy and epi-illumination (at 340 or 380 nM) were used to observe Fura-2 fluorescence (above 495 nM) within the cells. When observed at 380 nM, mechanical stimulation of a cell resulted in a specific reduction in fluorescence of the individual cell. Subsequently, a loss of fluorescence occurred in the neighboring cells in all directions, again, with a lag-time that was proportional to the distance of the cell from the stimulated cell. The time course of the spreading reduction in fluorescence and the communication of the frequency response between cells were similar. At 340 nM, similar spatial changes in fluorescence were observed in response to mechanical stimulation but instead of fluorescence reductions, fluorescence increases were observed. These results are consistent with the view that an elevation of intracellular calcium occurs during intercellular communication.

M-PM-C5 MEASUREMENT OF INTRACELLULAR pH IN THE FROG LENS AND ITS EFFECT ON INTERCELLULAR COMMUNICATION. R.T. Mathias, G. Riquelme and J.L. Rae*. Department of Physiology and Biophysics, SUNY at Stony Brook, N.Y. 11794; *Mayo Clinic, Rochester, MN. 55905.

The cells of the lens are electrically interconnected by low resistance gap junctions. These junctions allow the anterior epithelial cells to provide much of the transport needed by the fiber cells in order to maintain a constant intracellular volume and remain transparent. Thus, gap junctions are essential to the physiology of the lens and we have been studying factors which regulate the conductance of these junctions. Outer cortical fiber cell junctions will reversibly uncouple in response to changes in bath pH, however, this uncoupling does not extend to fiber cells located in the inner cortex. We have used ion sensitive, intracellular microelectrodes (liquid hydrogen ion exchange resin, WPI Instruments) to monitor the intracellular pH at various locations and under various conditions. In normal Ringer (pH = 7.4), the outer cortical pH is $7.0\pm.2$ and the effective intracellular resistivity, $R_i$, (a parameter proportional to junctional resistance) is about 3.5KΩcm, whereas the inner cortical pH is $6.8\pm.2$ and $R_i$ = 9KΩcm. When the bath is bubbled with 100% $CO_2$, the outer cortical pH falls to $6.2\pm.3$ and $R_i$ increases about 50 fold. Under the same conditions, the inner cortical pH falls to $6.5\pm.2$ and to the resolution of our measurement, $R_i$ does not change.

For electrochemical equilibrium, the normal intracellular pH would have to be about 6, so hydrogen ions are evidently transported out of the lens. The radial gradient in pH suggests that transport is carried out by epithelial or surface fiber cells. The lack of uncoupling of inner fiber cells in a low pH environment suggests that fiber cell junctions lose their pH sensitivity as a function of radial location, differentiation or age.

Supported by NIH grants EY06391, EY03282 and EY06005.

M-PM-C6 CONDUCTANCE OF GAP JUNCTIONS IN DROSPLILA SALIVARY GLANDS DEPENDS ON BOTH TRANSJUNCTIONAL AND INSIDE-OUTSIDE VOLTAGES. V.K. Verselis, T.A. Bargiello*, D.C. Spray and M.V.L. Bennett (Intr. by B.A. Wittenberg) Albert Einstein College of Medicine, Bronx, NY 10461 and Rockefeller University*, N.Y., NY 10021.

Gap junction channels, which span the apposed membranes of the coupled cells and the intervening gap, present two possibilities for voltage gating, one dependent on transjunctional voltage ($V_j$) and the other on voltage between the cytoplasm and the extracellular space of the gap ($V_{i-o}$). Gap junctions between salivary gland cells of Drosophila are sensitive to both these voltages. With both cells held at the same potential, i.e. with $V_j$=0 junctional conductance, $g_j$, is greater for more negative $V_{i-o}$. The $g_j$-$V_{i-o}$ relation is sigmoid, reaching a maximum plateau at large negative potentials (> -40 mV) and approaching 0 near $V_{i-o}$ = 0. The $V_{i-o}$ sensitivity is fit by a Boltzmann relation for 3 charges moving down the entire voltage gradient and is comparable to that in Chironomus (Obaid et al., J. Memb. Biol. 73: 69, 1983). When the potential of one cell ($V_1$) is fixed and the potential of the other ($V_2$) varied, a non-zero $V_j$ is established and $V_{i-o}$ for the 2nd cell is changed. Moderate hyperpolarization of cell 2 increases $g_j$ less than predicted for two independent series gates, one in each cell membrane controlled by $V_{i-o}$ for that cell. Further hyperpolarization decreases $g_j$ consistent with channel closure by $V_j$. The kinetics of changes induced by large $V_j$ are faster than those induced by large $V_{i-o}$. Thus, junctional currents ($I_j$) generated by large steps to one cell consist of two phases. The early phases are symmetric for the two voltage polarities, but the later phases are in the opposite directions. Thus for both hyperpolarization and depolarization of one cell, the magnitude of $I_j$ decreases initially due to closure by $V_j$. For depolarization $I_j$ continues to decline slowly whereas for hyperpolarization $I_j$ slowly increases after the initial decrease. The data are consistent with paired voltage sensors for channel closure that are located where they are affected by both $V_j$ and $V_{i-o}$.

**M-PM-C7** GAP JUNCTIONS BETWEEN SQUID BLASTOMERES: VOLTAGE DEPENDENCE PRODUCED DURING UNCOUPLING BY OCTANOL IS SIMILAR TO THAT DURING CYTOPLASMIC ACIDIFICATION. M.V.L. Bennett*, J.C. Saez* and K. Graubard**. Marine Biological Laboratory, Woods Hole, MA 02543, Albert Einstein Col. Med.*, Bronx, NY 10461, and U. Washington**, Seattle, WA 98195.

Although octanol at mM levels decreases conductance of many gap junctions, its mode of action is obscure. Data presented here further characterize its effects. We studied squid blastomeres in cleavage stage embryos which are joined by gap junctions and are closely coupled electrically as previously shown in isolated pairs. Junctional conductance, $g_j$, is reduced to low levels by cytoplasmic acidification and then can exhibit voltage dependence (Biophys. J. 45: 219-230, 1984; pp. 109-133 in Synaptic Function, eds: G.M. Edelman et al., 1987). Octanol also decreases $g_j$ and a similar voltage dependence can be detected. When reduced by octanol (c. 1mM) $g_j$ depends on both inside-outside and transjunctional voltage, $V_{i-o}$ and $V_j$. Generally: 1) Equal depolarization of both cells decreases $g_j$ and equal hyperpolarization increases $g_j$, although $V_j$ is zero. 2) Hyperpolarization of either cell so that $V_j$ is non-zero increases $g_j$ to a greater extent than when the same hyperpolarization is applied to both cells; this observation demonstrates a contribution of $V_j$ to the increase. 3) Depolarization of either cell increases $g_j$ but to a lesser extent than equal hyperpolarization of either cell; evidently the effect of $V_j$ is opposed by the more positive level of $V_{i-o}$. 4) To a variable degree the voltage dependence is asymmetrical in that $V_j$ of one polarity is more effective than the other. 5) $g_j$ may increase many fold but to only a small fraction of pre-octanol $g_j$. 6) $g_j$ changes are slow and require seconds. The data are consistent with there being two gates in series in each channel, each gate with both $V_j$ and $V_{i-o}$ sensitivity. Decrease in $g_j$ by octanol often showed some sensitization during successive applications, which prevented careful determination of a dose response curve. At higher concentrations voltage dependence appears and then disappears after $g_j$ is completely blocked; voltage dependence then transiently reappears during recovery on washing. Octanol decreases $g_j$ in the absence of external divalent cations and $Na^+$. Uncoupling is not reversed by 10 mM $NH_4Cl$ implying that it is not a pH effect. The similarity of voltage dependence caused by octanol and by cytoplasmic acidification indicates that in squid blastomeres these two apparently disparate agents ultimately act on a common gating mechanism.

**M-PM-C8** PROPERTIES OF GAP JUNCTIONS BETWEEN PAIRS OF PANCREATIC BETA CELLS OF MICE. E. Martha Perez-Armendariz, D.C. Spray, and M.V.L. Bennett, Albert Einstein College of Medicine, Bronx, NY 10461

Dye and electrical coupling and gap junctions have been demonstrated between beta cells of isolated islets of Langerhans. Furthermore there is evidence for increase in coupling by treatment with compounds which enhance insulin secretion. The small size of beta cells has made it difficult to determine the biophysical characteristics of the junctions, and the mechanisms of modulation of junction conductance remain unknown. We have developed an experimental system that allows direct measurement of junctional properties. Pairs of beta cells cultured for 6 hrs in the presence of 16mM glucose were voltage clamped independently by patch clamp pipettes in the whole cell recording mode. The pipette solutions contained either 135mM KCl or 135mM CsCl and 0.5mM $CaCl_2$, 2mM MgCl, 5.5mM EGTA, 5.0mM Hepes, and 3mM Mg-ATP. The external solution contained 135 mM NaCl,5 mM KCl, 5 mM $CaCl_2$, 5mM $NaHCO_3$, 10 mM Hepes and 16mM Glucose. To monitor junctional current the voltage in each cell was held at 0 mV or -60 mV and voltage steps of both polarities were applied alternately in both cells. Also I-V curves were obtained by application of slow voltage ramps. Cell input resistances were several gigaohms. With KCl in the pipettes outward rectification was observed which was associated with a large increase in noise, presumably due to single K channel events. Cells recorded from with CsCl filled pipettes were electrically linear with much less current noise. 8 of 17 pairs of cells were electrically coupled. The junctional conductance was 230 + 89 pS (mean + SD) which was constant over a range of at least + 45mV. No indication of single channel currents was obtained although the mean conductances would be provided by only a few channels of the size previously reported for gap junctions. The beta cell channels may be of lower conductance. Alternatively the channels are of the same size, but do not open and close under the recording conditions. If gap junctions typical of intact tissue are retained in the isolated pairs and their single channel conductance is large, most channels are closed. Experiments involving uncoupling treatments should clarify this issue.

**M-PM-C9**

**INOSITOL PHOSPHATE GENERATION DURING ACTIVATION OF THE HUMAN T-CELL LINE, JURKAT.** **Kamlesh Asotra and K. George Chandy*. Department of Physiology, University of California, Los Angeles, CA 90024 and *Deartment of Medicine, Division of Basic and Clinical Immunology, University of California, Irvine, CA 92717.**

**Using anion-exchange high performance liquid chromatography (HPLC) we have studied the activation of phosphoinositide metabolism in myo-[$^3$H]-inositol labeled human T-cell line, Jurkat. We first tested the effect of two monoclonal antibodies (mAbs, OKT3 and 9.3) which induce T-cell activation by different mechanisms and, in combination, synergize to induce interleukin-2. Three inositol phosphates namely inositol 1-phosphate ($InsP_1$), inositol 1,4-bisphosphate ($InsP_2$) and inositol 1,4,5-trisphosphate ($InsP_3$) extracted from Jurkats after various treatments were separated with a uBondapak $NH_2$ HPLC column isocratically with 60 mM ammonium acetate, pH 4 for the initial 20 min and then by applying a linear gradient between 60 mM and 2 M ammonium actetate, pH 4 over the next 100 min. Anti-CD3 mAb (OKT3) which activates via T-cell receptor complex, induced a transient 270% increase in $InsP_3$ levels at 2 min which decreased to become 35% more than the resting levels at 12 min. OKT3 increased $InsP_2$ and $InsP_1$ by 53-fold and 21-fold, respectively, compared with the resting cells. Anti-Tp 44 mAb (9.3) which activated via T-cell receptor-independent manner, produced only 220% increase in $InsP_3$ but 160% and 5% increase in $InsP_2$ and $InsP_1$, respectively. We also tested the effects of high external $K^+$ (160 mM), quinine (500 µM), verapamil (100 µM) and 4-aminopyridine (10 mM) all of which depolarize the T-cell membranes. High external $K^+$, quinine and verapamil increased $InsP_3$ levels by themselves. Quinine or verapamil potentiated the OKT3-induced inositol phosphate generation. In contrast, 4-aminopyridine reduced OKT3-induced production of inositol phosphates. The reason for the differences in effect of these depolarizing agents is unclear. In conclusion, membrane depolarization may contribute to the generation of inositol phosphates during T-cell activation.** **We thank Dr. Julio Vergara for the use of HPLC system and advice.**

**M-PM-C10** **CALCIOSOME, A CYTOPLASMIC ORGANELLE: THE INOSITOL 1,4,5-TRISPHOSPATE ($InsP_3$) SENSITIVE $Ca^{2+}$ STORE OF NON MUSCLE CELLS?** P. VOLPE, K.-H. KRAUSE, S. HASHIMOTO, F. ZORZATO, T. POZZAN, J. MELDOLESI and D. LEW (introduced by L.A. Sordahl). *Institute of General Pathology, University of Padova, Italy, Department of Pharmacology, University of Milano, Italy, Infectious Diseases Unit, University Hospital, Geneve, Switzerland.*

In non muscle cells the organelle specifically devoted to the uptake of $Ca^{2+}$ and to its release in response to receptor-triggered generation of $InsP_3$ has been suggested to correspond to the endoplasmic reticulum (ER). Subcellular fractionation of HL60 (human leukemia) cells revealed, however, that the markers of the $InsP_3$-sensitive $Ca^{2+}$ store can be dissociated from the markers of the ER and of other known cytoplasmic organelles, but remain associated with the distribution of a protein similar to calsequestrin (CS), the high capacity moderate affinity $Ca^{2+}$ binding protein contained within the lumen of muscle sarcoplasmic reticulum (SR). Immunocytochemical results provided direct evidence for the existence in non muscle cells of a hitherto unrecognized organelle homologous to SR: 1) CS-like proteins are expressed by HL60, PC12 cell lines and pancreatic, liver and brain cells. 2) In ultrathin cryosections, anti (skeletal muscle CS) antibodies decorate specifically a population of small organelles distinct from typical elements of the ER and Golgi complex and morphologically distinguishable from mitochondria, multivesicular bodies, lysosomes and secretory granules. The CS-positive organelles are distributed throughout the cytoplasm with some preference for the subplasmamembrane area. We propose this newly recognized organelle to be named calciosome.

**M-PM-C11** CONCANAVALIN A ACTIVATES A POTASSIUM CHANNEL IN CULTURED APLYSIA NEURONS VIA AN INTRACELLULAR SECOND MESSENGER. S.S. Lin, D. Dagan*, and I.B. Levitan. Department of Biology and Graduate Department of Biochemistry, Brandeis University, Waltham, MA 02254 and *Department of Physiology and Biophysics, Technion Faculty of Medicine, Haifa, Israel.

The lectin Concanavalin A (Con A) has been shown to affect a number of properties of Aplysia neurons. It alters their responses to the neurotransmitter glutamate (Kehoe, Nature 274(1978) 866-869), and both enhances neurite outgrowth and changes the type of synapses formed between neurons grown in culture (Lin and Levitan, Science, 237(1987)648-650). The mechanism(s) by which Con A induces these various types of neuronal plasticity is not known. We report here that, in cell attached membrane patches on cultured medial neurons, the activity of a 100 pS potassium channel increases when the cell is exposed to Con A. This increase in activity is due to a large decrease in the mean closed time of the channel with little if any change in the mean open time. Since the lectin is applied in the bathing medium outside the patch electrode and has no direct access to the channel in the patch, it must affect the channel's activity via an intracellular second messenger. Work is currently under way to determine possible intracellular messengers involved in altering channel activity. Supported by NSF grant BNS84-00875 to I.B.L.

**M-PM-C12** TEMPERATURE DEPENDENCE OF THE TIME COURSE OF THE SECRETORY RESPONSE TO ACETYLCHOLINE RECEPTOR ACTIVATION AND MEMBRANE DEPOLARIZATION IN ADRENAL CHROMAFFIN CELLS. Valentin Cena and Eduardo Rojas. Laboratory of Cell Biology and Genetics, NIH, Bethesda, MD20892

Adrenal chromaffin cells secrete catecholamines (CA) and ATP in response to acetylcholine (ACh) and high $[K^+]_o$. The release process is extremely fast making it difficult to measure the early phase of the secretory response. Recently we were able to resolve the time course of the secretory response by measuring the release of ATP using luciferin-luciferase included in the external medium (Rojas et al. FEBS lett. 185:323, 1985). For the three secretagogues studied, ACh, nicotine (Nic) and high $[K^+]_o$, the early phase of release followed first order kinetics. The following model was used to fit the data:

$$[ATP]_o(t) = [ATP]_{max}(1-\exp(-(t-\delta)/\tau))$$

where $\delta$ represents a delay in the start of the secretory response. Increasing the temperature from 23 to 37 °C induced a marked decrease in the time constant ($\tau$) needed to fit the data. While $\tau$ for the ATP secretion evoked by ACh (which involves activation of nicotinic as well as muscarinic receptors) decreased from 30.4 to 6.4 sec, $\tau$ for the ATP secretion evoked by activation of just nicotinic receptors decreased from 14.1 to 7.9. The time constant of the early phase of release evoked by high $[K^+]_o$ (60 mM) decreased from 59.1 to 13.4 sec with the same increase in temperature. The activation energies, estimated from Arrhenius plots, were 12 kcal $mole^{-1}$ $degree^{-1}$ for both Ach and high $[K^+]_o$. In the case of nicotine-induced release, the activation energy was significantly smaller, i.e. 7 Kcal $mole^{-1}$ $degree^{-1}$. The delay $\delta$ decreased when the dose of secretagogue was increased. For example, at 23 °C $\delta$ decreased from 14.2 to 0.64 sec when [ACh] was augmented from 0.1 to 100 uM. The delay $\delta$, representing a number of transitions preceding the actual release of ATP, also decreased when the temperature was increased from 23 to 37 °C. This suggests that the concentration of trigger molecules in the active state depends both, on the degree of receptor occupancy and $Ca^{2+}$-channel activation. Thus, the data presented here using a new method to monitor on-line the secretory activity suggest that, after $Ca^{2+}$ entry, ACh and membrane depolarization induce ATP (and CA) secretion through a common pathway.

**M-PM-C13** THE ROLE OF EXTERNAL ATP IN THE ACTIVATION PROCESS OF CALCIUM DEPENDENT POTASSIUM CHANNELS IN BOVINE AORTIC ENDOTHELIUM CELLS: A SINGLE CHANNEL STUDY. R. Sauvé, L. Parent, C. Simoneau, G. Roy. Dépt de Physiologie, Univ. de Montréal, Montréal, Canada H3C 3J7.

ATP and ADP are known to play an important role in the internal calcium mediated release of vasodilating substances by endothelium cells. Since numerous electrophysiological events can be related to internal calcium concentration changes, an extracellular patch clamp study was thus undertaken to determine the effect of external ATP on the ionic permeability of cultured bovine aortic endothelium cells (BAE). Our results essentially indicate **1)** that the BAE cell membrane contains a 50 pS $K^+$ channel (200 mM KCl) which can be activated by internal $Ca^{++}$ at concentrations ranging from 1 to 10 µM; **2)** that there is, in cell attached experiments, a substantial increase in the $K^+$-$Ca^{++}$ channel activity following the addition of ATP or ADP (10 µM) to the external medium. However, AMP, adenosine and non-hydrolysable ATP analogs were found to be ineffective to induce $K^+$-$Ca^{++}$ channel openings at concentrations less than 10 µM; **3)** that the channel activation process triggered by ATP occurs in two distinct phases: a first phase which would be solely dependent upon the presence of external ATP and a second phase which would require in addition external $Ca^{++}$; **4)** that the second phase can be suppressed by calcium channel blockers such as $Co^{++}$ (4 mM) or by depolarizing the cells with high $K^+$ external solutions. Based on these results, it is suggested that the action of ATP on BAE cells comes essentially from release of $Ca^{++}$ from intracellular $Ca^{++}$ stores coupled to a voltage and ATP dependent influx of $Ca^{++}$ from the extracellular space. This work was supported by the Medical Research Council of Canada by a grant from the Fonds de la recherche en santé du Québec.

**M-PM-D1** HETEROGENEITY OF $Na^+/H^+$ EXCHANGE IN BRUSH BORDER MEMBRANE VESICLES FROM RAT INTESTINE. Gerhard Ehrenspeck and Ulrich Hopfer, Dept. of Physiology and Biophysics, Case Western Reserve University, School of Medicine, Cleveland, OH 44106

To quantitate the effect of vesicle heterogeneity on $Na^+/H^+$ exchange, we analyzed the time-course of $^{22}Na^+$ exchange at equilibrium and the vesicle size distribution with the Computer Program CONTIN. As shown in the Figure, the efflux data revealed a distribution of rate constants (k) consisting of three peaks. The areas under the peaks (distorted by the logarithmic scale) indicate the relative contribution of the vesicle subpopulations to the macroscopic $^{22}Na^+$efflux. The heterogeneity in rate constants is increased by pretreatment of the rats with dexamethasone (Dex). In contrast, quasi-elastic light scattering indicates a relatively homogeneous size distribution of the vesicles. Dexamethasone increases the mean rate constant and permeability constant for $Na^+$, but has no effect on the mean vesicle size (Table). This approach provides a new dimension of analysis of vesicle transport properties. The data show that the common assumption of functional vesicle homogeneity is not always justified.

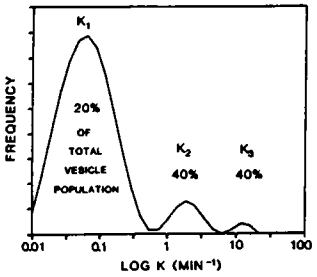


| | <k> ($min^{-1}$) | Vesicle <R> (nm) | <P> ($nm\ sec^{-1}$) |
|---|---|---|---|
| Control | 4.4 ± 0.3 | 116 ± 1 | 2.8 |
| Dex | 11.6 ± 0.6 | 118 ± 1 | 7.6 |

**M-PM-D2** HETEROGENEITY OF $Cl^-$TRANSPORT IN BRUSH BORDER MEMBRANE VESICLES FROM RAT SMALL INTESTINE. Raj Singh and Ulrich Hopfer, Dept. of Physiology and Biophysics, Case Western Reserve University, School of Medicine, Cleveland, OH 44106

To evaluate vesicle heterogeneity with respect to $Cl^-$exchange, we used the FORTRAN Program CONTIN to analyze both the time-course of $^{36}Cl^-$efflux (40 mM) at equilibrium and the quasi-elastic light scattering from vesicles (size distribution). The efflux data indicate that the vesicles are composed of at least two subpopulations with different rate constants of exchange (Figure). The vesicle size (from light scattering) was relatively homogeneous (See Table: $\langle R\rangle_z/\langle R\rangle_v$; Z-average radius/volume average radius). SITS (4-acetamido-4'-isothiocyanostilbene-2,2'-disulfonate) and DPC (Diphenylamine-2-carboxylic acid) overlapped in their inhibition at high concentrations (5 mM & 1 mM, respectively). The inhibition of SITS and DPC was additive at lower concentrations (0.5 mM), suggesting concentration-dependent differential effects on $Cl^-/OH^-$-exchange and $Cl^-$-conductance, respectively.

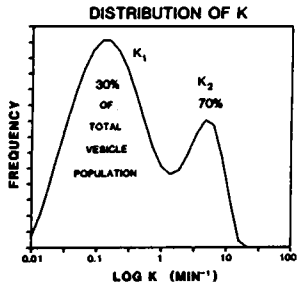


| | <k> ($min^{-1}$) | <R> (nm) | $\langle R\rangle_z/\langle R\rangle_v$ | <P> ($nm\ sec^{-1}$) |
|---|---|---|---|---|
| Control | 5.5 ± 0.2 | 130 ± 1 | 1.02 | 4.0 |
| SITS (5mM) | 0.7 ± 0.1 | 130 ± 1 | 1.02 | 0.5 |
| DPC (1mM) | 2.2 ± 0.1 | 130 ± 1 | 1.02 | 1.6 |

**M-PM-D3** ORIGIN OF INVERTED PD OF THE IN-VITRO FROG FUNDUS BATHED IN Cl-FREE MEDIA. W. S. Rehm, G. Carrasquer, M. A. Dinno and M. Schwartz. Departments of Medicine and Physics, University of Louisville, Louisville, KY 40292 and University of Mississippi, University, MS 38677.

Gastric K-H ATPase in the form of vesicles is neutral and it is suggested that the proton pump in the intact tissue is neutral (NP). However for the intact fundus substantial evidence favors that the proton pump is electrogenic (EP). For example, the nutrient side is normally positive, but with Cl-free media this side becomes negative and inhibitors of acid secretion abolish the inverted PD -- findings predicted by EP, i.e. $E_H$, the emf of the pump accounts for inverted PD and abolition of $E_H$ explains action of inhibitors. With the NP theory the inverted PD would be due to diffusion potentials, which result from ion ratios between the cell and external fluids. On the basis of previous findings (e.g. AJP 240;G267, 1981) it is generally agreed that the inverted PD is not due to Na, $HCO_3$, Mg, Ca or Pi diffusion potentials. Advocates of NP theory for intact tissue suggest that the K diffusion potential between cell and lumen is responsible for the inverted PD and that reduction in magnitude of this potential accounts for abolition of inverted PD with inhibition. But we show in both Cl and Cl-free media with high K on the secretory side (e.g. 80 mM), which would markedly reduce the K diffusion potential, that inhibitors produce a marked increase in PD. As a further test of NP it could be argued that the increase in PD resulting from inhibitors could be due to an increase in PD across the nutrient membrane of the tubular cells. We show with high K on both sides (e.g. 80 mM) which will markedly reduce both K diffusion potentials that inhibitors still produce the typical increase in PD with Cl-free solutions. (NSF support)

**M-PM-D4** SINGLE CHLORIDE CHANNEL ACTIVITY IN RESPIRATORY EPITHELIAL CELLS FROM A PATIENT WITH CYSTIC FIBROSIS. Jeffrey J. Smith, Murray Korc and Raphael Gruener. Depts.:Physiology, Pediatrics & Internal Medicine, University of Arizona College of Medicine. Tucson, AZ 85724.

Recent reports (Frizzell et al. Science 233:558, 1986; Welsh & Liedtke, Nature 322:467, 1986), using the patch-clamp technique, showed that single $Cl^-$ channel activity was absent from intact, cultured epithelial cells isolated from airways of patients with CF. Normal $Cl^-$ channel activity was, however, demonstrable in excised patches and by increasing intracellular $Ca^{++}$ in intact CF cells. These investigators suggested, independently, that CF $Cl^-$ channels remain closed because of abnormal intracellular regulation and that this may account for the transport defects in CF. Using cultured nasal polyp epithelial cells, from a patient with confirmed CF, we recorded single channel activity from intact and excised patches. Cytokeratin probes verified epithelial cell identity. The reversal potential, I-V behavior and pharmacologic responses were consistent with $Cl^-$ channel activity (Tris & methanesulfonate substitution; epinephrine challenge). Computer analysis (pClamp) revealed two separate channels based on distinct conductances (20 and 40 pS). Open time durations associated with these channels were 15 and 3 msec, respectively. These values were similar to non-CF cells under identical conditions. Closed time durations in CF cells were 3x longer than in non-CF cells, indicating a markedly reduced probability of channel openings. Since we routinely found $Cl^-$ channel activity, reduced channel density is unlikely in CF. These findings indicate a quantitative, rather than a qualitative, reduction in $Cl^-$ channel activity in CF cells.
Supported by grants from the Arizona Disease Control Research Commission, The Flinn Foundation of Arizona, The Arizona Lung Association, and a fellowship from The Cystic Fibrosis Foundation.

**M-PM-D5** ION CHANNELS ACTIVATED BY OSMOTIC AND MECHANICAL STRESS IN MEMBRANES OF OPOSSUM KIDNEY CELLS. J. UBL, H. Murer* & H.-A. Kolb. Faculty of Biology, University of Konstanz, D-7750 Konstanz, Federal Republic of Germany, and *Department of Physiology, University of Zürich-Irchel, CH-8037 Zürich, Switzerland

The patch clamp method was applied to study the response of cultured opossum kidney (OK) cells to media of various osmolarity. Whole cell records in isotonic media (310 mOsm) show a resting membrane potential of about -70 mV. Hypotonic bath causes within a few minutes depolarization to membrane potentials of about -30 mV. Exchange of the hypotonic media by the isotonic medium restores the resting membrane potential within a few minutes. Superfusion of OK-cells with hypotonic media (190 mOsm) in the cell-attached mode of the patch pipette induces after a variable delay in the minute range a stepwise activation of up to six ion channels of homogeneous single channel properties. The mean conductance of the membrane patch increases up to a factor of about twenty. The ion channels can be activated in the same membrane patch by application of a negative hydrostatic pressure to the pipette interior. The channel has a single channel conductance of about 22 pS and is permeable to $Cl^-$, $K^+$ as well as to $Na^+$. The results provide evidence that volume regulation involves mechanoreceptor operated ion channels.

**M-PM-D6** CONTINUOUS CELL VOLUME MEASUREMENTS: APICAL Cl/FORMATE EXCHANGE IN THE ISOLATED RABBIT RENAL PROXIMAL TUBULE. L Schild, P.S. Aronson and G.Giebisch. Dept of Cellular and Molecular Physiology.333 Cedar Street, New Haven, CT 06510-8026.

From Studies on microvillus membrane vesicles, Cl/Formate exchange represents a possible mechanism for transcellular Cl movement in the mammalian renal proximal tubule.We now used continuous measurements of epithelial cell volume by high contrast TV images to study this anion exchange in the intact epithelium. Formate (5mM) in the tubule lumen (pH6.8) reversibly increased epithelial cell volume by 3.9 % ±0.4, the maximal rate of change (dV/dt) normalized per mm of tubule length was 1.11 ± 0.1 nl/min. Changes in cell volume due to formate and dV/dt decreased by 50% when luminal formate was 1 mM, or when luminal pH was raised to 7.4. This suggests that formate induced cell swelling is due to non-ionic diffusion of formic acid into the cell, and subsequent cell accumulation of ionized formate. The estimated permeability coefficient of the apical membrane for formic acid is $6.10^{-2}$ cm.sec$^{-1}$. Cl removal from the bath and the lumen increased formate-induced cell swelling to 10.82% ± 0.3, but did not change dV/dt (1.23 ± 0.1). Replacing Cl by gluconate in the lumen or adding DIDS to the luminal side increased formate-induced cell swelling to 7.56 ± 0.6 and 6.09 ± 0.5 respectively, dV/dt remained unchanged. Finally, cell swelling induced by acetate was not affected by Cl. Conclusion: Cl prevents formate-induced cell swelling by recycling formate across the apical membrane via the Cl/Formate exchanger. For this mechanism to be efficient, cell membranes have to be more permeable to Cl than to formate. This approach provides a usefull model for the study of Cl transport across cell membranes.

**M-PM-D7** VOLTAGE-DEPENDENT CURRENTS RECORDED FROM PIGMENTED CILIARY BODY EPITHELIAL CELLS GROWN IN CULTURE. N.A. Farahbakhsh and G.L. Fain, Jules Stein Eye Institute, UCLA School of Medicine, Los Angeles, CA 90024.

The epithelium of the ciliary body lies along the margin of the eye and adjacent to the lens and is thought to be responsible for secretion of aqueous humor. This epithelium consists of two cell layers: a non-pigmented cell layer (facing the posterior chamber) and a pigmented cell layer (adjacent to the blood vessels). These cells are electrically coupled through extensive gap junctions. Tissue culture provides a means to isolate and study these cells individually.

We have used the whole-cell mode of the patch-clamp technique to study the membrane properties of pigmented ciliary body epithelial cells grown in culture from adult rabbits. During the recordings, the cells were perfused with a Ringer's solution containing [in mM]: NaCl, 111; $NaHCO_3$, 35; KCl, 4.3; $CaCl_2$, 1.7; $MgCl_2$, .8; glucose, 7; sucrose, 10 and bubbled with 95% $O_2$/5% $CO_2$ (pH 7.4) at 22° C. In most experiments patch electrodes contained [in mM]: KCl, 140; NaCl, 10; $CaCl_2$, .5; $MgCl_2$, 2; EGTA, 5.5; Hepes, 10; ATP, 1.5; GTP, .1 (pH 7.1).

Whole-cell recordings revealed a voltage-activated inward current, carried by Na and blocked by 30 nM TTX; a residual inward current that persisted in the absence of Na or in the presence of TTX; a voltage-activated outward current carried by K and blocked by 2 mM Ba or 10 mM TEA; and an inwardly-rectifying current for transmembrane voltages negative to -60 mV. This latter current was also blocked by the same concentrations of Ba and TEA. For voltages negative to -160 mV, the inwardly-rectifying current showed a "sag" which disappeared when Na, Ca and Mg in the extracellular Ringer's were replaced by K. Supported by NS07101 to NAF and by NIH EY00331 and EY01844 to GLF.

**M-PM-D8** NACL TRANSPORT IN PRINCIPAL CELLS (PC) OF RABBIT CORTICAL COLLECTING TUBULE (CCT). Kevin Strange, Wright State Univ. Sch. Med. Dept. of Physiol. & Biophys., Dayton, OH.

$10^{-4}$ M peritubular ouabain causes rapid and dramatic PC swelling, but has no effect on intercalated cell volume in CCT dissected from mineralocorticoid-treated rabbits. PC swell at an initial rate of 57.1 ± 4.9%/min (n=11) to a maximal volume 174.1 ± 16.2% (n=3) above control with no apparent structural damage. Ouabain swelling is completely blocked by luminal $Na^+$ or bilateral $Cl^-$ removal demonstrating that volume changes are due to apical NaCl entry. CCT exposed to ouabain for 45-60 seconds swell at an initial rate of 56.6 ± 7.3%/min (n=6) and then shrink -7.8 ± 3.4% below control volume after ouabain removal. The mean initial rate of shrinkage was -34.7 ± 4.4%/min which presumably reflects reactivation of the Na/K pump. Following a 10 minute recovery period, reexposure to ouabain causes PC to swell at a rate of 30.0 ± 4.1%/min, a value 53% lower than the original rate of swelling ($P<0.005$). Subsequent ouabain removal causes PC to shrink at a rate of -32.5 ± 4.8%/min which is not significantly different from the original rate of shrinkage ($P>0.25$). These results suggest down-regulation of apical NaCl entry mechanisms. With prolonged ouabain exposure (4-6 mins) PC reach their maximal volume and then shrink -23.9 ± 6.3% (n=3) below control volume following ouabain removal. Subsequent ouabain exposure has no effect on PC volume suggesting complete cessation of NaCl entry. Maximally swollen PC continuously exposed to ouabain activate volume regulatory decrease mechanisms and shrink at an initial rate of -3.25 ± 0.43%/min (n=4) to a new steady-state volume 13.0 ± 4.1% (n=3) above control. Ouabain removal after achievement of this new volume causes no further cell shrinkage suggesting indirectly that volume regulation may involve NaCl loss. NIH Grant AM 37317.

**M-PM-D9** SECRETAGOGUE INDUCED ION CHANNELS IN THE APICAL MEMBRANE OF ISOLATED OXYNTIC CELLS. J.R.Demarest, D.D.F.Loo and G.Sachs. Dept.of Physiol./Anat. Univ. of CA, Berkeley, CA 94720; Dept. of Physiol. UCLA, Los Angeles, CA 90024; CURE VA Wordsworth Med.Ctr.,Los Angeles CA 90073.

The apical membrane of the acid secreting oxyntic cell of the gastric mucosa is thought to posses $Cl^-$ and $K^+$ permeability mechanisms in addition to an electroneutral $H^+$,$K^+$-ATPase. The location of these cells within the glands of the epithelium has only permitted characterization of the apical permeability in membrane vesicles. Using isolated oxyntic cells from Necturus gastric mucosa, that maintain distinct membrane polarity and exhibit marked increase in exposed apical membrane area in responce to cAMP ($10^{-3}$ M) and isobutylmethylxanthine (IBMX, $10^{-4}$ M), we have employed the patch clamp technique to determine if ion permeation occurs through conductive channels. Cell attached patches (pipette solution:114 mM KCl,100 nM $Ca^{2+}$,10 mM HEPES) formed on the apical membranes of resting cells (i.e. not secreting acid, inhibited with $10^{-4}$ M cimetidine) contain 6pS channels in 15% of the patches while the majority exhibit no channels. Upon stimulation of these cells with cAMP and IBMX, 6pS channels began to appear in 90% of the patches after ~15 min. Open probability ($P_o$) increased progressively for 10 to 20 minutes in all patches containing channels. $P_o$ increased with hyperpolarization in cell attached and excised inside-out patches. These channels in excised patches were unaffected by $K^+$ for $Na^+$ substitution or $Ba^{2+}$ ($10^{-3}$ M) in the bath. In 10% of the cell attached patches another, larger conductance channel was observed. We conclude that there are stimulation-induced $Cl^-$ channels in the apical membranes of oxyntic cells.(Supported by NIHDK38664, NIHAM17328, USVA SMIA and SKB Foundation.)

**M-PM-D10** SINGLE FILE WATER CHANNELS IN THE RABBIT PROXIMAL TUBULE CELL MEMBRANE. Guillermo Whittembury and Paola Carpi-Medina, I.V.I.C., PO Box 21827, Caracas, Venezuela.

$P_{os}$, the water osmotic and $P_d$, the water diffusive permeabilities have been measured: $P_{os}$, in isolated tubules, from the rate of cell volume change under an osmotic difference applied across the apical and across the basolateral cell membrane (Pflügers Arch. 400:343-348, 1984; 402:337-339,1984; Kidney Int.30:187-191,1986); $P_d$ in isolated cells and tubules suspended in artificial plasma with 5 mM $MnCl_2$ which equilibrates in the extracellular space and shifts the NMR signal from extracellular protons, thus unmasking the intracellular signal (Proc Xth Int.Congr.Nephrol.London, Abstr.592, 1987). $P_{os}$ and $P_d$ were evaluated: (a) under control conditions and after exposure to various pCMBS (parachloromercuribenzenesulfonate) concentrations; and at different temperatures to calculate $E_a$, the energy of activation of $P_{os}$ and $P_d$. pCMBS inhibits $P_{os}$ and $P_d$ in a dose-dependent manner. The sulfhydryl reagent dithiothreitol reverts pCMBS action. Expressed per $cm^2$ of real cell membrane area, in µm/sec, the control values are: $P_{os}$, 396; $P_d$, 22; $P_{os}/P_d$, 13-18; with pCMBS: $P_{os}$, 32; $P_d$, 10; $P_{os}/P_d$, 3. $E_a$ values (kcal/mol) are: $P_{os}$, 3.2 (control); 9.2 (pCMBS); $P_d$, 5.2 (control); 9.1 (pCMBS). These and previous observations (Biochim.Biophys.Acta 775:365-373,1984) indicate that proximal cell membranes must be pierced by water channels which are altered by pCMBS. The permeabilities remaining with pCMBS indicate water permeation through the lipid bilayer part of the membrane. From $P_{os}/P_d$ of 13-18 an unreasonably large pore radius of 12-15 Å is calculated, which would not hinder entry of known extracellular markers. Alternatively, in a single file pore 13-18 water molecules would tandem along the pore. There are similarities between our results and those obtained in human RBC and ADH-stimulated toad urinary bladder. SUPPORTED BY FUNDACION POLAR, CONICIT and PNUD.

**M-PM-D11** SODIUM NMR IMAGING OF THE RABBIT KIDNEY, IN VIVO.
S.D. Wolff* and R.S. Balaban. (Intro. by M.B. Burg.)
NIH, Bethesda, MD, 20814. *Howard Hughes Research Scholar.

**Sodium concentration gradients in the kidney and their temporal regulation have been studied for many years in ex vivo tissue slices and through micropuncture studies. These techniques suffer from their invasive nature and subsequent related artifacts. We have developed a nondestructive model using $^{23}Na$ NMR in which we can image the sodium concentration within a rabbit kidney in vivo. These images were collected at 4.7 T in a 33 cm bore magnet with a custom saddle coil placed around the kidney. $^{23}Na$ transverse images of the kidney with a signal to noise ratio of 30:1 were obtained in 2 minutes. The voxel resolution of these images was 1 mm x 1 mm x 5 mm. The effect of acute saline infusion on the concentration and distribution of sodium within the kidney was examined. Consecutive sodium images were taken during an i.v. infusion of saline followed by furosemide (2 mg/kg). Inner medullary sodium content decreased by ~50% in less than 15 minutes after the infusion while cortical sodium content increased slightly. $T_1$ (~52 msec) and $T_2$ (~32 msec) relaxation times were measured before and after saline infusion. The differences in Na image intensity obtained after saline infusion could not be explained by changes in these relaxation times. These data demonstrate that $^{23}Na$ NMR imaging can be used to dynamically follow the distribution of sodium in the kidney in vivo.**

**M-PM-D12** Transendothelial ionic exchange underlies endocardial control of myocardial performance. Dirk L.Brutsaert and Ann L.Meulemans, University of Antwerp, Antwerp, Belgium.

We have previously shown that the endocardial endothelium (EE) modulates myocardial mechanical performance. As the mechanism is presently unknown, we evaluated EE control of ion (Ca++-K+) mediated changes in myocardial performance.

Peak isometric twitch tension (TT) and time to 1/2 isometric relaxation (RT/2) were measured in isolated cat papillary muscle (n=20, Krebs-Ringer solution, 35°C) over a wide range of $[K+]_E$ (2.35; 3.5; 5.9; 8; 10 mM) for 3 levels of $[Ca++]_E$ (1.25; 2.5; 7.5 mM) before and after damaging (1% Triton X-100, for 1s) the EE.

With intact EE, despite some shortening of RT/2 with increasing K+, TT was unaffected between 3.5 and 10 mM K+, regardless of Ca++; TT decreased somewhat (12+/-4%) only in 1.25 mM Ca++ at 10 mM K+ and it slightly increased (from 10+/-3% at 7.5 to 15+/-5% at 1.25 mM Ca++) at 2.35 mM K+.

After EE damage at 5.9 mM K+, RT/2 had typically shortened (6+/-3% at 7.5, 16+/-3% at 2.5, 20+/-3% at 1.25 mM Ca++) and TT had decreased in a Ca++-dependent manner (NS at 7.5, 34+/-5% at 2.5, 46+/-3% at 1.25 mM Ca++). Although TT at all Ca++ was hardly affected by changing K+ below 5.9 mM K+, TT decreased when K+ was increased from 5.9 to 8 and 10 mM K+; this decrease was Ca++dependent (35+/-6% at 7.5, 14+/-5% at 2.5, NS at 1.25 mM Ca++). Despite the EE damage-induced shortening of RT/2 at all Ca++, a further shortening of RT/2 was seen with increasing K+, similar to the K+-induced shortening in the presence of intact EE.

The data demonstrate that EE protects the myocardium from varying environmental K+ possibly via transendothelial Ca++ mediated K+ efflux.

**M-PM-E1** THE INFLUENCE OF DOUBLY-ATTACHED CROSSBRIDGES ON MECHANICAL BEHAVIOR OF SKELETAL MUSCLE FIBERS UNDER EQUILIBRIUM CONDITIONS. Aydin Tozeren. Department of Mechanical Engineering, The Catholic University of America, Washington, DC 20064.

A simple model of a double-headed crossbridge is introduced to explain the retardation of force decay following an imposed stretch in skeletal muscle fibers under equilibrium conditions. The critical assumption in the model is that once one of the heads of a crossbridge, say head 1, is attached to one of the actin sites available for attachment, the attachment of the second head will be restricted to a level of strain determined by the attachment of head 1. The crossbridge structure, namely the connection of both heads of a crossbridge to the same tail region, is assumed to impose this constraint on the spatial configurations of crossbridge heads. The unique feature of the model is the prediction that, in the presence of a ligand (PPi, ADP, AMP-PNP) and absence of $Ca^{2+}$, the half time of force decay is many times larger than the inverse rate of detachment found in solution. This prediction is in agreement with measured values of half times of force decay in fibers under similar conditions (Schoenberg and Eisenberg, 1985, Biophys. J. 48:863-871). It is predicted that a crossbridge head is more likely to reattach to its previously strained position than remain unattached while the other head is attached, leading to the slow decay of force. Our computations also show that the apparent cooperativity in crossbridge binding observed in experiments (Brenner et al. 1986, Biophys. J. 50:1101-1108) can be partially accounted by the double-headed crossbridge attachment. Model predictions fit the aforementioned data best when the crossbridge stiffness does not change significantly with the dissociation of one of the two attached heads. This observation suggests that crossbridge stiffness is determined either by the extensibility (flexibility) of the double helical tail region or its junction to the thick filament backbone.

**M-PM-E2** EXPLAINING THE LAG BETWEEN FORCE AND STIFFNESS DURING THE RISING PHASE OF A TETANUS. M. A. Bagni[†], G. Cecchi[†] and M. Schoenberg[*], [†]Dipartimento di Scienze Fisiologiche, Universita degli Studi, I-50134, Firenze, Italy and [*]NIAMS, NIH, Bethesda, MD, 20892, USA

In the Huxley-Simmons model of muscle contraction, force generation is due to a rapid conformational change between two attached crossbridge states. The model predicts an ~ 1 ms lag of force relative to stiffness during the rising phase of a tetanus, but not the 10-15 ms lag which is seen experimentally (Ford et al., J. Physiol. 372:595:1986; Cecchi et al., Pflug. Arch. 409:39:1987). This has been interpreted as suggesting that during contraction an additional stiff, slowly-attaching, non-force producing crossbridge state precedes the force producing states postulated by Huxley and Simmons (Huxley and Kress, J. Musc. Res. Cell. Mot. 6:153:1985). However, this explanation for the lag is not satisfying as a) there is no biochemical evidence for such a state, and b) this explanation for the lag fails to explain 1) why the magnitude of the lag between force and stiffness seen during the rising phase of a tetanus is different from that seen during the relaxation phase and during the redevelopment of force following a large quick release, 2) why, despite the different lags, plots of stiffness versus force for all 3 conditions above are virtually identical and 3) why, for a given size step, the rate-constant of the isometric force transient is faster during the rising phase of a tetanus than it is during the plateau. We will show that we can explain all the above findings, without postulating any additional crossbridge states, simply by having the force generating transition envisioned by Huxley and Simmons be a cooperative one, one where the rate-constant for the back reaction decreases with increasing attachment of crossbridges. While there is currently no direct evidence for this model, the model makes several predictions, some of which have been confirmed by preliminary experimentation.

**M-PM-E3** CONTRACTION OF MUSCLE FIBERS GENERATED BY SPIN-LABEL ANALOGS OF ATP. N. Naber and R. Cooke. (Introd. by A. Waring). Dept. of Biochemistry and CVRI, Univ. of California, San Francisco, CA 94143.

We have monitored the mechanics of contraction of glycerinated muscle fibers using spin-labeled analogs of ATP as substrate. EPR spectra provided information on the orientation of the spin-probe. Spin labels were attached to the 3' position of the ribose ring. In permeable soleus fibers both analogs (50-100 μM) generated 60% of the isometric tension and 30% of the shortening velocity found for ATP. The soleus fibers bind nucleotides tightly and both tension and contraction velocity were saturated at these nucleotide concentrations. However, the analogs did not cause relaxation of the fibers, even at high concentrations 200-300 μM. The analogs were hydrolyzed by isometric fibers at a rate that was approximately 50% of that of ATP. A similar contractile response was obtained using 3'dATP, showing that it is the loss of the 3' OH, not the presence of the label that is responsible for the partial inhibition in contractile response. EPR spectra of diphosphate analogs bound to muscle cross-bridges showed that the analogs were ordered with respect to the fiber axis in these inactive fibers. During active isometric contractions, with substrate concentrations maintained by high levels of creatine phosphate, approximately 90% of the bound probes remained aligned at the same orientation found for diphosphate analogs. We conclude that the loss of the 3' hydroxyl results in the partial inhibition of some transition that occurs when myosin is bound tightly to actin within the power-stroke. Although myosin heads are cycling relatively rapidly, and generating significant tension, most are bound to actin with well ordered nucleotide sites. Supported by USPHS AM 30868.

**M-PM-E4** **EFFECT OF MONO- AND BIFUNCTIONAL SULFHYDRYL REAGENTS ON THE STIFFNESS OF SKINNED RABBIT PSOAS FIBERS.** **Vincent A. Barnett and Mark Schoenberg, NIAMS, NIH, Bethesda, MD 20892.**

**When the bifunctional agent para-phenylenedimaleimide (pPDM) covalently crosslinks the SH1 and SH2 sulfhydryls of myosin in solution, it greatly reduces the affinity of myosin for actin (Reisler et al., 1974, Biochem.,13:3837). pPDM treatment has also been used in fibers to alter acto-myosin interactions (Chaen et al.,1986, J.B.C.,261:13632). In order to study in more detail the effect of sulfhydryl modification in fibers, we treated chemically skinned rabbit psoas fibers (5°C) with pPDM, or the monofunctional sulfhydryl reagent phenylmaleimide (PM). The fibers were treated either relaxed at normal ionic strength, relaxed at low ionic strength, or in rigor. The interaction of the crossbridges with the actin filament was monitored by measuring the fiber stiffness in rigor and in normal ionic strength relaxing solution. Modification of relaxed fibers at normal ionic strength for 15 min with either 0.2 mM pPDM or 0.1 mM PM causes a large decrease in rigor stiffness with little or no change in resting stiffness. In contrast, modification of fibers in rigor with either pPDM or PM causes only a slight change in rigor stiffness but a significant increase in resting stiffness. Fibers treated in low ionic strength relaxing solution showed changes more similar to fibers treated in rigor than to ones treated in normal ionic strength relaxing solution; they too showed little change of rigor stiffness with significant increases in resting stiffness. This supports the idea that at low ionic strength large numbers of crossbridges are attached in relaxed fibers and suggests that modifiers such as pPDM and PM may make it possible to estimate the fraction of crossbridges attached in relaxed fibers at different ionic strength. The similarity of action of pPDM and PM suggests either the presence of a contaminant crosslinker in PM or, more likely, that the effects of pPDM are due to sulfhydryl modification rather than crosslinking per se.**

**M-PM-E5** THE INFLUENCE OF FIBER TYPE AND MUSCLE SOURCE ON THE CALCIUM SENSITIVITY OF RAT MUSCLE FIBERS. B. Laszewski-Williams, R.L. Ruff and A.M. Gordon, Dept. of Phyiology, Univ. of Wash., Seattle, WA 98195 (BL-W & AMG) and Dept. of Neurology VAMC & CWRU, Cleveland OH 44106 (RLR)

We investigated the influence of muscle source and fiber type on various properties of rat skeletal muscle. Single fibers from predominantly slow muscles [soleus (SOL) and adductor longus (AL)], mixed muscle [posterior gracilis (PG)], and predominantly fast twitch muscle [extensor digitorum longus (EDL)] were chemically skinned. Segments of the fibers were characterized histochemically and calcium-tension relationships were determined. Fiber type and muscle source had significant effects on the negative log of the calcium concentration associated with half-maximal tension (pK). Slow twitch fibers had larger values of pK than did fast twitch fibers. Slow twitch fibers from the predominantly slow muscles, SOL and AL, had similar values of pK, but smaller values than slow twitch fibers from the mixed muscle, PG. Fast-glycolytic fibers from the predominantly fast muscle, EDL, had a higher pK than fast-glycolytic fibers from the mixed fiber type muscle, PG. There were no differences between the pK associated with fast-glycolytic and fast-oxidative-glycolytic fibers. There were no consistent effects of fiber type or muscle source on the Hill coefficient. Supported by NIH grant NS08384 to Dr. Gordon and Veterans Administration Merit Reviewed Funding to Dr. Ruff.

**M-PM-E6** DIFFUSION COEFFICENTS OF CYTOSOLIC PROTEINS IN RABBIT MUSCLE. David Maughan and Elisabeth Wegner, Department of Physiology & Biophysics, University of Vermont, Burlington, VT 05405

The myofilament lattice of rabbit muscle is a compact structure with distances of about 14, 17 or 29 nm between filament surfaces (actin-myosin, actin-actin, or myosin-myosin spacings) at 2.2 um sarcomere length. Cytosolic proteins have comparable dimensions: consequently, hindered diffusion or even exclusion of some proteins from certain regions of the lattice may occur and is probably important in determining the location and rate of cytoplasmic biochemical reactions. Diffusion coefficients of 7 endogenous proteins (5 glycolytic enzymes plus myokinase and parvalbumin) in relaxed muscle fibers, skinned under oil, were calculated from the rate at which these proteins diffuse from a skinned psoas (fast glycolytic) fiber into a skinned soleus (slow oxidative) fiber brought into contact with it. Radial diffusion coefficients were obtained from fibers placed in side-by-side contact. Proteins from fiber samples were separated by SDS-PAGE, silver stained, identified, and quantified by comparison with purified rabbit protein standards (Sigma). The radial diffusion coefficients of the proteins examined were, as a group, about a tenth (0.10±0.04 SD) of their coefficients in water. The diffusion coefficients were generally inversely proportional to their Stokes radii. Similar results were obtained from measurements of radial diffusion of proteins from psoas skinned fibers into a physiological relaxing solution. The magnitude of retardation was consistent with a simple model of protein diffusion through a lattice opening of 24 nm, assuming that the diffusivities of cytosolic molecules are, as a group, reduced by a factor of 2 relative to water due to viscosity or tortuosity (Kushmerick & Podolsky, Science, 166, 1297-1298, 1971). This lattice dimension accords with the range of interfilament distances noted above, suggesting that radial diffusion of these proteins is severely hindered in the myofilament lattice. [Funded by NIH]

**M-PM-E7 INTER-FILAMENT INTERACTIONS IN MUSCLE VISUALIZED IN FROZEN-HYDRATED THIN SECTIONS.**
B.L.Trus[1], A.McDowall[2], J.Dubochet[2], M.Unser[3], R.J.Podolsky[4] and A.C.Steven[4].
[1]DCRT/NIH, [2]EMBL/Heidelberg, [3]BEIB/NIH, [4]NIAMS/NIH.

For the purpose of determining net interactions between actin and myosin filaments in muscle cells, perhaps the single most informative view of the myofilament lattice is its averaged axial projection. We have studied frozen-hydrated transverse thin sections with the goal of obtaining axial projections that are not subject to the limitations of conventional thin sectioning (suspect preservation of native structure) or of equatorial X-ray diffraction analysis (lack of experimental phases). In principle, good preservation of native structure may be achieved with fast freezing, followed by low-dose electron imaging of unstained vitreous cryo-sections. In practice, however, cryo-sections undergo large-scale distortions, including irreversible compression; furthermore, the required use of under-focussed bright-field imaging results in a non-linear relationship between the projected density of the specimen and the optical density of the micrograph. To overcome these limitations, we have devised methods of image restoration and generalized correlation averaging, and applied them to cryo-sections of rabbit psoas fibers in both the relaxed and rigor states. At ~9nm resolution, actin filaments appear more prominent relative to myosin filaments, compared to what is seen in conventional thin sections. This may indicate that a significant fraction of crossbridges averages out in projection so as to contribute only to the baseline of projected density. Entering rigor encurs a loss of density from an annulus around the myosin filament, with a compensating accumulation of density in an annulus around the actin filament. This re-distribution of mass represents attachment of the "visible" fraction of cross-bridges.

**M-PM-E8** INCORPORATION OF A FLUORESCENTLY LABELED ACTIN CAPPING PROTEIN INTO THE Z-LINE OF KI-EXTRACTED MYOFIBRILS. Theodore J. Mullmann and Shin Lin. Department of Biophysics, The Johns Hopkins University, Baltimore, MD 21218.

Muscle capactin, an actin capping protein with 36K and 32K Da subunits, inhibits G-actin association/disassociation at the "barbed end" but does not sever actin filaments *in vitro* (Mullmann & Lin, *J. Cell Biol.* 103, 391a (1986)). To investigate its cellular localization and function, we labeled highly purified capactin from chicken breast muscle with lissamine rhodamine sulfonyl chloride (R-capactin) without significant loss of activity (inhibition of nucleated polymerization of pyrene-actin in 0.4 mM $MgCl_2$). When R-capactin was incubated at 10 ug/ml with myofibrils extracted with 0.6 M KI, incorporation of the labeled protein into the Z-line regions could be seen by fluorescence microscopy. In contrast, no incorporation was seen in unextracted myofibrils; immunoblotting with antibodies to capactin showed that the protein was in the KI-extract of the myofibrils. No incorporation of R-capactin was seen when extracted myofibrils were preincubated with 100 ug/ml of unlabeled capactin, demonstrating that a saturable number of sites were involved. In other controls, rhodamine-BSA at concentrations of 100 ug/ml did not stain the extracted myofibrils. Rhodamine-phalloidin also stained the Z-lines of the extracted myofibrils, showing that some F-actin remained at these regions. R-capactin incubated at 100° C for 10 min no longer inhibited actin polymerization but could still be incorporated into extracted myofibrils. The results of this study suggest that capactin binds to an undetermined factor present at the Z-lines of myofibrils, possibly functioning as a link between this factor and the ends of actin filaments. (Supported by GM-22289)

**M-PM-E9** STRUCTURAL STATES IN THE Z BAND OF SKELETAL MUSCLE CORRELATE WITH STATES OF ACTIVE AND PASSIVE TENSION. M.A. Goldstein, L.H. Michael, J.P. Schroeter and R.L. Sass. Dept. of Medicine-Cardiovascular Sciences Section, Baylor College of Medicine, Houston, TX 77030.

In skeletal muscle Z bands, the ends of the thin contractile filaments interdigitate in a tetragonal array of axial filaments held together by periodically cross-connecting Z filaments. Changes in these two sets of filaments are responsible for two distinct structural states observed in cross-section, the small square (ss), and the basket-weave (bw) forms. We have examined Z bands and A bands in relaxed, tetanized, stretched, and stretched-and-tetanized rat soleus muscles by electron microscopy and optical diffraction. In relaxed muscle, the A band spacing decreased with increasing load and sarcomere length, but the Z lattice remained in the ss form and the Z spacing changed only slightly. In tetanized muscle at sarcomere lengths up to 2.7μm, the Z lattice assumed the bw form and the Z spacing was increased. The increased Z spacing was not the result of sarcomere shortening. Computer reconstructions of cross-sectional EM's were used to further define structural features of the two lattice states. We conclude that passive tension is not sufficient to cause this change in the Z lattice; active tension is required.

Supported by NIH grants HL17376 and HL30809.

**M-PM-E10** IN SITU DISSOCIATION AND SUBSEQUENT REASSEMBLY OF MYOSIN FILAMENTS IN RABBIT SKELETAL MUSCLE. M.L.F. Barbosa and R. J. Podolsky. Lab. of Physical Biology, NIAMS, NIH, Bethesda, MD 20892.

We have observed by electron microscopy that myosin filaments in skinned muscle fibers change their organization when transferred from a 50mM rigor solution at pH 7.0 to a 50mM rigor solution at pH 8.5. At the higher pH, the filament swells and becomes a hollow cylinder. Incubation in rigor solutions of ionic strengths lower than 50mM at pH 8.5 causes dissociation of the myosin filaments despite the rigor condition. Incubation of skinned fibers in 5mM rigor solutions at pH 8.5 removes the M bridges, and causes partial dissociation of the myosin filaments at the M region. Dissociated filaments reassemble after addition of 3mM magnesium, or by transferring the fiber to a 50 mM rigor solution at pH 7.0. Reassembled myosin filaments are no longer organized in a superlattice. Our results confirm the importance of electrostatic interactions in maintaining the structure of the myosin filament backbone (Maw, M.C. and Rowe, A.J. 1980. Nature. 24:412-414), and agree with the proposed participation of the M bridges in holding the superlattice structure (Luther, P.K. and Squire, J.M. 1980. J. Mol. Biol. 141:409-439). Since the dissociation of the filaments takes place in fibers in the rigor state, the myosin "subfilaments" are probably either parallel to each other or twisted in a helical configuration of very high pitch.

**M-PM-E11** HIGH AND LOW RIGOR STATES IN SKELETAL MUSCLE SHOW DIFFERENT A-BAND ELECTRIC CHARGES E.M. Bartels and G.F. Elliott, Biophysics Group, The Open University, Oxford Research Unit, Boars Hill, Oxford, England.

Two different rigor states, low and high rigor, were described by M. Kawai and P.W. Brandt (J.Gen. Physiol. (1976) 68:267). The two states were determined by the prehistory of the muscle and the low rigor state showed a lower rigor tension but a higher stiffness than the high rigor state.

Donnan potentials have been measured from the A- and I-bands of glycerinated rabbit psoas in the two rigor states. From the Donnan potentials the protein charge concentrations have been calculated as described by Naylor et al (Biophys. J. (1985) 48:47). Since the two rigor conditions appear in the same chemical environment the filament lattice volume is the same in the two states, and the protein charge concentation is a direct measurement of the charges on the filaments. We induced the two rigor states by modifications of Kawai and Brandt's techniques. The results in rigor solution are given in Table 1. (n = 80, s.d. given).

| Table 1 | | Protein Charge Concentr.(mM) | | | Protein Charge Concentr.(mM) |
|---|---|---|---|---|---|
| Low Rigor State | A | -67 ± 5 | High Rigor State | A | -90 ± 6 |
| | I | -34 ± 6 | | I | -34 ± 6 |

The results show that the I-band charge is not affected while the A-band charge differs significantly in two rigor states. The highly charged state is the state with the high tension. This agrees well with our observation (E.M. Bartels and G.F. Elliott, Acta Physiol. Scand. (1984) 131:A20) that the electric charges increases during contraction.

**M-PM-E12** THE ACTIVE LATERAL EXPANSION FORCE OF A SINGLE SKELETAL MUSCLE FIBER. Henry H. Gale, Dept. Physiol., Creighton Univ. Med. Sch., Omaha, NE 68178.

Previously (Gale, J. Gen. Physiol. 70:7a, 1977) the active transverse outward force of isolated, whole, dog gastrocnemius muscles was measured as a function of muscle thickness, length, and active tension. Lateral pushing force depended on relative thickness and was independent of length and of tension. Here isolated, intact single barnacle (Balanus nubilus) fibers larger than 1 mm diameter were stimulated tetanically with alternating polarity rectangular pulses of submaximal voltage at 20° C. Lateral expansion force was measured during the tetanus plateau with a force transducer indented into the side of the fiber. As in whole muscle, pushing force increased as local fiber thickness was decreased by compression of the fiber between the force transducer and a mechanical stop on the opposite side of the fiber; giving the width-push relation. At the same time fiber length was separately changed and longitudinal tension was metered. Over the length range, fiber lateral expansion force declined progressively with longitudinal stretch -unlike whole muscle where the width-push relation was length independent- while longitudinal tension rose and fell with stretch giving the usual length-tension relation. Maximum active fiber expansion force was ~ 250 g/cm$^2$ compared with ~ 1 kg/cm$^2$ for whole muscle. Peak fiber tension was 1.5 kg/cm$^2$. Extrapolation above submaximal stimulus levels to the expected maximum value for barnacle muscle longitudinal tension, 6 kg/cm$^2$, gives an extrapolated lateral push of 1 kg/cm$^2$, equal to that of maximally stimulated whole muscle. In both preparations lateral expansion force varies independently from tension, suggesting separate lateral and longitudinal force generators in active muscle.

**M-PM-F1** INTERPRETATION OF THE OPTICAL SPECTRA OF THE FENNA-MATTHEWS ANTENNA COMPLEX
Robert M. Pearlstein, Physics Department, Indiana-Purdue University, 1125 East 38th Street, P.O. Box 647, Indianapolis, IN 46223 U.S.A.

Red shifts and other spectral features of bacteriochlorophyll (BChl) in antenna complexes have been attributed in varying degrees to BChl-protein or BChl-BChl (exciton) interactions. In the case of the one BChl antenna complex with an x-ray structural model, the Fenna-Matthews (F-M) structure, the interpretation of the BChl $Q_Y$-region spectra has been a long-standing and apparently intractable problem. As a result, progress in understanding the spectra of all BChl antenna complexes has been hampered. A new theoretical model is presented here of the optical spectra of the F-M structure. In this model, only standard, Y-polarized, $Q_Y$-transition moments are assumed. However, two new assumptions are introduced. First, the principal mechanism for the protein-induced portion of the red shift is taken to be modification of intra-BChl configuration-interaction (CI) resulting from van der Waals contact of aromatic amino acid (AAA) rings with the BChl macrocycle. In a simple theory, it is shown that AAA-modified CI results in $Q_Y$-band red shifts correlated with increased intrinsic $Q_Y$ dipole strengths. Second, it is proposed that, in solution (the experimental medium for the optical spectra), the individual F-M trimers themselves form dimers (i.e., dimers of trimers) in which two protein subunits in different trimers bind with their respective flat beta-sheet portions juxtaposed. This produces additional (inter-subunit) BChl-BChl exciton interactions, one or two of which are comparable in magnitude to the intra-subunit interactions. Optical spectra calculated according to this new theoretical model are in reasonable agreement with experiment. The consequences of the model for the interpretation of other BChl antenna complexes are discussed.

**M-PM-F2** BACTERIOCHLOROPHYLL c INTERACTIONS IN OLIGOMERS AND CHLOROSOMES OF GREEN PHOTOSYNTHETIC BACTERIA. Daniel C. Brune, George H. King, and Robert E. Blankenship, Department of Chemistry, Arizona State University, Tempe, Arizona, 85287-1604, USA.

Bacteriochlorophyll (BChl) c is the major antenna pigment in chlorosomes of the thermophilic green gliding bacterium Chloroflexus aurantiacus. The spectral features of BChl c in chlorosomes have been attributed to pigment-pigment interactions and are precisely duplicated by those of BChl c oligomers that form spontaneously in nonpolar solvents. We are now investigating the interactions between BChl c and analogous pigment molecules in organic solvents in order to elucidate their interactions in chlorosomes. BChl c from C. aurantiacus spontaneously self-associates in the absence of added water to form at least three different species, with red absorption maxima at 680 nm, 710 nm, and 740 nm. The 740 nm-absorbing species forms in aliphatic hydrocarbons and tends to precipitate from solution, indicating a large size. The 710 nm oligomer predominates in mixtures of hydrocarbon solvents and $CCl_4$ or $CS_2$, while the 680 oligomer (probably a dimer) is most apparent in dry $CH_2Cl_2$. A Fourier transform infrared (FTIR) spectrum of the 740 nm oligomer exhibits a peak at 1653 $cm^{-1}$ due to the 9-keto group that shifts to 1680 $cm^{-1}$ upon disruption of the oligomer (as indicated by a shift of the 740 nm peak to 670 nm) with pyridine vapor. Exposing a dried chlorosome film to pyridine vapor produces identical changes in the visible and FTIR spectra, indicating participation of the 9-keto group in pigment-pigment interaction both in the 740 nm oligomer and in chlorosomes. Experiments with pyrochlorophyll a shows that this pigment does not form a 740 nm oligomer under conditions that produce the 740 nm oligomer of BChl c. Instead it forms a 680 nm-absorbing product that may be analogous to the BChl c dimer that forms in $CH_2Cl_2$. These results suggest that the 2-hydroxyethyl substituent, as well as the 9-keto group, is required for formation of the 740 nm and probably also the 710 nm-absorbing oligomer of BChl c. Supported by a grant from the U.S. Department of Energy.

**M-PM-F3** TEMPERATURE DEPENDENCE OF EXCITATION TRANSFER IN Chloroflexus aurantiacus. Bruce P. Wittmershaus, Daniel C. Brune, and Robert E. Blankenship, Department of Chemistry, Arizona State University, Tempe, Arizona, 85287-1604, USA.

The system of light-harvesting antenna-proteins of the green photosynthetic bacterium Chloroflexus aurantiacus contains at least three major BChl complexes. Oligomers of the major antenna pigment, BChl c, are contained in membrane-attached structures known as chlorosomes. The region of the chlorosome in contact with the membrane (the baseplate) contains the BChl a complex, B795. The BChl a antenna pigment-proteins, B808-868, are found within the membrane. The current hypothesis is that excitations created in BChl c in the chlorosomes are transferred to B795 in the baseplate, then to the membrane complex B808-865 and finally are trapped by the reaction center. On decreasing the temperature of whole cells from their growth temperature of 55 C to 10 C, fluorescence from B808-868 reversibly increases 2- to 3-fold. Reduction of the secondary electron acceptors of the reaction center or addition of inhibitors produces a similar increase in fluorescence at 55 C, but has little effect at 10 C. The rate of energy transfer from B808-868 to the reaction center is proposed to decrease with decreasing temperature. These results suggest a lipid phase transition is occurring, which may reduce the mobility of the quinones in the electron transfer chain as the temperature is lowered, causing a decrease in the turnover rate of the reaction center and its ability to accept excitations from B808-868. Fluorescence from BChl c and B795 vary less than 5% from 55 to 10 C. The excitation spectrum of fluorescence from B795 remains unchanged. Energy transfer within the chlorosome appears to be unaffected by the change in temperature, as does the quenching of excitations in the chlorosomes. The transfer efficiency of excitations from BChl c to B808-868, as measured by comparing absorption and fluorescence excitation spectra, is 69% +/-13% at 55 C. Supported by a grant from the U. S. Department of Energy.

**M-PM-F4** CONSTRUCTION OF A RC DELETION MUTANT IN R. SPHAEROIDES. C. Schenck, T. Roberts, B. Brasher and D. Gaul*, Intr. by M. Elkind, Dept. Biochem., Colorado S.U., Ft. Collins, CO 80523

Reaction center(RC) function is being investigated by a molecular genetic and biophysical approach. We have constructed a strain of R. sphaeroides in which the RC L and M genes have been deleted. This mutant is useful for examining the effect of site-directed mutations in the RC genes.

Plasmid pSS3 containing LH1 and RC alleles was used as a source of structural genes. A double deletion construct was made in vitro which removed two-thirds of the L gene, all of the M gene, the ORF downstream from M and all regulatory sequences 5' to the LH1 $\beta$-subunit gene. The double deletion was introduced into pRK404 and the deletion plasmid was crossed into a high-frequency recipient. Tetracycline-resistant exconjugants were photographed in infrared fluorescence to screen for double-homologous recombinants. High fluorescence (hf) colonies appeared at a frequency of $10^{-3}$. All hf exconjugants demonstrated typical LH1 and LH2 electronic spectra.

An RC deletion strain was obtained by curing merodiploid hf exconjugants with 4$\mu$M acridine orange in minimal medium. The resultant tetracycline sensitive cells retain the hf phenotype, do not grow photosynthetically and do not revert. SDS-PAGE shows that RC L,M and H polypeptides are missing in mutant membranes and Southern blotting confirms the deletion construct in genomic DNA. The figure shows flash-induced $\Delta$A attributable to RCs in membranes. The lack of an observable $\Delta$A in the mutant confirms the absence of a functional reaction center.

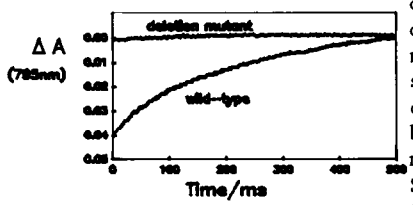


Supported by USDA, Colorado Agric. Expt. Sta, ACS Petro. Res. Fund
*NSF Plant Biology Postdoctoral Fellow

**M-PM-F5** NEAR-INFRARED ABSORPTION SPECTRA, EXTINCTION COEFFICIENTS AND ACID DENATURATION OF LIGHT-HARVESTING COMPLEXES OF *RHODOBACTER SPHAEROIDES* MUTANTS.

James N. Sturgis*, C. Neil Hunter†and Robert A. Niederman*. *Department of Biochemistry, Rutgers University, Piscataway, NJ and †Department of Pure and Applied Biology, Imperial College of Science and Technology, London UK.

In order to study the *in situ* spectral properties of the B800-850 and B875 light-harvesting complexes, mutant strains NF57 (B875$^-$, RC$^-$) and M21 (B800-850$^-$) were isolated after treatment of *R. sphaeroides* 8253 with N-methyl-N'-nitro-N-nitrosoguanidine (Ashby, M.K., Coomber S.A. & Hunter C.N. *FEBS Lett 213*, 245-248, 1987). Extinction coefficients were determined for the B800, B850 and B875 bands in membranes of these mutant strains and were found to be 226±10, 170±5 and 118±5 mM$^{-1}$BChl cm$^{-1}$, respectively. These values are in reasonable agreement with those reported for detergent-isolated complexes (Clayton, R.K. & Clayton B.J. *Proc. Natl. Acad. Sci. USA 78*, 5583-5587, 1981), although detergent solubilization caused a broadening on the blue side of the B875 and B800 bands. The data obtained for the mutant strains were used to deconvolute BChl species in membranes of the wild-type.

Treatment of M21 membranes with acid resulted in the rapid conversion of about half the B875 BChl absorption band into 'free' BChl with an absorption near 770 nm (Fig.1); the remaining absorption was shifted ~4 nm to the red. During prolonged incubation (30-180 min), the peak at 880 nm shifted slowly to 844 nm with an isosbestic point at 860 nm. Kinetic analysis seemed to indicate that the fast loss of B875 BChl absorption initiated the subsequent slow shift. The changes occurred with rate constants of ~0.29 and ~0.02 min$^{-1}$, and apparent pK$_a$ values near 5.3 and 3.5, respectively. They could not be reversed by addition of alkali. Exposure of M21 membranes to alkali up to pH 12 had no effect. Possible titratable groups responsible for the fast and slow changes are histidyl imidazole and glutamyl-$\gamma$-carboxyl groups, respectively, within the putative B875 BChl binding site. The sequential loss of the B875 band also suggests that the large spectral redshift of B875 BChl is not due to exciton interactions of dimeric BChl. When chromatophores of strain NF57 were treated with acid, the B850 absorption band was stable down to pH 2; however, the B800 band was lost with a complicated titration behavior. (Supported by NSF grant DMB85-12587)

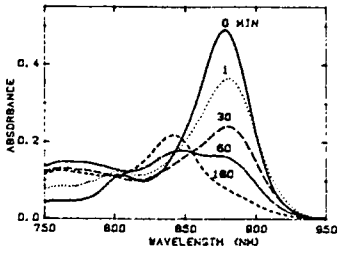


Fig.1 Spectra of M21 membranes incubated at pH 2.2 in 0.1M citrate buffer.

**M-PM-F6** SINGLE CRYSTAL ELECTRON SPIN RESONANCE STUDIES OF THE REACTION CENTER PROTEIN FROM *Rhodopseudomonas sphaeroides* WILD TYPE STRAIN 2.4.1. Harry A. Frank[a], Shahriar S. Taremi[a], David E. Budil[b], Peter Gast[b], and James R. Norris[b], [a]Department of Chemistry, University of Connecticut, Storrs, CT 06268 and [b]Chemistry Division, Argonne National Laboratory, Argonne, IL 60439

Single crystals of the photochemical reaction center protein isolated from the photosynthetic bacterium *Rhodopseudomonas sphaeroides* wild type strain 2.4.1 were obtained. At low temperatures the crystals display pronounced anisotropy in their triplet state electron spin resonance (ESR) spectra. A detailed analysis of the angle dependence of the resonance field positions revealed two magnetically nonequivalent primary donor molecules per unit cell. This agrees with the the symmetry assignment of $P_{2_12_12_1}$ deduced from previous X-ray diffraction studies (1). However, the ESR data could not be fit assuming that the unit cell axes coincide with the crystal morphological axes. Rather, in order to explain the data it was necessary to assume a rhombic crystal cross section with the unit cell axes lying along the diagonals of the rhombus. The unit cell *b* and *c* axes were found to make angles of 26 ± 2° and 64 ± 2° respectively, with one of the faces of the crystal. This work is supported by grants from the NSF (PCM-8408201), USDA (86-CRCR-1-2016) and NIH (GM-30353).

(1) Frank, H. A., Taremi, S. S. and Knox, J. R. (1987) J. Mol. Biol. **197**, (in press).

**M-PM-F7** THEORETICAL CALCULATIONS OF DYNAMICS OF THE PRIMARY ELECTRON TRANSFER IN PHOTOSYNTHETIC BACTERIAL REACTION CENTERS. Z.T.Chu, A.Boeglin, S.H.Lin, Dept. of chemistry, Arizona State University, Tempe, AZ. 85287-1604

This work proposes a new model regarding the role played by the accessory bacteriochlorophyll in the primary electron transfer(ET) reaction dynamics in bacterial reaction centers(RCs). Quantum mechanical calculations of the dynamics based on this model by using the density matrix method have been performed. The interplay of vibrational relaxation and electron processes(electron transfer, electron energy transfer,etc.) is taken into account. The calculation results indicate that the ET reaction in RCs is irreversible and that the fast vibrational relaxation is not necessary for the ultrafast ET reaction to occur in RCs. It is shown that the accessory bacteriochlorophyll could act as an intermediate in ET, but the spectroscopic observation of the state $P^+B^-H$ depends on the exact details of the electronic coupling constants and the energies of the states involved.

**M-PM-F8** The Possible Existance of a Charge Tranfer State which Precedes the Formation of $(BChl)_2^+ BPh^-$ in Rb. sphaeroides Reaction Centers. P.L.Dutton, G. Alegria and M.R.Gunner. Dept.Biochem.Biophys. Univ. of Penna. Phila.Pa 19104.

Langmuir-Blodgett RC monolayers placed between electrodes were used to determine the electric field (E) dependence of the quantum yield $\phi(E)$ for the formation of $(BChl)_2^+Q_A^-$ (BBA 851 38). There are several possible sources for the observed loss in $\phi(E)$ with fields opposing charge separation:Electron transfer from $BPh^-$ to $Q_A$ is unlikely to be the sole cause because a) no increase in the rate of decay of $(BChl)_2^+Q_A^-$, diagnostic of lowered $E_{1/2}$ $Q_A$ is seen, and b) the weak effect that the reduction in $-\Delta G^\circ$ (effected by $Q_A$ replacement) has on $\phi$. An increase in the recombination rate from $BPh^-$ to $(BChl)_2^+$ is tentatively considered E insensitive.Rather,we consider it likely that the first step(s), that is $(BChl)_2^* \rightarrow (BChl)_2^+ BPh^-$,which involves charge separation of 1.6nm ($\Delta G^\circ$ 260±100meV),is sensitive to E. Initially this electron transfer step is identified by a single rate,k.However, as shown in the figure, the behaviour of k(E) is unusual;in fact such a large field dependency supports the proposal that an intermediate state exists between $(BChl)_2^*$ and $(BChl)_2^+BPh^-$ which possesses significant charge transfer character and perhaps involves the monomeric BChl.

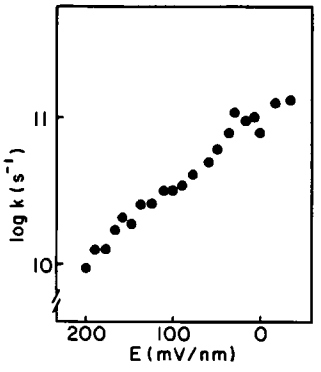


NSF DMB. 85-1833, DOE-ER 13456.

**M-PM-F9** TEMPERATURE DEPENDENCE OF THE PRIMARY ELECTRON TRANSFER IN PHOTOSYNTHETIC PURPLE BACTERIA

J.L. Martin, G.R. Fleming[§], and J. Breton[+]. (Intr. by P. Ripoche)
Laboratoire d'Optique Appliquée, Ecole Polytechnique--ENSTA, INSERM U275, 91128 Palaiseau Cedex, France;[§]On sabbatical leave from the Department of Chemistry, The University of Chicago, Chicago, Illinois 60637 USA;[+]Service de Biophysique, CEN/Saclay 91191 Gif-sur-Yvette Cedex, France.

The primary electron transfer rates in reaction centers (RCs) from Rps. viridis, Rb. sphaeroides and fully-deuterated Rb.sphaeroides have been measured with 100-fs resolution over the temperature range 8K to 300K. Our data indicate that the puzzling similarity in electron transfer rate for Rps. viridis and Rb. sphaeroides holds only at room temperature. The primary electron transfer rates increase with decreasing temperature. We observe at 10K a transfer time of 1.2 ± 0.1 ps in Rb. sphaeroides and 0.7 ± 0.1 ps in Rps. viridis. Complete deuteration of Rb. sphaeroides reaction centers produces no significant changes in the electron transfer rate. The involvement of the protein in the electron transfer process and the validity of conventional electron transfer theory to describe the primary charge separation will be discussed.

**M-PM-F10 LOW TEMPERATURE FEMTOSECOND SPECTROSCOPY OF THE INITIAL STEP OF ELECTRON TRANSFER IN REACTION CENTERS FROM PHOTOSYNTHETIC PURPLE BACTERIA**

J. BRETON*, G.R. FLEMING[+] and J.-L. MARTIN
Lab. d'Optique Appliquée, Ecole Polytechnique, ENSTA, INSERM U275, 91128 PALAISEAU CEDEX, FRANCE
*Service de Biophysique, CEN/Saclay 91191 GIF-SUR-YVETTE CEDEX, FRANCE

The initial step of charge separation has been monitored with 100-fs time resolution in reaction centers (RCs) from Rps. viridis and Rb. sphaeroides R-26 at 10K. In addition, to the native RC from Rb. sphaeroides R-26, we have also investigated RCs in which the accessory $B_M$ molecule has been removed by borohydride treatment. The main results which will be presented and discussed are :
1. The absorbance changes measured at several wavelengths in the near IR bands for excitation at 870nm at 10K, which are interpreted in terms of the formation of the state $P^+H_L^-$ with no spectral evidence for a detectable concentration of $P^+B_L^-$.
2. The large contribution from an initial bleaching in the 850-nm band in Rps. viridis RCs, at 10K, which confirms that this band can be mainly assigned to the high-energy exciton band of P.
3. The presence in all these RCs of a fast transient bleaching of the B molecule upon excitation around 600nm, which relaxes with a 400-fs time constant at both room and low temperature.

[+]On sabbatical leave from Dept. of Chemistry, Univ. of Chicago, CHICAGO, ILLINOIS 60637, USA

**M-PM-F11** ENDOR OF EXCHANGEABLE PROTONS OF THE REDUCED INTERMEDIATE ACCEPTOR IN RCS FROM RB. SPHAEROIDES R-26*; G. Feher, R.A. Isaacson, M.Y. Okamura, U.C.S.D., La Jolla, CA; W. Lubitz, Freie Universität, Berlin, Germany.

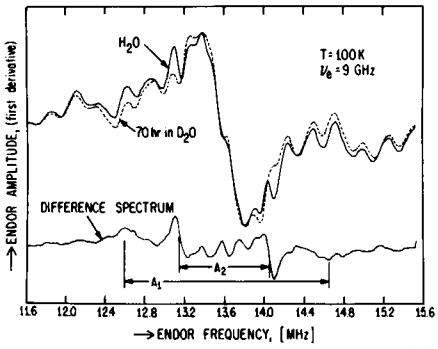


ENDOR spectra of the exchangeable protons coupled to the reduced intermediate acceptor (bacteriopheophytin$^-$) were obtained from difference spectra of RCs incubated in $D_2O$ and $H_2O$ respectively (see Fig). Exchangeable protons include ring protons (on the pyrrole nitrogens and on C-10) and H-bonded protons from the amino acid residues of the RC. We assign the major splittings $A_1$ and $A_2$ to A∥ and A⊥ of the hyperfine tensor of the carboxylic acid proton from Glu L104 which is H-bonded to the carbonyl oxygen on ring V[(2)]. This assignment was based on evidence from the line shapes and positions, indicating an approximate dipolar nature of the splittings ($|A\parallel| \approx |2A\perp|$), the functional dependence on temperature of the hyperfine couplings (hfc)[(1)] and the absence of these splittings in Bphe$^-$ in aqueous solvents. From the dipolar hfc and the calculated spin densities on the oxygen which ranged from 0.05[(3)] to 0.10[(4)], a hydrogen bond distance of 1.6 Å to 2.0 Å was deduced.
1) G. Feher, M.Y. Okamura; D. Kleinfeld; Protein Structure: Molecular and Electronic Reactivity, 399-421, Springer Verlag (1987) Eds: R. Austin et al. (see Fig. 15). 2) J.P. Allen, G. Feher, T.O. Yeates H. Komiya and D.C. Rees (1987) PNAS 84, 5730. 3) M. Plato, private communication. 4) L. Hanson and J. Fajer, private communication. *Work supported by the NSF, DFG and NATO.

**M-PM-F12** ENDOR OF THE REDUCED INTERMEDIATE ELECTRON ACCEPTOR IN BACTERIAL AND PHOTOSYSTEM II REACTION CENTERS*; W. Lubitz, M. Plato, Freie Universität, Berlin; G. Feher, R.A. Isaacson, M.Y. Okamura, U.C.S.D., La Jolla, CA 92093

Recently we reported on a highly resolved ENDOR spectrum of the intermediate acceptor radical anion I$^-$ freeze-trapped in bacterial RC's (1). We have now identified some of the hyperfine couplings (hfc's) with specific nuclei of the radical (Table) and of its surrounding (following abstract). Furthermore, the anion radicals of bacteriochlorophyll BChla and bacteriopheophytin BPha were studied in inert and coordinating solvents in the liquid and frozen state. In the Table the isotropic methyl proton hfc's of pyrrole rings I and III are compared. From MO calculations, RHF-INDO/SP (2), the observed changes can be related to interactions with the protein surrounding. These interactions are believed to influence (presumably optimize) electron transfer rates in the RC. ENDOR data were also obtained from I$^-$ in PS II (see also ref. 3) and are compared with the respective pigment anion radicals in 1,2-dimethoxy ethane.

| SAMPLE | | $A_{iso}(CH_3)$ ring I | \|MHz\| ring III |
|---|---|---|---|
| I$^-$ | (a) | +8.1 | +9.9 |
| BPh a$^-$ | (b) | +7.6 | +9.0 |
| BPh a$^-$ | (c) | +7.5 | +8.8 |
| BPh a$^-$ | (d) | +7.1 | +8.3 |
| BChla$^-$ | (b) | +9.2 | +10.8 |
| BChla$^-$ | (c) | +8.4 | +9.8 |
| BChla$^-$ | (d) | +7.6 | +9.2 |
| I$^-$ | (e) | +4.7 | +13.0 |
| Ph a$^-$ | (d) | +5.4 | +9.9 |
| Chl a$^-$ | (d) | +5.4 | +10.6 |

(a) RC's *Rb. sphaeroides* R-26, 100 K, (b) aqueous pyridine, 145 K, (c) 2-methyl THF, ~ 100 K (d) DME, 255-270 K, (e) PS II, (55 Chl/RC), 100 K.

(1) G. Feher, R.A. Isaacson, M.Y. Okamura, W. Lubitz, Biophys. J. (1986) 37, 337a; (2) M. Plato, E. Trankle, W. Lubitz, F. Lendzian, K. Mobius, Chem. Phys. (1986) 107, 185; (3) A. Forman, M.S. Davis, I. Fujita, L. K. Hanson, K. M. Smith, J. Fajer, Israel J. Chem. (1981) 21, 265.
*Work supported by the NSF, DFG and NATO.

**M-Pos1 THE EFFECT OF PROLINE RESIDUES ON THE FOLDING OF PHAGE T4 LYSOZYME**

**Bao-lu Chen, Walter A. Baase, Hale Nicholson and John A. Schellman**
**Institute of Molecular Biology, University of Oregon, Eugene, OR 97403-1229**

**The denaturation of T4 lysozyme and its mutants with single amino-acid substitutions in Gdn-HCl solution is slow at low temperatures (relaxation times in minutes to hours). The folding mechanisms of these proteins are found to be in accord with two-state behavior at pH 5 to 6. This is judged by comparing unfolding and refolding rates at conditions close to the middle of the transition as monitored by circular dichroism at 223 nm.**

**Wild type T4 lysozyme has three proline residues at positions 37, 86 and 143. In order to study the effect of proline isomerization on the folding process, we have applied the "double jump" experiment. We find there is no kinetic evidence of an additional slow phase in the conformational transition. We have measured two mutant proteins (Leu 39 to Pro and Ala 82 to Pro) with an extra proline residue (four prolines in the protein) made by site-directed mutagenesis. These mutants also show the same relaxation times for the forward and backward reactions with no indication of intermediate steps associated with the cis-trans isomerization of proline. We are investigating mutant proteins with single and mutiple substitutions of the three prolines of the wild type.**

**This work has been supported by PHS Grant GM20195 and by NSF Grant 8609113.**

**M-Pos2** THERMODYNAMIC STABILITY OF DIPHTHERIA TOXIN. G. Ramsay, D. Montgomery, D. Berger and E. Freire. Department of Biology, The Johns Hopkins University, Baltimore, MD 21218

The thermal stability of monomeric, nicked, nucleotide free and nucleotide bound diphtheria toxin has been investigated by high sensitivity differential scanning calorimetry. At pH 8 and low ionic strength, the thermal unfolding of the nucleotide free toxin is characterized by a transition temperature ($T_m$) of 51°C and an enthalpy change ($\Delta H$) of ~250 kcal/mole. The thermal unfolding of the nucleotide bound toxin, on the other hand, is characterized by a $T_m$ of 57°C and a $\Delta H$ of ~300 kcal/mole. The larger $\Delta H$ for the nucleotide bound toxin reflects the enthalpy associated with the release of the nucleotide from the toxin upon unfolding and/or any excess enthalpy arising from a nucleotide induced conformational change in the native form of the toxin. Both toxin species have asymmetric excess heat capacity profiles which can be deconvoluted into two independent two-state transitions most likely corresponding to the A and B fragments. The thermal stability of the nucleotide bound toxin has been studied as a function of pH and ionic strength. The pH dependence of $T_m$ is sigmoidal and characterized by an inflection point centered at pH 5.3. Between pH 7 and pH 4, the melting temperature decreases 27°C. The location of the midpoint of the pH transition is independent of salt concentration but at high ionic strength (0.2 M NaCl) all the Tm's are 5°C lower than in the absence of added salt. The enthalpy change for the unfolding transition is also pH dependent and shows a marked decrease as the pH is lowered below 6 until no detectable change is observed at pH 3. These results provide a thermodynamic basis for the mechanism of toxin insertion into the membrane. (Supported by NIH grant GM-37911.)

**M-Pos3** POINT CHARGE CONTRIBUTIONS TO DIFFUSION-LIMITED CATALYSIS BY SUPEROXIDE DISMUTASE. Jacqueline J. Sines, Stuart A. Allison, Dept. of Chemistry, Georgia State Univ., Atlanta, GA 30303 and J. Andrew McCammon, Dept. of Chemistry, Univ. of Houston, Houston, TX 77004

Brownian dynamics simulations are used to analyze long-range and local dielectric effects of individual charges in the superoxide dismutase dimer. Studies are based on a grid model of the bovine erythrocyte protein in oxidized ($Cu^{+2}$) form with linearized Poisson-Boltzmann modelling of electrostatic forces. Point charges associated with protein residues and the active site copper atom are varied. Results are presented for a range of salt concentrations spanning physiological levels. Simulation of catalysis by $Cu^{+1}$ SOD produced rates and salt dependence identical to the oxidized form within the statistical range of the data. Pronounced rate variations are seen in simulations in which active site residues are altered, with increasing rates associating with increasing positive charge. The introduction of an offsetting central charge only slightly reduces these effects, evidence of their local nature. In contrast, outlying residues yield rates which are consistent with purely long-range effects as simulated by a dummy charge in the center of the protein. Simultanaeous neutralization of glutamic acid 131 and arginine 134 produced a relatively small 10% decrease in the rate. SUPPORT: DMB-8451873 from NSF.

**M-Pos4** REDUCTION STUDIES ON RIBONUCLEOTIDE REDUCTASE FROM ESCHERICHIA COLI. A. Gräslund[a], M. Sahlin[b], B.-M. Sjöberg[b], L. Petersson[a], and A. Ehrenberg[a]. (Intr. by S. Scheiner.)
[a]Department of Biophysics and [b]Department of Molecular Biology, University of Stockholm, S-10691 Stockholm, Sweden.

Ribonucleotide reductase from E. Coli consists of two nonidentical subunits, proteins B1 and B2. The active form of protein B2 carries an antiferromagnetically coupled pair of high-spin ferric ions, linked by a μ-oxo bridge, and a stable free radical, which is an oxidized form of tyr-122 in the polypeptide chain. The iron center and the free radical are close enough in space to exhibit magnetic interaction (Sahlin et. al. (1987) Biochemistry, 26, 5541-48).

The free radical and the iron center of protein B2 were reduced either electrochemically or chemically by dithionite in the presence of suitable mediators such as benzyl viologen or phenosaffranin. The process was followed by optical spectroscopy and EPR. Regeneration of the active state of the protein was achieved by exposure to oxygen. These in vitro reduction-oxidation processes mimic the action of a NAD(P)H: flavin oxidoreductase enzyme system in E. Coli, whereby the essential free radical is introduced into an inactive non-radical form of protein B2 and the enzymatically active form is restored (Fontecave et. al. (1987) J. Biol. Chem. 262, 12325-31 and 12332-36).

**M-Pos5** PROTEIN SPIN LABELING WITH MALEIMIDE. J.R. Perussi, M.H. Tinto, O.R. Nascimento, M. Tabak - Instituto de Física e Química de São Carlos, Universidade de São Paulo, C.P. 369, 13560 - São Carlos, SP, Brasil.

Characterization of the effective spin labeling of several proteins with maleimide nitroxide has been made. It is commonly accepted that spin labeling of human hemoglobin (Hb) results in the binding of two labels at the two β-93 cysteine residues. In previous work[1] we have studied the kinetics of maleimide (MAL) binding to Hb showing that the reaction is quite complex. Quantitation of the amount of bound spin label showed that it is much less then the expected. Using calibration curves and measuring the areas of bound and free signals after the end of reaction a considerable reduction of the total spin labels concentration was observed. This is interpreted as due to the reduction of MAL catalyzed by Hb and dependent on the presence of free SH groups. Hb previously blocked with N-ethylmaleimide was unable to reduce the spin label. In the case of bovine serum albumin (BSA) was also observed this reaction while horse myoglobin was unable to reduce the nitroxide. The reduction of TEMPOL was also observed in the presence of Hb and BSA. The dependence on SH group concentration is very different for both nitroxides. Our results suggest that a carefull analysis of the binding should be performed in protein spin label studies.

1. J.R. Perussi, M.H. Tinto, V. Massaro, O.R. Nascimento, M. Tabak (1986), Bull. Magn. Res. 8, 209.

Support: FAPESP, CNPq, FINEP and CAPES.

**M-Pos6** PHYSICAL PROPERTIES OF CONSTRAINED TRYPTOPHAN, M.Sattler, L Tilstra, W. Colucci, F. R. Fronczek, M. D. Barkley. Intr. by: B. J. Hales

A constrained tryptophan derivative, 3-carboxy-1,2,3,4-tetrahydro-2-carboline, has been synthesized. In this derivative the α-amino group is incorporated into a six-member ring. The crystal structure has been solved. The conformation of the new ring is suggestive of a twisted chair with C-5 below and N-2 above the plane of the indole moiety (the plane of the paper).

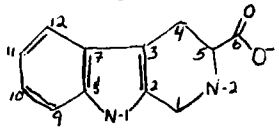


Another possible conformation is one in which C-5 is above and N-2 below the plane of the paper. The twisted chair is converted to a reverse twisted chair by rotation about the C-4, C-5 bond. MM-2 calculations suggest that the reverse twisted chair conformer is approximately one-third as stable as the twisted chair.

The fluorescence decays of the zwitterion and the anion are measured at 20°C. The decay curves are adequately fit by monoexponential functions at pH 5.5, 7.5, and 11.3. The lifetime decreases from 6.7 ns to 4.9 ns over this pH range. Indole also exhibits monoexponential fluorescence decay with a similar decrease in the lifetime over this pH range. The lifetimes obtained for the monoexponential decay of indole and biexponential decay of tryptophan agree with literature values. NMR measurements at pH 11.3 show a shift relative to tryptophan.

**M-Pos7** ELECTRIC BIREFRINGENCE STUDIES OF NON-POLYMERIZABLE SKELETAL AND SMOOTH MUSCLE TROPOMYOSINS. Charles A. Swenson and Nancy C. Stellwagen, Department of Biochemistry, University of Iowa, Iowa City, IA 52242.

Electric birefringence studies have been performed on non-polymerizable tropomyosins to assess their relative flexibilities in solution. The non-polymerizable tropomyosins were prepared by carboxypeptidase treatment of tropomyosins isolated from rabbit skeletal and from turkey gizzard smooth muscle. The electric birefringence measurements have been made as a function of electric field strength, pulse length, concentration, ionic strength and temperature. The temperature dependencies of the measured rotational relaxation times, after correction for solution viscosity, are interpreted as changes in structural rigidity and the results are compared with the thermal denaturation profiles as measured for these molecules in a differential scanning calorimeter. We will also present data on the electro-optical parameters for these molecules. Supported by grants from AHA and NIH, GM-29690.

**M-Pos8** **EFFECTS OF SINGLE SITE MUTATIONS AT THE INTERCHAIN INTERFACES OF E. COLI ASPARTATE TRANSCARBAMOYLASE.** D. S. Burz and N. Allewell, Wesleyan University, Middletown, CT 06457; J. M. Sturtevant, Yale University, New Haven, CT 06520.

E. coli aspartate transcarbamoylase contains 6 c chains and 6 r chains, organized as two catalytic trimers ($c_3$) and three regulatory dimers ($r_2$). Changes in the subunit interactions are known to underlie the allosteric regulatory mechanism, and mutations at these interfaces have been shown to produce major changes in the allosteric properties of the enzyme {Robey and Schachman, J. Biol. Chem. 259, 11180 (1984); Middleton and Kantrowitz, PNAS 83, 5866 (1986); Wales and Wild, in preparation}. In order to interpret these results, it will be necessary to examine the effects of these mutations on protein stability and subunit interaction energies. We have begun to use differential scanning calorimetry, analytical gel chromatography and hydrogen exchange to examine these questions. Results to date indicate that four mutations (Arg 130R -> Gly, Glu 50C -> Gln, Glu 239C -> Gln, Tyr 165C -> Phe) alter $T_{1/2}$ and $\Delta H$ of melting of the $r_2$ subunits of $c_6r_6$, but have negligible effects on the thermal transition of the $c_3$ subunits. One mutation, Arg 269C -> Gly, reduces $T_{1/2}$ for both $r_2$ and $c_3$ subunits to 62°C. Addition of the bisubstrate analog PALA increases $T_{1/2}$ for the $c_3$ transition, partially resolving it. Differences in Stokes radii and changes upon addition of effectors can be demonstrated by analytical gel chromatography, providing information on the quaternary structure of each mutant and the ability of effectors to induce conformational transitions. Experiments examining stability as a function of urea concentration are underway. Supported by NIH grants AM-17335 (to NMA) and GM-04725 (to JMS) and NSF grant DMB-8421173 (to JMS).

**M-Pos9** TERTIARY AND QUATERNARY STRUCTURAL DIFFERENCES BETWEEN TWO GENETIC VARIANTS OF BOVINE CASEIN BY SMALL-ANGLE X-RAY SCATTERING. Helmut Pessen[1], Thomas F. Kumosinski[1], Harold M. Farrell, Jr.[2], and Harry Brumberger[1]. [1]Eastern Regional Research Center, USDA, Philadelphia, PA 19118 and [2]Department of Chemistry, Syracuse University, Syracuse, NY 13244-1200.

The colloidal casein complexes of bovine milk consist of four fractions. Two genetic variants, A and B, of $\alpha_{s1}$-casein (the predominant fraction) result in milks with markedly different physical properties, such as solubility and heat stability. To investigate the molecular basis for these differences, small-angle X-ray scattering was performed on colloidal micelles (with $Ca^{+2}$) and on submicelles (without $Ca^{+2}$). Scattering curves for submicelles of both variants showed multiple Gaussian character interpretable in terms of two concentric regions of different electron density, i.e., a 'compact' core and a relatively 'loose' shell. In the A variant, there was a third Gaussian, reflecting a negative interaction due to high charge-to-mass ratio. The data for the micelles, for which scattering yields cross-sectional information, could be analyzed by a sum of three Gaussians; for these, the corresponding two lower radii of gyration represent the two concentric regions of the submicelles, while the third reflects the packing ratio of submicelles within the micellar cross-section. Most of the molecular parameters obtained showed small but consistent differences between A and B, but for several the differences were particularly notable: A has a larger radius of gyration for the 'loose' region (96 Å vs. 88 Å), a greater molecular weight of the 'compact' region (82,000 vs. 60,000), and a much higher packing ratio (6:1 vs. 3:1). Reasons for these differences are to be sought in sequence differences and in differences in calcium-binding sites and charge distribution.

**M-Pos10** SMALL-ANGLE X-RAY SCATTERING INVESTIGATION OF THE MICELLAR AND SUBMICELLAR FORMS OF BOVINE CASEIN. Thomas F. Kumosinski[1], Helmut Pessen[1], Harold M. Farrell, Jr.[1], and Harry Brumberger[2]. [1]Eastern Regional Research Center, USDA, Philadelphia, PA 19118; [2]Dept. of Chemistry, Syracuse University, Syracuse, NY 13244-1200.

Whole casein occurs in milk as spherical colloidal complexes, called micelles. On removal of $Ca^{+2}$, these dissociate into smaller noncolloidal complexes (submicelles). To investigate the controversial question whether the structural integrity of these hydrophobically stabilized submicelles is maintained within the electrostatically stabilized micelle, small-angle X-ray scattering was performed on whole casein under submicellar ($Ca^{+2}$ removed) and micellar ($Ca^{+2}$ re-added) conditions. Submicellar scattering curves showed two Gaussian components which could be interpreted in terms of a particle with two concentric regions of different electron density, a relatively compact core and a looser shell. Calculated distance distribution functions and normalized scattering curves were consistent with an overall spherical particle with concentric inner core of higher electron density. Micellar scattering data, which can yield only cross-sectional information, could be analyzed by a sum of three Gaussians with no residual function. The two Gaussians with the lower radii of gyration could be interpreted as indicating the two concentric regions of different electron density of inhomogeneous spherical particles; the third Gaussian was shown to reflect the packing density of these particles within the micellar cross-section, which was 3:1 for this system. These results are a clear indication that submicellar inhomogeneous particles containing hydrophobically stabilized inner cores persist within the colloidal micelle.

**M-Pos11** RELAXATION KINETICS OF CALMODULIN-CALCIUM INTERACTIONS. Herbert R. Halvorson, Henry Ford Hospital, Detroit, Michigan 48202

Interactions between calcium and calmodulin were studied by repetitive pressure-jump relaxation kinetics, using the altered fluorescence of reversibly bound ANS to provide a signal. The reaction is driven by the volume change (expansion) upon calcium binding. Lengthy signal-averaging permitted study of relaxations with small amplitude. The relaxations can be grouped into three distinct phases. The slowest is a conformational change with a 10 $s^{-1}$ rate constant, identical with a rate for calcium dissociation assigned to the C-terminal domain by Martin et al (EJB 151:543, 1985). The intermediate rate process is ascribed to the N-terminal domain and the apparent dissociation rate constant agrees with that found by Martin et al. The fastest process corresponds to elementary calcium binding with an association constant of 5-10 x $10^7$ $M^{-1}$ $s^{-1}$. This is slower than typical calcium-ligand interactions by an order of magnitude and may reflect the complexity of the chelation process.

These data excluded a significant role for the C-terminal domain in a dynamic regulatory process, the response to a lowered calcium concentration being too slow. The probable functional significance of the C-terminal domain binding site is to assure the existence of a calmodulin-enzyme complex at resting levels of calcium concentration. The dynamics of regulation then become the responsibility of the N-terminal domain. Progress on the expression of the N-terminal interaction site will be reported.

Supported in part by GM 23302

**M-Pos12** FACTOR ANALYSIS OF THE NEAR UV ABSORPTION SPECTRUM OF PLASTOCYANIN. S.R. Durell, E.L. Gross; Biophysics Program and Dept. of Biochem.; The Ohio State University; Columbus, OH. 43210

The near UV absorption spectrum of Plastocyanin (PC) is a superposition of absorption due to the tyrosine residues, the phenylalanine residues, and transitions involving the copper center. The copper center transitions are metal-ligand charge transfer and copper 3d-4s,4p Rydberg transitions. The effects that the redox state of the copper atom and environmental perturbations, such as pH and ionic strength, have upon the absorption of the individual chromophores provides useful information about the conformation of the protein. Unfortunately, the composite nature of the spectrum makes it difficult to discern the effects upon each separate chromophore. We have used a method of factor analysis, developed by Dr. R.T. Ross, to separate 16 absorption spectra (4 species of PC in both redox states and at two pH values) into two independent spectral components. The first component has a maximum at 278 nm and represents absorption due mainly to the tyrosine residues; the second component has a maximum at 250 nm and represents absorption due to the phenylalanine residues and the copper center. The absorption magnitude of the first component varied correctly according to the number of tyrosines in each PC species, with smaller variations in response to redox state and pH. The change of absorption magnitude of the second component between the oxidized and reduced forms of PC was the same in the 4 different species. This suggests that the redox state dependent change in the geometry of the copper center is an important feature conserved among different species of PC. We have also experimented with analyzing a tri-linear data set that combines circular dichroism and fluorescence spectra with the absorption spectra. This second approach may facilitate the assignment of bands in the complex near UV CD spectrum of PC.

**M-Pos13** STRUCTURE OF RECOMBINANT HUMAN TUMOR NECROSIS FACTOR
Tsutomu Arakawa, Linda O. Narhi and David A. Yphantis*, Amgen, 1900 Oak Terrace Lane, Thousand Oaks, Ca 91320 and *Department of Molecular and Cell Biology, University of Connecticut, Storrs, CT 06268 and Department of Biology and Institute of Molecular Biology and Biotechnology, University of Crete, Iraklion, Crete
Both recombinant human tumor necrosis factor (TNF) and the natural protein exhibit a variety of biological activities. We have examined the structure of TNF in solution: sedimentation equilibrium experiments showed TNF to be in the form of a trimer (MW=52,000) at both pH 8.6 and pH 6.0 with distinct dissociation into monomers at pH 6.0. Gel filtration experiments at pH 8.6 showed TNF to be comparable in behavior to ovalbumin (46,000) with no evidence of dissociation. Gel permeation HPLC of TNF at both pH 6.0 and pH 7.0 at protein concentrations higher than 0.2 mg/ml gave a Stokes radius of 2.3nm, a value smaller than that expected from a globular trimer. Thus the TNF trimer has a very compact structure. In agreement with the sedimentation measurements, gel permeation HPLC at pH 6.0 indicates dissociation, probably from trimer to monomer, with decreasing protein concentration. Gel permeation HPLC also indicates dissociation of the TNF trimer on dilution at pH 7.0: The component with 2.3nm Stokes radius is gradually replaced by a 2.2nm Stokes radius component. This apparent dissociation at pH 7.0 may involve a dimer, since an asymmetric dimer can be as large as a compact trimer in hydrodynamic effective volume. Appropriate sedimentation experiments are under way. (Supported in part by NSF Grant #BBS-8612159).

**M-Pos14** SPECTROSCOPIC AND HYDRODYNAMIC CHARACTERIZATION OF SYNTHETIC HUMAN AND PORCINE RELAXIN.
Steven J. Shire*, David L. Foster** and Ernst Rinderknecht**; *Pharmaceutical Research and Development Department, and **Process Recovery Department; Genentech, Inc.; So. San Francisco, CA.

Relaxin is a protein hormone of ~6000 molecular weight which plays a major role in reproductive biology in various species[1]. The protein consists of 2 polypeptide chains linked by disulfide bonds and maintains homology with insulin in terms of the relative spacing of cysteine residues in the amino acid sequence. The far UV circular dichroism (CD) spectrum from 250 to 190nm of synthetic human relaxin is similar to that obtained for porcine zinc free insulin whereas the spectrum obtained for porcine relaxin is substantially different. In particular, the CD band at ~209nm is more negative for porcine relaxin than human relaxin (~-24000 compared to -14000 deg $cm^2$ $dmol^{-1}$). Sedimentation equilibrium analytical ultracentrifuge measurements at 20°C yield whole cell weight average molecular weights at $C_o$=0.2mg/mL of 9900 and 6600 for human and porcine relaxin respectively. The centrifuge results suggest that human relaxin exists in a monomer-dimer equilibrium under solution conditions investigated whereas porcine relaxin is essentially monomeric. This is consistent with the circular dichroism experiments since zinc free insulin is also capable of dimerization[2]. These experiments also appear to support the conclusions of Schwabe and Harmon[2] regarding the effect of the dye benzopurpurine 4-B on the far UV CD spectrum of porcine relaxin. The shift of the porcine relaxin CD spectrum to a more "insulin like" spectrum was attributed to protein association mediated by interaction with the dye.

(1) G.D. Bryant-Greenwood, Endocrine Reviews 3, 62 (1982).
(2) C. Schwabe and S.J. Harmon, BBRC 84,374 (1978).

**M-Pos15** EFFECT OF pH ON FLUORESCENCE LIFETIME AND ANISOTROPY OF TYROSYL RESIDUES IN CARDIAC TROPONIN C. Ronglih Liao[1], Chien-Kao Wang[1], Iain Johnson[2], Bruce Hudson[2], and Herbert C. Cheung[1]. (1) Department of Biochemistry, Univ. of Alabama at Birmingham, Birmingham, AL 35294 and (2) Department of Chemistry, Univ. of Oregon, Eugene, OR 97403

We have measured the fluorescence emission and anisotropy decays of the three tyrosyl residues of cardiac troponin C (CTnC) using a cavity-dumped laser that was synchronously pumped by a Nd:YAG laser. The emission decay excited at 290 nm and observed at 320 nm was best represented by a sum of three exponentials. At 20°C and neutral pH, $\tau_1$ ~ 0.4 ns, $\tau_2$ ~ 1.6 ns, and $\tau_3$ ~ 3.7 ns. Saturation of TnC with $Ca^{2+}$ induced ~ 10% increase in the lifetimes. When the temperature was lowered to 5°C, the lifetimes also increased by ~ 10%. A reduction of pH from 7.2 to 5.2 resulted in a 20% increase in all three components of the emission decay.

The anisotropy decay showed two correlation times. At 20°C and neutral pH, $\phi_1$ ~ 1.0 ns and $\phi_2$ ~ 11.7 ns. $\phi_1$ arises from rapid motions of the tyrosyl residues while $\phi_2$ reflects the overall protein motion. The latter result is 50% larger than that expected of an equivalent sphere with 20% hydration. In the presence of $Ca^{2+}$, $\phi_1$ ~ 1.6 ns and $\phi_2$ ~ 9.8 ns. The effect of acid pH is a reduction of $\phi_2$ by 17%. This result obtained at acid pH is different from that obtained with skeletal TnC (STnC). In an accompanying poster, we present data showing that at acid pH $\phi_2$ for STnC as deduced from anisotropy decay of the two tyrosyl residues is some 30% higher than at neutral pH. These results suggest very different hydrodynamic properties of the two proteins at low pH (Supported in part by NIH AM25193).

M-Pos16 A COMPARISON OF TYROSINE FLUORESCENCE AND ANISOTROPY DECAYS OF SKELETAL TROPONIN C AND BOVINE BRAIN CALMODULIN. Chien-Kao Wang[1], Ronglih Liao[1], Iain Johnson[2], Bruce Hudson[2], and Herbert C. Cheung[1]. (1) Dept. of Biochemistry, Univ. of Alabama at Birmingham, Birmingham, AL 35294 and (2) Dept. of Chemistry, Univ. of Oregon, Eugene, OR 97403

Using time-resolved picosecond fluorescence spectroscopy, we examined the fluorescence emission and anisotropy decays of tyrosyl residues in skeletal troponin C (STnC) and bovine brain calmodulin (BCaM). With excitation at 290 nm and emission at 320 nm, the decays exhibited tri- and tetra-exponential kinetics for STnC and BCaM, respectively. At 20°C and neutral pH, the following lifetimes were observed: (1) apo-STnC, 0.4, 1.3, and 2.7 ns, and (2) apo-BCaM, 0.09, 0.4, 1.4, and 3.9 ns. The longest lived component of the emission in STnC comprises ~ 42% of observed intensity, however, the corresponding component in BCaM contributes only ~ 5%. Binding of $Ca^{2+}$ to the proteins induced an increase of the average lifetimes ~ 23% (STnC) and ~ 24% (BCaM). When temperature was lowered to 5°C, the lifetimes also increased ~ 24% (STnC) and ~ 12% (BCaM). A decrease of pH from 7.2 to 5.2 resulted in an increase of the lifetimes ~ 20% (STnC) and ~ 22% (BCaM).

The anisotropy decays exhibited two rotational correlation times for both proteins. AT 20°C and neutral pH, (1) apo-STnC, $\phi_1$ ~ 0.18 ns, $\phi_2$ ~ 10.1 ns, and (2) apo-BCaM, $\phi_1$ ~ 0.13 ns, $\phi_2$ ~ 7.2 ns. The $\phi_2$ values suggested that both proteins were not highly asymmetric at pH 7.2. Addition of $Ca^{2+}$ to the proteins resulted in an increase of $\phi_2$ ~ 22% in STnC and ~ 5% in BCaM. A decrease of pH from 7.2 to 5.2 led to an increase of $\phi_2$ ~ 37% for STnC and ~ 31% for BCaM. These results suggested that hydrodynamic properties of STnC and BCaM are similar at low pH (Supported in part by NIH AM-25193).

M-Pos17 INDOLE PROTON EXCHANGE RATES OF NATIVE AND THERMALLY DENATURED T4 PHAGE LYSOZYME MUTANTS CONTAINING SINGLE TRYPTOPHAN RESIDUES

Cynthia L. Phillips, Lawrence P. McIntosh, and F. W. Dahlquist
Institute of Molecular Biology, University of Oregon, Eugene, OR 97403

Proton exchange rates in proteins are sensitive to local structure and solvent accessiblity. Indole N-H proton exchange rates in wild type and mutant T4 phage lysozymes were measured using proton nuclear magnetic resonance $T_1$ and $H_2O$ saturation transfer experiments. Wild type T4 lysozyme has three tryptophan residues at positions 126, 138, and 158; whereas each of the three mutants has two of the tryptophan residues replaced by tyrosine residues. The indole proton resonances in the native wild type protein have different chemical shifts, whereas in the denatured protein all three have the same chemical shift, thus the neccessity of studying the mutants to measure single indole proton exchange rates in the denatured T4 lysozymes. Near the midpoint of the thermal denaturation of the mutant proteins (30 deg. C, pH 2.5, 25 mM $H_3PO_4$), both the native and denatured indole proton resonances are resolved. In native T4 lysozyme, the three tryptophans show different exchange kinetics. Preliminary results show the indole protons in the three denatured proteins exchange at comparable rates, implying similar indole environments in the denatured state. In addition, the denatured protein indole protons exchange slower than N-acetyltryptophanamide, suggesting there is lowered proton accessibility in the denatured proteins.

M-Pos18 USES AND IMPLICATIONS OF LINEAR ENTHALPY-ENTROPY COMPENSATION PATTERNS OBSERVED IN PROTEIN REACTIONS. Rufus Lumry, University of Minnesota, Minneapolis, Minnesota, 55455.

Enthalpy-entropy compensation plots are proving to be ubiquitous in data from studies of physiological functions of proteins (cf. The Fluctuating Enzyme, Wiley 1986). Each plot corresponds to a linear-free-energy relationship among the subprocesses of a protein linkage system. The linearity in any case is due to weak coupling, close adherence to a mean-field approximation or the large "free-energy capacity" of proteins conformations, i.e., significant free-energy changes produce small conformation readjustments. The linear behavior makes linkage-analysis relatively simple and reveals normal modes of the protein machine, i.e., orthogonal combinations of subprocesses responding to changes in single independent variables. Compensation plots are characterized by their slopes, $T_c$, and when these are reliably close to physiological temperatures, the width of the fluctuation distribution function is large, so large as to indicate that the fluctuations of conformation and coupled subprocesses which describe the operation of the machine occur with high probability in the resting protein free of ligand or substrate. Hemoglobin is a well studied example with $T_c$ values rarely outside the range 285-310K. Surprisingly, enzymes appear to behave similarly. Given the $T_c$ values for a protein system, the phenomenological G, H and S changes in the single steps of function can be decomposed into contributions from the individual subprocesses, as will be illustrated with chymotrypsin. $T_c$ values for proteins appear to fall in restricted ranges, e.g., water-protein interactions, 280-310K and 360-385K; disruption and proton-exchange of knots, 330-360K; substrate binding, 200-240K; transition-state formation in primary-bond rearrangements, 430-500K. Compensation behavior is frequently observed in studies of mutant families of single proteins.

**M-Pos19** MULTINUCLEAR SPIN RELAXATION STUDIES OF MYOFIBRILLAR PROTEIN HYDRATION AND SALT BINDING.

T.F. Kumosinski*, I.C. Baianu** + and P.J. Bechtel**@, *USDA, ARS Eastern Regional Res. Center, 600 E.Mermaid Lane, Philadelphia,PA, and **University of Illinois at Urbana,+Dept. of Food Science, Physical Chemistry and NMR Laboratories, 567 Bevier Hall,905 S. Goodwin Avenue, and @Depts. of Animal Science and Physiology, Muscle Biology Laboratory, Urbana, Illinois 61801.

A complex, nonlinear dependence of $^{17}O$ and $^{23}Na$ NMR relaxation rates of myofibrillar protein and salt concentrations in aqueous solutions was previously reported. Over a wide range of protein and salt concentrations, the NMR absorption peaks for $^{17}O$, $^{2}H$, $^{7}Li$ and $^{23}Na$ were single Lorentzian, consistent with a two-site, fast exchange model. Previous reports have shown that the dependence of the $^{2}H$ NMR relaxation rates on protein concentration in $D_2O$ solutions with salt can be fitted quantitatively only by taking into account the protein activity coefficients. The $^{17}O$ NMR transverse relaxation rates of NaCl and LiCl solutions in $D_2O$ exhibited also a nonlinear dependence on salt concentration. This variation could be readily modeled, at all salt concentrations, by a simple Debye-Huckel expression for the activity of the electrolytes using nonlinear regression analyses on a digital computer. $^{23}Na$ NMR transverse relaxation rates of myofibrillar protein (MFP) solutions in $D_2O$ with varying salt concentrations,for a fixed protein concentration, could be analyzed by assuming both salt/water binding and chemical exchange contributions to the nuclear spin relaxation. A simple binding isotherm allowed us to fit quantitatively the variation of the bound relaxation rate with the salt concentration, and yielded a soudium binding constant of 54 1/mole, corresponding to one salt binding site to an average domain size of 5.6 kD within MFP. The variation with salt in the chemical exchange contribution reflects the preferential binding term of the second virial coefficient of activity of the MFP.In MFP solutions,water is exchanged as the hydrated ion species.

**M-Pos20** A GENERAL SOLUTION TO COMPLEX TRANSIENT KINETIC MECHANISMS.

H.D. White, A. Strand, and X.Z. Zhang, Dept. of Biochem., E. Virginia Medical School, 700 Olney Rd., Norfolk, VA.

We have developed a general method for solving transient kinetic equations using LaPlace transforms, which can be used to transform systems of differential equations that describe pre-steady state kinetics to systems of linear algebraic equations. The 'transformed' equations have the same form as steady state rate equations and can be 'solved' using the same rules that have previously been devised for steady state equations by King and Altman. The general form of the presteady state solution is:

$$I(t) = I_o + \sum_{i=1}^{n-1} I_i e^{-k_i t}$$

where I(t) is the time dependence of the physically observed property of the system, $I_o$ is the value of I(t) at t=0, n is the number of intermediates in the mechanism, $k_i$ are the observed rate constants (reciprocals of the relaxation times), t is time, and $I_i$ are the amplitude coefficients associated with each observed rate constant. We have written a program in compiled basic to run on a personal computer to evaluate $I_i$ and $k_i$. The program will evaluate the coefficients of a mechanism with six intermediates and five relaxations times in less than one second on a 8 MHz PC equipped with a math coprocessor. The most complex mechanism that we have solved, a mechanism of actomyosin ATP hydrolysis containing 12 intermediates, required approximately 30 minutes. We believe that this method could be used to evaluate the differences in transient kinetic properties of complex biochemical mechanisms such as the four and six state models of actomyosin ATP hydrolysis. This work is supported by a research grant from the American Heart Association.

**M-Pos21**

INTERACTION OF A SPIN-LABELED ANALOG OF ADENOSINE TRIPHOSPHATE WITH THE CHEMOTAXIS PROTEIN, CHEY.

L. Kar[1], Y. Lee[1], P. Matsumura[2] and M. Johnson[1], Departments of Medicinal Chemistry and Pharmacognosy[1] and Biological Sciences[2], University of Illinois at Chicago, Chicago, IL 60680.

The chemotaxis protein, CheY, plays a fundamental role in the mechanism of flagellar rotation in E. coli. As an initial step toward understanding the functional behavior of CheY, we are studying its interaction with a variety of small molecules. We have performed epr and $^{1}H$ and $^{31}P$ nmr experiments to study the interactions of a nitroxide spin labeled analog of adenosine triphosphate (SL-ATP), of ATP, and of adenosine monophosphate (AMP) with CheY. We find that, in the presence of low SL-ATP concentrations, the proton nmr spectrum of CheY exhibits strong suppression of two or three resonances in the aromatic region, and of one resonance in the aliphatic region, indicating that SL-ATP exhibits fairly strong, stereochemically specific binding to the protein. Results from epr measurements with SL-ATP and nmr measurements with ATP and AMP both suggest that binding is primarily mediated through the phosphate groups, and that the adenosine plays little or no role in binding. The significance of these results for CheY function will be discussed.

Supported in part by grants from the National Institutes of Health and the National Science Foundation.

**M-Pos22** ULTRACENTRIFUGAL ANALYSIS OF REVERSIBLE SIMULTANEOUS HOMOGENEOUS AND HETEROGENEOUS DIMER FORMATION BY SMALL PEPTIDES. Marc S. Lewis, Samuel W. Luborsky and Kenneth M. Yamada, Division of Research Services and National Cancer Institute, National Institutes of Health, Bethesda, MD 20892.

An interaction involving both homogeneous and heterogeneous associations is one of the most complex systems which can be studied by analytical ultracentrifugation. We report here on such a system involving the interaction of the tetrapeptide argininyl-glycyl-aspartyl-serine (P1) obtained from fibronectin with the reversed sequence tetrapeptide seryl-aspartyl-glycyl-arginine (P2), both of which undergo reversible self-association to form dimers. The equilibrium constants for dimer formation for the individual peptides can be obtained by fitting the ultracentrifugal equilibrium concentration distributions with the mathematical model:

$$c_r = c_{b,i}\exp(AM(r^2 - r_b^2)) + QK_i c_{b,i}^2 \exp(2AM(r^2 - r_b^2))$$

where the c's are expressed on a concentration scale of grams per liter, fringe number or optical density and Q is a conversion factor to permit the use of equilibrium constants on a molar scale. With the values of $K_1$ and $K_2$ known, the heterogeneous association constant, $K_{1,2}$, can be obtained by fitting the mixed association concentration distribution with the mathematical model:

$$c_r = (c_{b,1} + c_{b,2})\exp(AM(r^2 - r_b^2)) + Q(K_1 c_{b,1}^2 + K_2 c_{b,2}^2 + K_{1,2} c_{b,1} c_{b,2})\exp(2AM(r^2 - r_b^2)).$$

At 20°C, values of 6.19, 1.98 and 8.89 liters/mol were obtained for $K_1$, $K_2$ and $K_{1,2}$ respectively, and the corresponding values of $\Delta G^\circ$ were -1.06, -0.40 and -1.27 kcal/mol, implying relatively weak assocoations.

**M-Pos23** **THE MECHANISM OF CRYOPROTECTION OF PROTEINS BY SOLUTES.** **John F. Carpenter and John H. Crowe, Department of Zoology, University of California, Davis, CA 95616.**

**Organic solutes have been used for decades to stabilize proteins during freeze-thawing. There has been much speculation about the mechanism by which these solutes exert their protective influence. However, to date there has been no mechanism proposed that could satisfactorily account, at least in our minds, for the fact that cryoprotection is afforded by a broad array of chemical compounds. Timasheff and his colleagues have already solved this dilemma for nonfrozen, aqueous systems. They have demonstrated (via thermodynamic arguments) that stabilization of proteins by a wide variety of solutes results, in every case, because the solutes are preferentially excluded from contact with the surface of proteins. To determine if the same mechanism is operative during freeze-thawing, we have tested the capacity of 28 different compounds (including sugars, polyols, amino acids, methylamines and lyotropic salts) to protect lactate dehydrogenase (LDH) from inactivation during freeze-thawing. The only characteristic that these solutes have in common, as group, is that have all been shown to be preferentially excluded from contact with the surface of proteins in aqueous solution. All the compounds tested, except NaCl, protected the enzyme, to varying degrees. Conversely urea and guanidine HCl, which are known to bind to proteins, enhanced the inactivation of LDH during freeze-thawing. Thus, we conclude that the mechanism advanced by Timasheff to explain stabilization of proteins by solutes in nonfrozen, aqueous systems applies equally as well to stabilization in the frozen state.** **(Supported by grant DMB 85-18194 from NSF).**

**M-Pos24** QUANTITATION OF THE ASSOCIATION BETWEEN PRETHROMBIN-1 AND FACTOR Vh Elizabeth A. Luckow, Charles T. Esmon* and Thomas M. Laue, Department of Biochemistry, University of New Hampshire, Durham NH 03824, *Oklahoma Medical Research Foundation, Oklahoma City OK 73104.

Regulation of the strength of the association between blood coagulation factor Va and prothrombin governs, in part, the rate of thrombin production by the prothrombinase complex (serine protease Xa, protein-cofactor Va, $Ca^{2+}$ and phospholipid). This association is mediated by the Vh subunit of Va. Prethrombin-1 (pre1) serves as a substrate for prothrombinase and does not undergo self-association as prothrombin can. Mixtures of Vh-pre1 in 0.05 M Tris (pH 7.65), 0.1 M NaCl, 1 mM benzamidine and either 2 mM EDTA or 2 mM $Ca^{2+}$ were examined using equilibrium sedimentation. Samples were analyzed at speeds of 12, 16, 20, 24 and 28 thousand rpm, and at temperatures of 11.4, 18.0, 23.3 and 30.9 °C at 28 thousand rpm. Analyses of these data suggest: 1) the interaction between Vh and pre1 has a 1:1 stoichiometry, 2) the apparent dissociation constant is 32 μM at 23.3 °C (+/- 2 μM), 3) the association is $Ca^{2+}$-independent and 4) small quantities of higher oligomers may be formed at high concentrations. This work is supported by a Grant in Aid (#850781) from the American Heart Association.

M-Pos25 GEOMETRY SWITCHING CHROMOGENS IN PROTEIN CONFORMATION MOTILITY. Rex Lovrien and Jaqueline Pietig, Biochemistry Dept., Univ. of Minnesota, St. Paul, MN 55108

Molecules having azobenzene groups like chrysophenine bind to proteins. They can be switched to and fro in their cis and trans geometries: Cis $\rightleftharpoons$ Trans, using light energy (filtered tungsten light) for Trans $\rightarrow$ Cis conversion, with quantum yields ca. 0.20 to 0.30. Absorption spectra difference between isomers is large and easily monitored in the near u.v. (M. Inscoe et al. (1959) J.A.C.S. 81, 5634). On binding to proteins, Cis $\rightarrow$ Trans conversion (dark reaction) have $t_{\frac{1}{2}} \sim$ 10-1000 sec. These kinds of chromogens have some especially advantageous features: (i) Because they engage in large geometry changes unlike other probes, they have a good chance to reflect protein conformational fluctuations if continuously bound (J.A.C.S. 96, 244 (1974)). (ii) Properly selected chromogens are impervious to general and specific acid-base catalysis using any mixture of low M.W. side chain equivalents. Hence protein-propelled catalysis of the dark reaction probably is an expression of the protein's conformational motility and pH dependencies thereof. (iii) These probes are tough and repeatedly reversible, not oxidatively damaged. (iv) They can be gotten in many structural variations. When bound to proteins like plasma albumin, the pH dependencies of the switching kinetics correlate closely with the pH dependencies of protein conformation properties. Clamping the proteins with lipids sharply inhibits their catalytic capacities, expected from the tendency of lipids to tighten such proteins as seen on the basis of other criteria that are expressions of motility. Supported by Bioprocess Institute, Univ. of Minnesota.

M-Pos26 **KINETICS OF THE ASSOCIATION OF FACTOR VIII WITH WILLEBRAND FACTOR.** Lollar, P., Parker, C.G. and Krishnaswamy, S. (Intr. by D.M. Warshaw) Depts. of Biochemistry and Medicine, University of Vermont, Burlington, VT 05405

Factor VIII (fVIII) and Willebrand factor (WF) are plasma glycoproteins that are necessary for normal hemostasis. When activated by proteolytic cleavage, fVIII is a cofactor for factor IXa in the activation of factor X in the intrinsic pathway of blood coagulation. WF is necessary for normal platelet adhesion and aggregation. WF circulates as a population of multimers ranging from 1 to 20 MDa as estimated by SDS agarose gel electrophoresis. Multimers are composed of identical 270 kDa subunits. WF binds fVIII to form a tight, noncovalently-linked complex. This interaction prolongs the half-life of fVIII in plasma. Previous studies using a 240 kDa heterodimeric form of porcine fVIII have shown that one fVIII molecule can bind each subunit of WF and that the weight-average sedimentation coefficient of WF increases from 21 to 40 S when it is fully saturated with fVIII (Lollar, P. and Parker, C.G., J.Biol.Chem. in press). We now find that the binding of fVIII to WF in solution is accompanied by a detectable increase in light scattering intensity. The kinetics of association of fVIII with WF were studied by stopped-flow right angle light scattering under conditions of excess fVIII at ionic strength 0.15, pH 7.4. The increase in light scattering with time was described well by a single exponential. The second order rate constant was $3 \times 10^7$ $M^{-1}s^{-1}$. No indication of a cooperative process was observed. These data are consistent with the interpretation that WF multimers contain multiple, identical and independent binding sites for fVIII. Additionally, this method promises to be a useful way to study the quantitative aspects of the interaction of fVIII with WF.

**M-Pos27** THE STRUCTURE OF PARTICLES IN MIXED BILE SALT-LECITHIN COLLOIDS BY SMALL ANGLE NEUTRON SCATTERING R.P. Hjelm[1], M.H. Alkan[2], and P. Thiyagarajan[3] [1]Los Alamos Neutron Scattering Center, Los Alamos National Lab., Los Alamos, NM; [2]Department of Pharmaceutics, University of Illinois at Chicago; and [3]IPNS Division, Argonne National Laboratory, Argonne, IL.

Mixed colloidal systems of bile salt and lecithin are of interest as drug delivery systems, as models of bile structure and action and as models of membrane structure. Small-angle neutron scattering was done on mixed dispersions of egg phosphatidylcholine and sodium glycocholate at different molar ratios as part of a project to construct a structural phase map of this system. Of interest here is to follow the structural transitions which occur on dilution of the system between lipid concentrations of 50 mg/ml and 1.0 mg/ml. This models the micelle to vesicle transition which occurs (due to dilution of bile salt below the critical micelle concentration) on injection of mixed micelles into the blood, or on passing of bile into the upper intestine. The data provide information on the size and shape of the colloidal particles. At 50 mg/ml the scattering curves suggest small, ellipsoidal micelles but the analysis is complicated by the presence of scattering from interparticle correlations at low Q. At lower concentrations larger aggregates of apparently complex morphology are seen. Samples diluted to concentrations of 2.5 mg/ml and less are constituted of spherical vesicles the size of which decreases with decreasing concentration. The size is also dependent on the relative amounts of bile salt and lecithin.

This work was supported by the USDOE

**M-Pos28** CALORIMETRIC STUDIES OF A HOMOLOGOUS SERIES OF 1,2-DI-ACYL-3-O-(α-D-GLUCOPYRANOSYL)-sn-GLYCEROLS. D.A. Mannock, R.N.A.H. Lewis and R.N. McElhaney, Department of Biochemistry, University of Alberta, Edmonton, Alberta, Canada, T6G 2H7.

Diacyl-α-D-glucosyl-sn-glycerols are membrane constituents of several Streptococci and of Acholeplasma laidlawii. We have synthesized a series of these compounds with acyl chain lengths from 10-20 carbon atoms, for the purpose of studying their thermotropic phase behaviour. Thermograms obtained using a Perkin-Elmer DSC-2C calorimeter at fast heating and cooling rates show a strongly energetic, lower temperature transition and a weakly energetic higher temperature transition. These have been assigned to the lamellar phase chain melting and the lamellar-hexagonal II phase transitions, respectively. The chain-melting transition temperature increases with increasing acyl chain length, whereas the temperature of the $L_\alpha \rightarrow Hex_{II}$ phase transition decreases. On annealing at low temperatures, additional gel phases are formed, indicating that the gel phase formed on initial cooling is metastable. The stable gel to $L_\alpha$ phase transition is very energetic and occurs at higher temperatures than the metastable gel to $L_\alpha$ phase transition, a pattern similar to that seen in the shorter-chain β-D-glucosyl compounds. The conversion from the metastable to the stable gel phase in the even-chain α-D-glucolipids takes seconds to a few hours. This is much faster than the transformation in the equivalent β-D-glucosyl compounds. In contrast, formation of the stable gel phase in the odd-chain α-D-glucolipids takes tens to several hundred hours, which is markedly slower than their β-D-glucosyl counterparts. Furthermore, the subgel phases seen in the longer-chain β-D-glucolipids are absent in the β-D-glucosyl compounds. These differences in behaviour suggest that altering the configuration of the sugar headgroup, viz. α or β, changes the packing behaviour of these molecules.

**M-Pos29** A MULTINUCLEAR NMR STUDY OF LIPOSOMES CONTAINING THE ANTIARRHYTHMIC DRUG AMIODARONE, Gordon L. Jendrasiak and Calvin Glisson, Departments of Radiation Oncology and Physics, East Carolina University, Greenville, NC and R. Stephen Porter, Likoff Cardiovascular Institute, Hahnemann University, Philadelphia, PA.

Amiodarone, a potent antiarrhythmic drug, is being widely used in cardiology. Its electrophysiological effects as well as its side effects seem to involve lipids. We report here a multinuclear NMR study of amiodarone in liposomes containing phosphatidic acid. Both H-1 and C-13 measurements suggest that amiodarone interacts with the phospholipid hydrocarbon chains in a quite different manner than does cholesterol. The phospholipid head-group signals, both H-1 and P-31, from amiodarone liposomes, are quite distinct from those from liposomes incorporating cholesterol. Relaxation time values for the two liposome systems are also very different. A paramagnetic cation interacts with cholesterol containing liposomes in a manner similar to that found for other liposomes whereas the amiodarone containing liposomes do not show this type of interaction. Preliminary results with liposomes containing stearylamine show similar results to the phosphatidic acid case. Since the pH of the two systems is quite different, it appears that hydrogen ion concentration may not be a major factor in determining the location of the drug in the liposome. Our NMR observations thus do not support a recently proposed model wherein amiodarone is buried deep within the hydrocarbon core of the liposomes.

M-Pos30 LOCALIZATION OF LIPID EXCHANGE SITES BETWEEN BULK LUNG SURFACTANTS AND SURFACE MONOLAYER : FREEZE FRACTURE STUDY. Arindam Sen, Marysue Mosgrober-Anthony and Sek-Wen Hui, Department of Biophysics, Roswell Park Memorial In stitute, Buffalo, NY 14263.

Air bubbles trapped in calf lung surfactants (CLS) and an extract of CLS (CLSE), as foam, have been used to provide a model air-water interface for study of surfactant structures at the interface. Freeze fracture replicas of the foam from CLS show tubular myelin figures (TMF) attached to the bubble surface. Replicas from samples of CLSE foam show vesicles in the bulk phase attached to bubble surfaces either directly or, more common, through "funnel-like" structures. Such funnel-like structures are also found in CLS foam. Foam from only dipalmitoylphosphatidylcholine however, does not show any evidence of interaction of bulk phase lipid with the bubble surfaces. These data have important implications with respect to activity of lung surfactants; and we interpret the funnel-like structures as regions at which rapid lipid exchange, between the bulk surfactants and surfactant monolayers at the air-water interface, occurs.

M-Pos31 DEUTERIUM NMR INVESTIGATION OF PHASE BEHAVIOR OF CHOLESTERYL ESTERS. Stuart S. Berr, Theodore P. Trouard, S.C. Shekar, and Michael F. Brown. Department of Chemistry, University of Arizona, Tucson, AZ 85721.

The crystalline, smectic, cholesteric, and isotropic phases of cholesteryl myristate have been studied using deuterium NMR. Cholesteryl myristate (CM) with the acyl chain both perdeuterated and selectively deuterated ([3-$^2H_2$]) were examined as pure compounds. In addition, deuterated CM was examined in mixtures with cholesteryl linoleate (CL) and cholesteryl oleate (CO), which approximate the composition of the cholesteryl esters found in atherosclerotic plaque (10:8:2 by mass). The influence of triolein, another plaque constituent (5% by mass), on the properties of the mixtures of CM/CL/CO was investigated. In all cases, high fidelity $^2H$ NMR lineshapes were obtained with use of the quadrupolar echo method. Moments of the $^2H$ NMR spectra were analyzed as a function of temperature to investigate the phase transitions and degree of orientational order of cholesteryl myristate in each of the various states. The profiles of the quadrupolar splittings of CM as a function of acyl chain segment position in the smectic phase resemble those of deuterated phospholipids in the smectic, liquid-crystalline ($L_\alpha$) phase. Spin-lattice relaxation rates $R_{1Z}(i)$ were determined as a function of chain position for the smectic phase of both the pure compounds and the mixtures, and analyzed in conjunction with the corresponding order parameters $S_{CD}(i)$ to obtain new information on the molecular dynamics. Supported by a Postdoctoral Fellowship from the American Heart Association (S.S.B.), a Research Career Development Award from the NIH (M.F.B.), and NIH Grant EY03754.

M-Pos32 MICROEMULSION MODEL SYSTEMS FOR LOW DENSITY LIPOPROTEINS: A $^{13}C$-NMR STUDY. Robert E. Reisinger, David Atkinson, and James A. Hamilton, Biophysics Institute, Departments of Medicine and Biochemistry, Housman Med.Res.Ctr., Boston University Schl.of Med.,Boston, MA 02118

As a model for the lipid interactions in low density lipoproteins, microemulsions comprised of dimyristoyl phosphatidylcholine (DMPC), cholesteryl oleate (CO), and varying amounts of cholesterol were studied by $^{13}C$-NMR at 50.3 MHz. Fractionated microemulsion with a uniform size distribution displayed thermal transitions at ~25° and ~40° by differential scanning calorimetry. The higher temperature transition is a CO liquid to liquid-crystal transition, and the lower, a phospholipid acyl chain transition. $^{13}C$-C3 and $^{13}C$-C4 enriched cholesterol were used to monitor the environment and molecular motions of cholesterol. Chemical shifts (C3=70.8 ppm, C4=41.9 ppm) were independent of cholesterol composition (4.0 to 20.0 mol % with respect to DMPC) and temperature. Cholesterol resonances were observed both above and below the 40° transition, but broadened beyond detection at the lower transition. Resonances for the CO ring carbons were narrow at 50°, broadened with decreasing temperature, and were not observed below 30°. Acyl chain resonances unique for CO (e.g., olefinic and allylic) were observed at 30° but broadened significantly below 25°. At 20° the overall spectrum was very broad, except for the choline peaks. We conclude that the surface and core undergo essentially independent phase transitions. Cholesterol is present primarily in the surface at all temperatures, is not detectably affected by the CO transition, but becomes immobilized below the DMPC transition. The marked broadening of CO olefinic resonances below the surface phase transition indicates some surface/core cooperativity, either via the direct or indirect interactions.

**M-Pos33** EFFECT OF ALKANES AND PEPTIDES ON THE PHASE STRUCTURE OF MODEL MEMBRANE LIPIDS

G. Lindblom, M. Sjölund and L. Rilfors
Department of Physical Chemistry, University of Umeå,S-901 87 UMEÅ, SWEDEN

Abstract: The phase equilibria in phosphatidylcholine (PC)-n-alkane-water systems have been studied to elucidate the driving forces for the transition between a lamellar liquid crystalline ($L_\alpha$) and a reversed hexagonal ($H_{II}$) phase. A tentative phase diagram for the system dioleoyl-PC (DOPC)-n-dodecane-water was determined. An $H_{II}$ phase was formed at room temperature at both low and high water concentrations in DOPC-n-dodecane-water mixtures. The phase equilibria were also studied in PC-n-dodecane-water systems containing PC with different degrees of acyl chain unsaturation. The water and dodecane concentrations required to induce the formation of an $H_{II}$ (or isotropic) phase increase in the order dilinoleoyl-PC ∿ DOPC <1-palmitoyl-2-oleoyl-PC<dipalmitoyl-PC. The effect of n-alkanes with different chain length ($C_8$-$C_{20}$) on the phase equilibria in DOPC-n-alkane-water mixtures was studied. The ability of the alkanes to promote the formation of an $H_{II}$ phas was strongly chain length dependent. Gramicidin (hydrophobic) had a similar influence on the phase equilibria as the alkanes. Melittin (amphiphilic) induced the formation of an isotropic phase, while insulin and duramycin (water soluble) had no, or a very limited, ability to induce a nonlamellar phase. Our results are discussed in the light of simple physical models dealing with the self-assembly of amphiphiles.

**M-Pos34** IN SITU FT-IR INVESTIGATION OF PHOSPHOLIPID MONOLAYER PHASE TRANSITIONS AT THE AIR/WATER INTERFACE. Melody L. Mitchell and Richard A. Dluhy, National Center for Biomedical Infrared Spectroscopy, Battelle-Columbus Division, 505 King Avenue, Columbus, OH 43201

The liquid-expanded to liquid-condensed phase transition of 1,2-dipalmitoy-sn-glycero-3-phosphocholine (DPPC) monolayers at the air-water interface has been investigated in-situ using external reflectance Fourier transform infrared spectroscopy. Infrared spectra have also been obtained for monolayer films of 1,2-dimyristoyl-sn-glycero-3-phosphocholine (DMPC, a liquid-expanded film) and 1,2-distearoyl-sn-glycero-3-phosphocholine (DSPC, a liquid-condensed film). All three phospholipid monolayer films were monitored in the conformation-sensitive C-H stretching region as a function of molecular area at the air-water interface. The measured frequencies of the symmetric and antisymmetric $CH_2$ stretching bands for the DPPC monolayer in the high molecular area, expanded phase (2853 $cm^{-1}$ and 2924 $cm^{-1}$, respectively) are comparable to those of bulk DPPC multilayer dispersions above its main thermotropic phase transition and indicate a fluid and disordered conformation in the hydrocarbon chains. The measured frequencies for the low molecular area, condensed phase of DPPC (2849 $cm^{-1}$ and 2919 $cm^{-1}$) indicate a rigid, mostly all-trans hydrocarbon chain conformation for the condensed phase monolayer, similar to the low-temperature, gel phase bulk DPPC dispersion. A continuous decrease in frequency with decreasing molecular area is observed throughout the transition region for the DPPC monolayer. These results demonstrate that the DPPC monolayer is heterogeneous with changing acyl conformations.

**M-Pos35** CONFORMATION OF Nα-ACETYL Tn-I(104-115) AMIDE BOUND TO TROPONIN C. A. Patricia Campbell, Robert S. Hodges, Jennifer Van Eyk and Brian D. Sykes, Department of Biochemistry & MRC Group in Protein Structure and Function, University of Alberta, Edmonton, Alberta, Canada, T6G 2H7.

The $Ca^{2+}$-mediated interaction between troponin I (Tn-I) and troponin C (Tn-C) in the thin filament of skeletal muscle is an important element in the regulation of the actomyosin ATPase. A synthetic analogue of the inhibitory region of Tn-I, Nα-acetyl Tn-I(104-115) amide, was made by solid phase peptide synthesis. This region represents the minimum sequence necessary for inhibition of actomyosin ATPase activity, and is found to bind to Tn-C. Conformational changes induced by the formation of the synthetic peptide-Tn-C ($Ca^{2+}$-saturated) complex were followed by the study of the transferred proton-proton nuclear Overhauser effect (TRNOE). In the unbound form, the peptide tumbles rapidly in solution, and the peptide proton-proton NOEs are small and positive; but when the peptide is bound to Tn-C it tumbles more slowly with the protein, and the NOEs are large and negative. The TRNOE allows the transfer of information concerning conformation via chemical exchange between the bound and the free state peptide. Thus, in the presence of Tn-C, negative NOEs are measured on the easily detected free ligand resonances following irradiation of other ligand resonances in order to obtain conformational information in the bound state. Two-dimensional TRNOESY spectra of the Tn-I peptide bound to $Ca^{2+}$-sat. Tn-C reveal the appearance of several medium-range nonsequential NOEs indicative of the formation of secondary structure in the bound peptide. Furthermore, long range NOEs between side chains of residues at opposite ends of the peptide indicate a closer approach of the N-term and C-term ends. Energy minimization and molecular dynamics computer programs using NOE distance constraints are being used to generate the bound peptide structure.

**M-Pos36** THE DETERMINATION OF THE SOLUTION STRUCTURE OF DNA BY NMR. James D. Baleja and Brian D. Sykes, Department of Biochemistry, University of Alberta, Edmonton, AB, Canada, T6G 2H7.

The quantitative determination of structure in solution by NMR has been developing rapidly and extensively in the last few years. Most methods depend on the derivation of interproton distances from the measurement of initial nuclear Overhauser enhancements (NOEs) between nuclei. For macromolecules, the NOEs are measured as off-diagonal crosspeaks in a two-dimensional NOE spectroscopy (NOESY) experiment. To first order an intense crosspeak can be easily interpreted as two protons that are close in space. Less intense crosspeaks represent a pair of protons with greater separation. However, the derived interproton distances are approximate because NOEs must be measured with finite mixing times to give adequate signal-to-noise ratios in NOESY spectra. Under these conditions cross relaxation can greatly alter crosspeak intensity. In our approach, approximate interproton distances and a molecular dynamics program are used to generate a starting model. The structure is then refined by incorporating the NOE intensities directly into an algorithm that compares the experimental data to the NOEs calculated using a full matrix analysis including the effects of spin diffusion. The structure is then moved to minimize the difference between the calculated and observed NOEs. To express the overall precision of the NOE data, we propose the use of a factor R:

$$R = \sum_i |NOE_{obs}(i) - NOE_{calc}(i)| \Big/ \sum_i |NOE_{obs}(i)|$$

$^1$H NMR assignments and structures for the DNA duplexes d(TCTATCACCG)·d(CGGTGATAGA), $d(CATGCATG)_2$, and $d(GTACGTAC)_2$ are presented. The first sequence is one-half of the major binding site for the cro repressor on λ DNA (OR3); the latter two have an alternation of purine-pyrimidine residues which is an important factor in promoting a B-Z transition in DNA. All structures are most like B DNA.

**M-Pos37** **REDUCTION OF NITROXIDES IN WHOLE BLOOD, ERYTHROCYTES AND PLASMA**
M. Sentjurc*, D. Apte+, and H. Swartz+, *J. Stephan Institute, Ljubljana, Yugoslavia, +Department of Physiology and Biophysics, University of Illinois, Urbana, IL 61801

Many of the proposed uses of nitroxides in animals and tissues will involve exposure of the nitroxides to blood. We therefore investigated the reduction of various types of lipophilic and hydrophilic nitroxides by whole blood, erythrocytes and plasma by electron spin resonance (ESR). It was found that the rates of reduction, in general, follow structure/reduction relationships similar to those reported for nucleated mammalian cell lines. Nitroxides on azethoxyl, proxyl and pyrrolidine rings were more stable than nitroxides on piperidine and doxyl rings. For neutral nitroxides reduction was faster in erythrocytes than in plasma, while for the cationic nitroxide, $CAT_1$, reduction in plasma was faster than in erythrocytes.

In order to distinguish between enzymatic and nonenzymatic reduction the blood and its fractions were treated by heat or by TCA to denature enzymes or were incubated with the SH inhibitor n-ethylmaleimide (NEM) or with ascorbate oxidase. It was found that ascorbate oxidase almost completely stopped the reduction of $CAT_1$ in all samples, while it did not affect the reduction of neutral nitroxides. Heating of blood and its fractions or treatment with TCA decreased the reduction by about 50%, while NEM had only a minor effect on the nitroxide reduction. From these results we conclude that the main source of reduction of nitroxides in plasma is ascorbate, while in erythrocytes other enzymatic and nonenzymatic mechanisms predominate. On the basis of the lack of effects of NEM, the mechanisms of reduction of nitroxides in blood appear to be different from those observed in nucleated mammalian cells. (NIH GRANTS RR01811, GM35534)

M-Pos38 REFINEMENT AND AUTOMATION OF THE MAIN CHAIN DIRECTED ASSIGNMENT ALGORITHM FOR THE ANALYSIS OF $^1$H SPECTRA OF PROTEINS. S. Nelson, D.M. Schneider, D.L. Di Stefano and A.J. Wand. Institute for Cancer Research, Fox Chase Cancer Center, Philadelphia, PA 19111

The recently introduced (1,2) main chain directed (MCD) assignment algorithm has been refined and extended. Several new closed loop connectivity patterns displaying the three main criteria of the MCD approach (self-correcting, high fidelity and high frequency) have been derived from further analysis of high resolution structures of proteins. In an effort to probe the reliability of the expanded MCD algorithm in the analysis of $^1$H NMR spectra of proteins, we have simulated COSY and NOESY spectra of a number of relatively large proteins. The simulations allow any level of resonance degeneracy and linewidth to be introduced. The extended MCD algorithm has been computerized and used to analyze simulated and real spectra. Analysis of simulated spectra suggest that the MCD algorithm can successfully assign the main chain elements of structured proteins up to at least 20 kDa in size. The required information is the definition of the frequencies of the NH-$C_\alpha$H-$C_\beta$H J-coupled subspin system of each residue and the digitized NOESY spectrum. Experimental data derived from human ubiquitin and hen egg white lysozyme have also been analyzed and the results of these studies will be presented.

1. Englander, S.W. & Wand, A.J. (1987) Biochemistry 26:5953-5958
2. Di Stefano, D.L. & Wand, A.J. (1987) Biochemistry 26, in press

M-Pos39 NMR INVESTIGATION OF NICOTINE-TREATED LIVE RATS. P. Blondet, P.N. Venkatasubramanian and M. Bárány, Dept. of Biol. Chem., Univ. of Illinois, Col. of Med., Chicago, IL 60612.

Male Sprague-Dawley rats (~150 gm) were injected subcutaneously with 3 μmoles nicotine/kg (as nicotine tartarate) 35-times during a 12 week period. $^1$H and $^{31}$P NMR spectra of nicotine injected and control anesthetised rats were recorded on a GE CSI 2T spectrometer with 2 cm surface coils from the brain, liver and leg muscle. $^{31}$P spectra were obtained with a one-pulse sequence. ($\theta/2 - \tau - \bar{\theta}/2$) Te ($\theta - \tau - \bar{\theta}$) Te (Williams, et al. JMR, 66, 562, 1986) and ($\theta - \tau/2 - SL - \tau/2 - SL$) Te ($\theta - \tau - \bar{\theta}$) Te spin lock (Blondet, et al. JMR, 69, 403, 1986) pulse sequences were used to record water suppressed $^1$H spectra. Observation of metabolite resonances in the aromatic region is feasible using very short spin echo delays. Using a long echo delay time and fasting the rat for 36 hrs partially suppressed the $(-CH_2-)_n$ lipid signal and enabled the observation of metabolite resonances in the aliphatic region. $=NCH_3$ of PCr/Cr (3.0 ppm) and $-\overset{+}{N}(CH_3)_3$ of choline (3.2 ppm) were visible in the muscle and brain $^1$H aliphatic spectra. $-CH_3$ of N-acetylaspartate gave the major signal in brain at 2.0 ppm. In the aromatic region of muscle spectra, $H_2\overset{+}{N}=C=$ of PCr (7.3 ppm) and C2-H of anserine (around 8.06 ppm) were seen. pH (7.11) was calculated from the latter (Arús and Bárány, BBA, 886, 411, 1986). H2 of ATP (8.3 ppm) gave a signal in brain and liver spectra. $^{31}$P spectra show resonances from ATP and PCr in the leg muscle and brain. Resonances from inorganic phosphate, sugar phosphates and phosphodiesters were seen in the brain and the liver. There were no observable differences between the spectra of control and nicotine injected rats after either 17 or 35 injections. (Supported by CTR).

M-Pos40 THE INTERACTION OF AN N-METHYLATED POLYAMINE ANALOG, HEXAMETHONIUM (2+), WITH DNA: $^{14}$N AND $^{23}$Na NMR RELAXATION RATE STUDIES, S. Padmanabhan, B. Richey, C.F. Anderson and M. T. Record, Jr., Depts. of Chemistry and Biochemistry, University of Wisconsin, Madison, Wisconsin, 53706

We have investigated the interactions of the divalent hexamethonium ($Hex^{2+}$) cation with double helical calf thymus DNA by $^{14}$N and $^{23}$Na NMR. In a titration of NaDNA with $HexBr_2$, we monitor the displacement of $Na^+$ from DNA by $Hex^{2+}$ by concurrent measurements of the Lorentzian $^{14}$N signals and the biLorentzian $^{23}$Na signals. Quadrupolar relaxation rates of $^{14}$N and $^{23}$Na are analyzed according to a simple two-state model to obtain parameters characterizing the $Hex^{2+}/Na^+$ exchange process. The stoichiometry of ion exchange is two $Na^+$ displaced per $Hex^{2+}$ accumulated. Approximately one half of the DNA phosphate charge is neutralized by accumulated $Hex^{2+}$ and $Na^+$.

The transverse and longitudinal relaxation rates observed for $^{14}$N were analyzed under the assumption that the quadrupolar relaxation processes of $^{14}$N in $Hex^{2+}$ associated with DNA is characterized by a single exponential correlation function with correlation time $\tau_{NB}$. The resulting value of $\tau_{NB}$, 7.8±0.8 nsec, is three orders of magnitude greater than that estimated for $Hex^{2+}$ in the absence of DNA, and is only 3-4 times greater than the correlation times reported for $^{23}$Na and other quadrupolar cations in DNA solutions. These comparisons indicate that the observed enhancements in the relaxation rates of $^{14}$N are due mainly to slowing of the motions that modulate the quadrupolar interaction of $Hex^{2+}$ near DNA.

**M-Pos41** NEXT GENERATION OF $^{19}F$ NMR pH INDICATORS. C. Deutsch and J. Taylor, Department of Physiology, University of Pennsylvania and Fox Chase Cancer Center, Phila., PA (Intr. by D.Wilson)

Over the last few years we have developed and tested a family of fluorinated amino acid $^{19}F$ NMR pH indicators (Deutsch and Taylor, 1987). Recently we have investigated aromatic fluorinated compounds, in which the flourine is directly bound to the aromatic ring. We hoped to exploit the resonance interaction between $NH_2$ and ortho and para fluorine substituents on the ring. This proved possible for a simple, available class of aromatic fluorinated amines, the fluoroanilines. Ortho and para substitutions give the largest chemical shifts per pH unit, while the meta substitution is substantially less; the pH sensitivity of these o- and p-substituted anilines is at least an order of magnitude larger than the fluoromethlylalanines. The $pK_a$s of the o-, p-, and m-fluoranilines are in the low acid range. However, we have modified these compounds so as to increase the $pK_a$, thereby generating a repertoire of sensitive molecules over a range of pHs. These new molecules are analogs of alanine that contain a N-(p-F-phenyl group). Advantages of the new indicators are (1) the chemical shift difference between the conjugate acid and base is large (10-15 ppm), (2) the $^{19}F$ NMR spectrum is a singlet (approximately 50 ppm upfield from trifluoroacetate) and therefore (3) proton decoupling is not necessary. (Supp. by NIH GM 36433).

**M-Pos42** THE INFLUENCE OF THE FREEZING PROCESS UPON THE BINDING OF FLUORIDE TO HEMEPROTEINS. A.-S. Yang and A.S. Brill, Dept. of Physics, Univ. of Virginia

The association of fluoride with ferric myoglobins and hemoglobins in aqueous buffers above freezing has been well-studied. We chose this reaction to investigate the feasibility of observing titration intermediates and estimating dissociation constants at the freezing temperature by EPR spectroscopy at cryogenic temperatures. A strong dependence of the apparent dissociation constant upon protein concentration was observed, a factor of four decrease in protein concentration (at monomer concentrations below 4 mM) being accompanied by about a four-fold increase in the tightness of binding. (The reduction of free fluoride by the amount bound to the protein has been taken into account.) It appears that this effect is associated with freezing-induced concentration of the ligand, a process which has been described in the literature. Bands of high concentration of electrolyte accompany the rejection of solute during the growth of ice crystallites, sweeping by the relatively slowly moving macromolecules. Thus, just before it is trapped in the solid phase, the protein can experience a much greater concentration of salt than was present in the original liquid sample. A mathematical model of this process, which depends upon nucleation rate and ice-crystal growth rate in the super-cooled aqueous solution, shows how the average concentration of mobile solute species can depend upon the concentration of all species present, including macromolecules. The effect of a second macromolecular species was tested by adding bovine serum albumin to the hemeprotein-fluoride system, and the results support the interpretation of the original data and the model.
Supported by NSF DMB85-17819.

**M-Pos43** CONFORMATIONAL ASPECTS OF THE INTERACTION OF SODIUM DODECYL SULFATE (SDS) WITH BRADYKININ (BK) AND RELATED PEPTIDES. Delbert D. Mueller, Raymond J. Vavrek, John M. Stewart and John R. Cann. Department of Biochemistry, Kansas State University, Manhattan, KS 66506 and Department of Biochemistry / Biophysics / Genetics, University of Colorado Medical School, Denver, CO 80262.

Earlier CD measurements (1) on the interaction of SDS with BK ($Arg^1$-$Pro^2$-$Pro^3$-$Gly^4$-$Phe^5$-$Ser^6$-$Pro^7$-$Phe^8$-$Arg^9$) and related peptides indicated formation of a 1:2 BK-SDS complex. Conformational aspects of the interaction have now been probed by NMR with appropriate controls. The $^{13}C$ NMR spectrum of 0.7 mM [99%-2-$^{13}C$-$Gly^6$]-BK in $H_2O$, pH 8.3, confirmed (2) the high cis/trans ratio=0.51 about the sixth peptide bond. Addition of 5.2 mM SDS at constant pH shifted the broadened trans resonance downfield by 0.7 ppm without shifting the broadened cis resonance and increased the cis/trans ratio to 0.78 . Thus, the cis and trans isomers of the peptide interact differently with SDS and the cis isomer is favored in the complex. $^{19}F$ NMR of [$Gly^6$,pF-$Phe^8$]-BK showed two resonances at -115.5 and -116.1 ppm in the ratio 0.48, indicating that pF-$Phe^8$ also senses the cis and trans isomers of $Pro^7$ in conformity with a previous model of the Gly-Pro-Phe sequence (2). In SDS there were two resonances at -119.3 and -122.1 ppm in slow chemical exchange.The minor (9%) downfield resonance may be an intermediate complex (1). $^1H$ NMR of BK and Ser-Pro-Phe-Arg in $D_2O$ attested to their strong interaction with SDS: Aromatic proton resonances were broadened and shifted, and $\alpha$-protons were broadened with accompanying changes in coupling constants. The tetrapeptide appears to be structured in $D_2O$: Changing the pH from 7.4 to 8.4 caused changes in aliphatic coupling constants while analysis of the aromatic region of the spectrum suggests restricted rotation of Phe. These results indicate that changes in the CD of Phe as well as conformational changes contribute to the change in CD of BK and Ser-Pro-Phe-Arg upon interaction with SDS (1).

1. Cann et al,Peptides 7, 1121 (1986); 2. London et al,J. Am. Chem.Soc. 101, 2455 (1979)

**M-Pos44** DIFFERENTIAL BROADENING OF $^{13}C$ DOUBLETS OF [2-$^{13}C$]ATP and [2-$^{13}C$]AMP BOUND TO PORCINE ADENYLATE KINASE. Bruce D. Ray and B. D. Nageswara Rao, Physics Department, IUPUI, P.O. Box 647, Indianapolis, IN 46223 and P. Rösch, Max-Planck-Institut für Medizinische Forschung, Jahnstrasse 29, 6900 Heidelberg, W. Germany.

Adenylate Kinase (E.C. 2.7.4.3) catalyzes the reversible reaction MgATP + AMP ⇌ MgADP + ADP. The two nucleotide binding sites on this enzyme are distinguishable by the fact that the AMP site binds these nucleotides uncomplexed by the cation whereas such a selectivity is absent at the ATP site. Furthermore, the AMP site is specific for adenine nucleotides whereas guanine nucleotides are accepted at the other site. In an attempt to characterize the active-site structure of this enzyme, [2-$^{13}C$]AMP, and [2-$^{13}C$]ATP were synthesized and the enzyme-substrate complexes of these nucleotides were examined by $^{13}C$ NMR. For both AMP and ATP, no changes were observed in either the chemical shift or the $^{1}H$-$^{13}C$ coupling constant upon binding to the enzyme. However, for both nucleotides, the proton-coupled spectra exhibited differential broadening of the two peaks of the $^{1}H$-$^{13}C$ doublet ($J(^{1}H$-$^{13}C)$ = 205 Hz). The primary cause for this effect is an 'interference' between the mechanisms of $^{13}C$ relaxation viz., $^{13}C$ chemical shift anisotropy and $^{13}C$-$^{1}H$ dipolar interactions, both of which are tensors of the second rank. The extent of differential broadening was different for the two nucleotides. This differential broadening was studied as a function of frequency at 50, 75, and 117 MHz. In addition, longitudinal relaxation times ($T_1$'s) were measured at 50 and 75 MHz. The results of these measurements together with their analysis in terms of rotational correlation time, $^{13}C$ chemical shift anisotropy, and $^{13}C$-$^{1}H$ dipolar interaction will be presented.

Work supported by the NSF grants DMB 86 08185 and PCM 80 18725 (for the purchase of NT-300) and NIH grant RR01077 (Purdue Biochemical Magnetic Resonance Laboratory).

**M-Pos45** INVESTIGATION OF THE INTERACTION OF TRIFLUOPERAZINE WITH BOVINE BRAIN S-100B PROTEIN. P.L. Pingerelli, A.L. Schlaepfer, and H. Mizukami. Division of Regulatory Biology and Biophysics, Department of Biological Sciences, Wayne State University, Detroit, Michigan 48202.

To investigate the influence of trifluoperazine (TFP) on the overall structure of S-100b and to identify where the drug might bind, the interaction of TFP with S-100b was studied using $^{1}H$ NMR and UV difference spectroscopy.

Our studies indicate that in the presence of $Ca^{2+}$, TFP and S-100b form a complex of molar ratios up to 2:1. Spectral evidence for the interaction between S-100b and TFP in the presence of $Ca^{2+}$ has come from the observation of $^{1}H$ NMR resonance broadening in the range 6.8 to 7.2 ppm, corresponding to Phe and His $C_4$ nuclei. These changes are distinct from those observed when excess $Ca^{2+}$ is added to apo-S-100b in the absence of TFP. Alternatively, the 3,5-protons from Tyr-16β were unaffected by addition of TFP to $Ca^{2+}$-bound S-100b.

The difference spectrum, using UV difference spectroscopy, produced when $Ca^{2+}$ was added to a 1:1 TFP/S-100b mixture was characterized by a negative difference absorption between 250 and 260 nm, while positive difference absorption was observed between 260 and 270 nm. This has been interpreted as a change in the exposure of S-100b-Phe residues to the solvent and was less than was noticed for the protein in the absence of TFP. No difference absorption at 287 nm for Tyr-16β was observed.

It is postulated that TFP binding to S-100b is a $Ca^{2+}$-dependent hydrophobic interaction which involves Phe and His residues but not Tyr-16β. (Supported by a B-Haley Graduate Research Award & GRA Provost Award, WSU).

**M-Pos46** INTERNAL DYNAMICS OF PROLINE ANALOGUES : A POTENTIAL MECHANISM FOR CATALYSIS OF PROLINE ISOMERIZATION, K.A. McGroddy, G.L.Millhauser and R.E.Oswald, Dept. of Pharmacology, NYSCVM, Cornell University, Ithaca,N.Y., 14853.

Variable temperature $^{1}H$ Nuclear Magnetic Resonance spectroscopy (NMR) was used to study the molecular dynamics of several model compounds including 1,1-dimethyl-4-acetyl piperazinium iodide (PIP), a potent cholinergic agonist, and its open-chained derivative N,N,N'-tetramethyl-N'-acetylethylenediammonium iodide (TED). Intramolecular exchange was observed in PIP at temperatures just slightly above room temperature, but TED showed no exchange below sixty degrees C. This exchange was found to be due to rotation about an internal imide bond. A lineshape analysis was then performed on the series of spectra in order to extract the rate constants for the process. A linear Arrhenius plot was generated from these rate constants, giving energies of activation for rotation about the bond of 18 kcal/mole for TED but only 12 kcal/mole for PIP.

The only difference between these two molecules is the restriction imposed by the piperazinium ring. This constrains a positively charged ammonium group to be near the imide nitrogen, which we believe destabilizes the double bond character of the imide bond, allowing for easier rotation. The positive nitrogen is free to move further away in TED, which allows for more double bond character and a correspondingly higher energy of activation.

These model compounds are potentially very useful for studying the catalysis of rotation about amide and imide bonds. Proline isomerization, or rotation about an imide bond, has been implicated as an important step in the folding of small proteins. It is characterized by an energy of activation on the order of 20 kcal/mole, but in certain cases involving partially folded intermediates, the barrier to rotation is much lower. This has never been satisfactorily explained. Catalysis due to the presence of a positively charged amino acid near the imide bond could possibly be an explanation for this observed effect.

M-Pos47 A ROLE FOR PHOSPHORYLCHOLINE AND PHOSPHORYLETHANOLAMINE AS BUFFERS AND pH MODULATORS, C. Tyler Burt, F. Jungawalla, and Benjamin Chen, NIEHS, Research Triangle Park, NC, 27709, E.K. Schriver Center, Waltham, MA, and Yale University Medical Ctr., Dept. of Radiology, New Haven, CT.

Recent NMR studies have highlighted the presence in many tissues (particularly tumors) of phosphorylethanolamine (PEth) and phosphorylcholine (PCh). While their primary role has been postulated as lipid intermediates, we now wish to suggest a secondary role that these compounds could play. That role is as pH buffers and modulators which are effective at low physiological pH's. To test this possibility, changes in PCh level in vitro were correlated to pH by $^{31}P$ NMR performed at 360 mHz. In unbuffered solution, treatment of phosphorylcholine with alkaline phosphatase results in alkalinzation of the solution to a pH above 7.5. The same result is found in diluted semen to which exogeneous phosphorylcholine is added. No change is seen in control semen for the same time period. NMR spectra in both cases show significant movement of the inorganic phosphate peak indicative of alkalinization, while there is relatively little shift in PCh. These findings suggest two pH related roles for phosphomonesters. The first in fluids such as semen, which for humans is rich in PCh, is as a rapid source of alkalizing capability. In semen, it could serve to modulate the low pH sperm are confronted with in the vagina. The second is to increase the buffering capacity in the physiologic acidic region, without increasing inorganic phosphate concentration. Buffers are most effective near their pK, which for PCh and PEth is near 5.7. It is of some interest, therefore, that those tissues which have the greatest potential to be made severely acidic either by natural ischemia, such as during birth or by the Warburg effect like tumors, have the highest levels of PEth and/or PCh.

**M-Pos48** QUENCHING OF THE INTRINSIC FLUORESCENCE OF RABBIT SKELETAL MUSCLE MYOSIN LIGHT CHAIN KINASE. Bonnie Bowman, James T. Stull, and David M. Jameson, Depts. of Physiology and Pharmacology, Univ. Tx. Hlth. Sci. Ctr., Dallas, Dallas, TX 75235

Previous studies have demonstrated that binding of rabbit skeletal muscle myosin light chain kinase (MLCK) to $Ca^{2+}$/calmodulin (Cm) results in a 30% increase in its intrinsic tryptophan fluorescence and an 8 nm blue shift of its maximum emission wavelength. MLCK has 4 tryptophan residues, 3 in the catalytic domain and 1 in the calmodulin binding domain. Calmodulin has no tryptophan residues. To investigate whether the observed changes in the emission spectrum are dominated by the contribution from trp 580 in the calmodulin domain, we examined the ability of acrylamide to quench the intrinsic fluorescence of both MLCK and Cm-MLCK. Stern-Volmer plots of the quenching of MLCK show a distinct downward curvature. Moreover, the Stern-Volmer constants (Ksv) increase with emission wavelength, 3.1 $M^{-1}$ at 310 nm to 7.3 $M^{-1}$ at 390 nm. Cm-MLCK is less readily quenched, the Ksv values increase from 0.9 $M^{-1}$ at 315 nm to 1.6 $M^{-1}$ at 375 nm. In comparison, the single tryptophan emission of a synthetic peptide of the calmodulin binding domain (P) quenched readily, Ksv = 17 $M^{-1}$, and Cm-P poorly, Ksv = 0.4 $M^{-1}$. These results suggest that the intrinsic fluorescence of MLCK and Cm-MLCK is due to several emitting species with different emission spectra. Although the data support the hypothesis that trp 580 is less accesssible to solvent once Cm has bound, a more rigorous argument will require both time-resolved fluorescence measurements and a global data analyis to determine the extent of its contribution to the observed steady state fluorescence changes (Supported in part by NIH HL23990 and NSF DMB8706440).

**M-Pos49** TRYPTOPHAN FLUORESCENCE IN SMALL PEPTIDES: IS THERE A CORRELATION OF THE DECAY KINETICS TO ROTAMER POPULATIONS? M.F. Lulka(1), J.B.A. Ross(1), W.R. Laws(1), P.G. Katsoyannis (1), N. Ohta(1), A. Buku(2), and H.R. Wyssbrod(2), Depts. of Biochemistry(1) and Physiology and Biophysics(2), Mount Sinai School of Medicine, One Gustave L. Levy Place, New York, NY 10029.

The complex kinetics of the fluorescence decay of a single tryptophan in peptides and proteins have not been resolved. However, we have recently demonstrated that the complex fluorescence decay of tyrosine in model compounds and small peptides can be explained by a kinetic model which predicts a single exponential decay for each rotamer about the $C^{\alpha}$-$C^{\beta}$ bond of the aromatic residue [Biochemistry 25, 599 and 607 (1986)]. To test this decay model on tryptophan, the tyrosine residue was replaced in oxytocin and a cyclic pentapeptide (CPP) to form 2-Trp OT and cyclo (-D-Trp-Pro-Gly-D-Ala-Pro-). An insulin analogue has also been synthesized, replacing the A-14 Tyr with Trp. Only 2 of the $C^{\alpha}$-$C^{\beta}$ Trp rotamers are populated in CPP (from proton NMR) and the fluorescence decay exhibits 2 wavelength-independent lifetimes in accord with the rotamer model. The model is insufficient, however, since the pre-exponential terms for the decay do not equal the rotamer populations and are wavelength dependent. Conversely, 2-Trp OT seems to fit the rotamer model with the fluorescence decay requiring 3 exponentials and the amplitudes agreeing with the rotamer populations. However, since the mean lifetime slightly increases on going to the red, other mechanisms may also be involved. While we have not yet determined the rotamer populations of the A-14 Trp insulin, the fluorescence data suggests the rotamer model. Supported by NIH grants DK-10080, HD/GM-17542, and DK-12925 and by NSF Instrumentation Grant DMB-8516318.

**M-Pos50** QUENCHING OF TYROSINE FLUORESCENCE IN OXYTOCIN AND OXYTOCIN ANALOGUES. Corbin Woodling and William R. Laws, Dept. of Biochemistry, Mount Sinai School of Medicine, One Gustave L. Levy Place, New York, NY 10029.

We have shown that the complex fluorescence decay kinetics of the single tyrosine residue in the neurohypophyseal hormone oxytocin (OT) can be explained by multiple ground-state populations due to the 3 phenol rotamers about the $C^{\alpha}$-$C^{\beta}$ bond [Biochemistry 25, 609 (1986)]. To define further the local environment of the phenol ring in OT, Stern-Volmer quenching experiments have been performed in 0.001 M HCl at 5°C using N-acetyltyrosinamide (NATyrA) for a reference compound. We have examined OT, desamino-OT (dOT), lacking the N-terminal amino group, and desaminodicarba-OT (dDCOT), where the disulfide has also been replaced by an ethylene bridge. The steady-state data for NATyrA, OT, dOT, and dDCOT quenching by acrylamide and pyridine-HCl (to 0.3 M) are non-linear, with upward curvature that can be explained by increasing static quenching [Anal. Biochem. 114, 199 (1981)]. While the static quenching parameter is essentially invariant for the different compounds, the Ksv values are smaller for OT, dOT, and dDCOT than for NATyrA, indicating diminished solvent access to the phenol ring in the hormone peptides. In contrast, the linear data for iodide quenching (to 0.3 M) of NATyrA and dOT indicates no static quenching but a reduced Ksv for dOT. The iodide quenching of the phenol in OT, however, is non-linear with downward curvature. The presence of more than one fluorophore with different Ksv parameters could explain this behavior; one possibility is that the N-terminal amino group could be differentially affecting the rotamers in their collisions with iodide ions. Supported by NIH grant DK-10080.

**M-Pos51** FLUORESCENCE LIFETIME ANALYSIS OF PHOSPHOGLYCERATE MUTASE. Joseph A. Schauerte and Ari Gafni, University of Michigan, Ann Arbor, Michigan 48102

Fluorescence lifetime studies of the glycolytic enzyme phosphoglycerate Mutase (PGM;EC 2.7.5.3) have shown fluorescence with the unusually long lifetime of 18 nsec. This long lived fluorescence is tentatively assigned to a red shifted tryptophan and was found in rat and rabbit PGM but was not found in PGM isolated from yeast. In addition, Diphosphoglycerate Mutase isolated from human erythrocytes (DPGM;EC 2.7.5.4), which has been shown to be related to PGM structurally, did not possess the long lived tryptophan component. The X-ray structure of yeast PGM has been reported and the amino acid sequence has been reported for yeast PGM and human DPGM. These molecules show a high degree of sequence conservation. Yeast PGM was shown to have 5 tryptophans per monomer (4 monomers per molecule) while human DPGM has 6 tryptophans per monomer (2 monomers per molecule). Rat PGM is shown to have 6 tryptophans per monomer by magnetic circular dichroism (active species is a dimer). While there is evidence that these molecules are related structurally, fluorescence lifetime studies indicate that the environment of one tryptophan is altered in rat and rabbit PGM. Stern-Volmer analysis indicates the tryptophan responsible for the long lived component is statically quenched by $I^-$ and $Cu^{2+}$.

The long lived tryptophan flourescence was immune to 2M Guanidine HCl, an environment that destroys enzyme activity, indicating that the tryptophan is in a stable portion of the PGM molecule. However 4M Guanidine HCl at pH 2.0 was capable of quenching the long lived fluorescence. The fluorescence lifetime was restored upon introduction of the protein to a non-denaturing environment, indicating the lifetime is not the result of a covalent modification.

**M-Pos52** THERMAL DENATURATION OF RIBONUCLEASE $T_1$ MONITORED BY TIME-RESOLVED TRYPTOPHAN FLUORESCENCE. Iain Johnson and Bruce Hudson, Department of Chemistry, University of Oregon, Eugene, OR 97403.

Time-resolved fluorescence of the single tryptophan residue has been used to examine the reversible thermal denaturation of ribonuclease $T_1$. In agreement with previous studies, the folded state of the protein at 20°C and pH 5.5 is characterized by a single exponential total fluorescence decay and a fluorescence anisotropy decay reflecting only overall rotational motion. Thermal unfolding occurs at about 55°C and is marked by a sharp decrease in the average fluorescence lifetime from 2.8 ns at 50°C to 1.0 ns at 60°C. The fluorescence decay in the unfolded state is highly nonexponential and analysis in terms of decay rate distributions (representative of conformational multiplicity) is presented and discussed. Incomplete reversibility results in decay components at $T<60$°C representing unfolded species which may be identified by selective quenching. Unfolding is also marked by the appearance at temperatures $>50$°C of a rapid fluorescence anisotropy decay component representing large angular excursions of the tryptophan residue free from the constraints of its densely packed native environment.

**M-Pos53** TIME-RESOLVED FLUORESCENCE STUDIES OF GLYCERALDEHYDE-3-PHOSPHATE DEHYDROGENASE. Chen-Lu Tsou*, Jay R. Knutson#, Raymond F. Chen#, and Shu-Jian Liang*, *Institute of Biophysics, Academia Sinica, Beijing, China, and #Laboratory of Technical Development, NHLBI, National Institutes of Health, Bethesda, Maryland 20892.

Rabbit muscle glyceraldehyde-3-phosphate dehydrogenase (GAPDH) has 4 identical subunits each with 3 trp residues. When carboxymethylated GAPDH is exposed to u.v., 2 of the 4 $NAD^+$ molecules at the active sites are transformed into covalently bound fluorescent photoproducts (Tsou, C.L. et al., Biochem. Soc. Trans. 11, 425, 1983). Using a single photon apparatus based on excitation with a synchronously pumped picosecond tunable dye laser, we have measured the fluorescence decay of native and modified GAPDH. Decay-associated spectra (DAS) were obtained with automatic computer-controlled sample changing, wavelength stepping, and data collection. Holo-GAPDH with 4 $NAD^+$ had multiexponential trp emission with $a_1$=0.74, $t_1$=0.63, $a_2$=1.72, $t_2$=1.59, $a_3$=0.26, $t_3$=2.83, and $t_m$=1.71 ns at 340 nm. The spectra associated with these lifetimes were obtained by global analysis. Bound photoproduct emission had $a_1$=0.45, $t_1$=2.2, $a_2$=0.55, $t_2$=4.3, and $t_m$=3.7 ns. DAS of the GAPDH-photoproduct complex suggest unequal energy transfer from the trps to the photoproduct. Anisotropy decay shows the photoproduct to be highly immobilized on GAPDH. Guanidine denaturation of GAPDH is slow enough to permit collection of fluorescence decay vs. time, showing sequential alteration of the DAS. These fluorescence studies support the concept that different parts of the protein denature at different rates.

**M-Pos54** RESOLUTION OF THREE-ROTATIONAL CORRELATION TIMES FOR PERYLENE BY FREQUENCY-DOMAIN FLUORESCENCE SPECTROSCOPY. Joseph R. Lakowicz, Ignacy Gryczynski, and Henryk Cherek, University of Maryland, Department of Biological Chemistry, Baltimore, Maryland 21201.

We report the first resolution of three rotational correlation times for a rigid asymmetric molecule. The possibility of three correlation times has been known since the pioneering work by F. Perrin, but to date only two correlation times have been observed experimentally for rigid asymmetric molecules. We examined the anisotropy decays for perylene using the frequency-domain method with modulation frequencies to 2 Ghz. Resolution of the amplitudes and correlation times was enhanced by global analysis of measurements performed with varying experimental conditions. In particular, the excitation wavelength ranged from 281 to 442 nm, in order to vary the orientation of the absorption moment relative to the molecular axes. Additionally, the decay time was progressively decreased by collisional quenching by bromoform. Global analysis of data for three excitation wavelengths and three quencher concentrations yielded correlation times of 0.43, 2.45 and 3.45 ns in propylene glycol at 10°C. The confidence intervals of the decay times do not overlap, even with consideration of correlation between the parameter values. The correlation times varied as expected with temperature. Importantly, the amplitudes were invariate with temperature, and were found to be 0.16, 0.10 and 0.03, respectively. These anisotropy parameters should be valuable for comparison with theories for slip and stick rotational diffusion.

**M-Pos55** RESOLUTION OF TWO EMISSION SPECTRA FOR TRYPTOPHAN pH = 7, USING PHASE-MODULATION EMISSION SPECTRA AT MULTIPLE MODULATION FREQUENCIES. Henryk Szmacinski, Ranjith Jayaweera, Wieslaw Wiczk, and Joseph R. Lakowicz, University of Maryland, Department of Biological Chemistry, Baltimore, Maryland 21201.

We recorded the wavelength-dependent phase angle and modulation spectra for the emission of tryptophan in water, pH = 7, 20°C. Data were obtained at modulation frequencies ranging from 11.4 to 261 MHz. Analysis of the phase-modulation emission spectra of tryptophan revealed a dominant emission centered at 355 nm and a minor (8%) broad component with a maximum near 335 nm. The minor component was not seen in N-acetyl tryptophanamide. The decay times of the minor and major spectral components were found to be 0.54 and 3.44 ns, respectively. Model studies with a mixture of PPD and NATA confirmed our ability to recover components which contribute only 8% to the total emission, even when the decay times have the closely spaced values of 1.10 and 3.16 ns, respectively, which agree with the independently measured values of 1.3 and 3.0 ns. All samples were purified by HPLC. Multi-frequency phase-modulation emission spectra should be generally useful for the resolution of multi-component emissions, including systems which undergo excited state reactions or energy transfer.

**M-Pos56** FLUORESCENCE ANISOTROPY OF MYOSIN-DYE CONJUGATES. EXCITATION WAVELENGTH DEPENDENCE OF STEADY-STATE AND TIME-RESOLVED MEASUREMENTS. D.G. Nealon and D.L. VanderMeulen, Baylor Research Foundation, Dallas, TX 75246; D.M. Jameson, Dept. of Pharmacology, UTHSCD, Dallas, TX 75235

Excitation polarization spectra for fluorophores generally demonstrate wavelength dependence of the intrinsic polarization, $P_o$, (or limiting anisotropy, $r_o$). Excitation into the lowest energy absorption band typically yields high (positive) $r_o$ values, whereas absorption into higher energy bands with differing orientation of the transition dipoles may produce negative values. We have studied the anisotropic rotations of the myosin 'head' utilizing the wavelength dependence of dyes such as eosin, fluorescein, and erythrosin conjugated to specific binding sites for myosin and its 'subfragments'. Rotational information from steady-state measurements was obtained using Perrin-Weber anisotropy plots obtained by varying solvent viscosity and/or temperature. Time-resolved measurements, including lifetime and dynamic polarization, were made using multifrequency phase and modulation fluorometry; multiple excitation wavelengths were used (e.g., 514 and 351 nm for eosin), corresponding to positive and negative limiting anisotropy. Both types of measurements show clear wavelength-dependent differences in the apparent rotational modes of bound probe. For 514 or 351 nm excitation of free eosin, rotation is essentially isotropic, with a Debye rotational relaxation time of ca. 0.5 ns. Bound to the $SH_1$ thiol of myosin, however, two components are evident for 514 nm (200 & 1 ns) and 351 nm (150 & 7 ns). The fractional weighting of the faster rate was much smaller for 351 nm ($< 10\%$) than for 514 nm ($> 30\%$), evidence for highly anisotropic rotation. (Supported by ONR FEL contract N0014-86-K-0186 [DN,DVM] and NSF grant DMB-8706440 [DMJ].)

M-Pos57 PADE-LAPLACE METHOD FOR THE ANALYSIS OF FLUORESCENCE DECAY. Zeljko Bajzer, Andrew Myers, Salah Sedarous, and Franklyn G. Prendergast. Department of Biochemistry and Molecular Biology, Mayo Foundation, Rochester, Minnesota 55905.

This novel approach to the analysis of multiexponential functions is based on the combined use of the Laplace transform and Pade approximants [E. Yeramian and P. Claverie, Nature 326(1987) 169]. It is similar in principle to the well-known Isenberg method of moments (with exponential depression) traditionally applied to the analysis of fluorescence decay. The advantage of the Pade-Laplace method lies in its ability to detect the number of components in multiexponential functions as well as their parameters. It is ideally suited for the analysis of time-resolved fluorescence decay curves. However, we have modified the original method so that it can be applied to the analysis of multifrequency phase and modulation measurements of fluorescence intensity decay. Basically, Fourier and Laplace transforms are combined to give the appropriate rational function which is then considered as the Pade approximant and analyzed according to the original method proposed by Yeramian and Claverie. The numerical integration involved in this analysis of phase/modulation data is more complicated than for simple Laplace transformation, which necessitates the use of higher orders of Pade approximants to effect recovery of the components. The method has allowed us to recover two and three lifetime components (and their fractional contributions) from phase/modulation data gathered on mixtures of fluorophores where the ratios of fluorescence intensities for the individual components were known. The method is now being used to analyze intensity decays of tryptophan fluorescence in proteins. Supported by GM 34847.

M-Pos58 CORRELATIONS OF TRYPTOPHAN FLUORESCENCE IN RIBONUCLEASE-T1 WITH MOLECULAR DYNAMICS SIMULATIONS OF THE SOLVATED PROTEIN STRUCTURE. Paul H. Axelsen and Franklyn G. Prendergast. Department of Biochemistry and Molecular Biology, Mayo Foundation, Rochester, MN 55905.

A molecular dynamics simulation of Ribonuclease-T1 has been conducted which accurately predicts the observed anisotropy decay of the single tryptophan residue at position 59 in this protein. Further analysis of this simulation has been performed in order to understand other photophysical properties of this residue, in particular, the fluorescence emission spectrum, the fluorescence lifetime and the accessibility of the tryptophan to quenching agents. We find that conformational changes occur near titratable residues in the simulation which may relate to the pH-dependent changes observed in the fluorescence intensity decay of TRP-59. In addition, this fluorophore is largely sequestered from bulk solvent by other residues, but features of the simulation suggest that several restricted and highly ordered encounters with water may be actually facilitated by the protein matrix. Comparative features of Ribonuclease-T1 and other single-tryptophan proteins with tryptophan residues analogously located but evincing very different photophysical properties will be presented. Supported by GM34847.

M-Pos59 EFFECTORS OF THE STEPS IN E. COLI RNA POLYMERASE TRANSCRIPTION INITIATION,
S. Leirmo and M. T. Record, Jr., Depts. of Chemistry and Biochemistry, University of Wisconsin, Madison, Wisconsin, 53706

Roe and Record (1985 J. Mol. Biol. 185, 441) proposed a three-step mechanism for open complex formation of the λPr promoter: initial binding, protein isomerization, helix opening. We have examined the effects of cation and anion concentration and type and DNA supercoiling on both the bimolecular and isomerization association rate constants. Cation release in the initial binding step alone accounts for most of the salt dependence of the overall process. The nature of the anion dramatically affects both initial binding and subsequent isomerization steps, with rate constants increased 2-50 fold by substitution of the organic anions acetate and glutamate for chloride, yet the net number of anions involved is small. Anion effects are expected to be protein-based since under these conditions E. coli RNA polymerase conformational equilibria are anion dependent while DNA helix opening is not. Substitution of a supercoiled for a linear template also increases both bimolecular and isomerization rate constants.

M-Pos60 KINETICS AND REGULATION OF HISTONE GENE EXPRESSION IN EARLY DEVELOPMENT.
Johanna G. Koster and Hans V. Westerhoff
Human Gen. Branch, NICHD and Lab. Mol. Biol., NIDDK, NIH, Bethesda, MD 20892, USA.

In many organisms there is a stage of rapid cell divisions early in embryogenesis. Since chromatin requires equal masses of histone protein and DNA, the rapid synthesis of DNA poses an extreme demand on the supply of histone protein at a period where the number of gene copies per embryo is still very small. To cope with this problem possible strategies for the organism include reiteration of histone genes, storage of histone protein and storage of histone mRNA in the oocyte.

We have set up a quantitative model for histone gene expression in the early development of Xenopus laevis and found that in addition to the above three strategies, the deceleration of DNA synthesis around 8 hours after fertilization (i.e., mid-blastula transition) is crucial in this organism. Comparison of calculated to experimental mRNA concentrations suggests that around 11 hours after fertilization regulation at a pretranslational level occurs that prevents excessive histone accumulation later in development.

(Supported in part by the Netherlands Organization for the advancement of pure research (ZWO).)

**M-Pos61** A KINETIC AND THERMODYNAMIC STUDY OF THE INTERACTION OF WHEAT GERM PROTEIN SYNTHESIS INITIATION FACTOR 3 WITH 40S RIBOSOMAL SUBUNITS AND 80S RIBOSOMES. D.J. Rounds and D.J. Goss, Chemistry Dept., Hunter College of CUNY, New York, NY 10021.

One of the primary events in the initiation of protein synthesis is eucaryotes is the dissociation of the 80S ribosome into subunits. This process is mediated by eucaryotic initiation factor 3 (eIF3). The rate constants for eIF3 association and dissociation with 40S ribosomal subunits and 80S monosomes have been determined. These rate constants were determined by laser light scattering with unmodified eIF3. The affinity of eIF3 for 40S subunits is about 30-fold greater than for 80S ribosomes. This difference in affinity resides mainly in the association rate constants. Rate constants of $8.8 \times 10^{7} M^{-1} s^{-1}$ and $7.3 \times 10^{6} M^{-1} s^{-1}$ were obtained for eIF3 binding to 40S subunits and 80S ribosomes, respectively. Thermodynamic parameters have been calculated from the temperature dependence of the association and dissociation reactions. From thermodynamic cycles, the affinity of eIF3-40S subunits for 60S subunits is about 30-fold lower than free 40S subunits for 60S subunits. A calculation shows that under these conditions and assuming simple equilibria, approximately 12% of ribosomal subunits would associate via a reaction of 40S-eIF3 with 60S subunits as opposed to a path where eIF3 dissociates from the 40S subunits prior to association with 60S subunits.

Grant Support: AHA NYC Affil., NSF 86007070, and PSC-CUNY Research Award.

**M-Pos62** INTRACELLULAR $K^+$ ACTIVITY REGULATES PROTEIN SYNTHESIS. Ying-Tung Lau[1,2] and Samuel B. Horowitz[1]. Department of Physiology and Biophysics, [1]Michigan Cancer Foundation, Detroit, MI, [2]Chang Gung Medical College, Tao-Yuan, Taiwan.

When Dumont Stage 4 Xenopus oocytes are immersed in oil, they become semi-closed systems in which one can alter the cellular $K^+$ content, and then measure both the intracellular $K^+$ activity ($a_K$) and the rate of amino acid incorporation (R). As $a_K$ is systematically varied, a characteristic response pattern of R emerges. When $a_K$ increases in the range of $a_K$ between ~100-135 mM, R is greatly stimulated; for every 10 mM $a_K$ increase, R is tripled. When $a_K$ increases to above ~140 mM, R decreases precipitously. The $R/a_K$ response pattern is anion-independent and is not caused by cellular hyperosmolality. Polypeptide synthesis examined by 2D-PAGE analysis shows that every polypeptide detected in control oocytes appears in increased abundance in KCl-stimulated oocytes. This suggests that $a_K$ affects a common synthetic step. The step appears not to be transcription since 1) the response persists in the presence of alpha-amanitin, and 2) rates of GTP incorporation are $a_K$-independent. Thus $a_K$ appears to control protein synthesis at the level of translation, with no immediate effect on transcription. Supported by NIH Grant HD 12512, GM 19548, and an institutional grant from the United Foundation of Greater Detroit.